

# بلورهای فوتونی

# Photonic Crystals

## فصل دوم : خلاصه ای از ویژگی های اساسی بلورهای فوتونی

زاهدان - دانشگاه سیستان و بلوچستان - دانشکده مهندسی برق و کامپیوتر -  
گروه مهندسی الکترونیک - دکتر محمدعلی منصوری بیرجندی

[mansouri@ece.usb.ac.ir](mailto:mansouri@ece.usb.ac.ir)

[mamansouri@yahoo.com](mailto:mamansouri@yahoo.com)

# References

## □ Main references

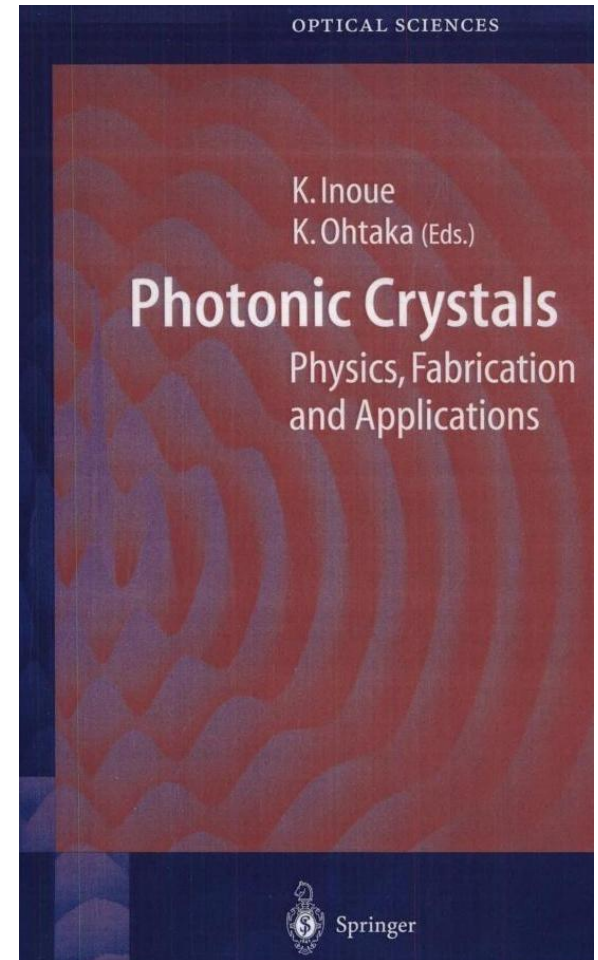
### ➤ Textbook:

● **Kuon Inoue, and Kazuo Ohtaka**

*Photonics Crystals: Physics,  
Fabrication and Applications*

Springer-Verlag Berlin Heidelberg, 2004

● **Lecture notes**



## 2 Survey of Fundamental Features of Photonic Crystals

*K. Inoue, K. Ohtaka*

---

### 2.1 One-Dimensional Photonic Crystal: Band Calculation

2.1.1 Bloch Theorem

2.1.2 Scaling Property of Photonic Band Structure

### 2.2 One-Dimensional Photonic Crystal:

#### Various Concepts and Characteristic Features of Photonic Bands

2.2.1 First Band at  $k \approx 0$

2.2.2 Photonic Bands for  $k$  near the BZ Boundary

2.2.3 Tendency of Photon Localization: Dielectric and Air Bands

2.2.4 Slow Group Velocity      2.2.5 Density of States

### 2.3 Concept of the Light Cone and Example of One-Dimensional Off-Axis Band

### 2.4 Band Structures of Two- and Three-Dimensional Photonic Crystals

2.4.1 Examples of Two-Dimensional Photonic Band

2.4.2 Example of Three-Dimensional Photonic Band

## 2 Survey of Fundamental Features of Photonic Crystals

*K. Inoue, K. Ohtaka*

---

### 2.5 How to Experimentally Explore the Band Structure

### 2.6 Defect Modes

### 2.7 Common and Fundamental Features of Photonic Band Structure

2.7.1 Existence of Photonic Band Gap

2.7.2 Existence of Defect or Local Modes

2.7.3 Anomalous Group Velocity

2.7.4 Remarkable Polarization Dependence

2.7.5 Manifestation of Peculiar Bands

### 2.8 Application of Photonic Crystals

References

## فصل ۲

# خلاصه ای از ویژگی های اساسی بلورهای فوتونی

۱-۲- بلور فوتونی یک بعدی (محاسبات باند)

۱-۱-۲- قضیه بلاخ

۲-۱-۲- خاصیت مقیاس پذیری ساختار باند فوتونی

۲-۲- بلورهای فوتونی یک بعدی (مفاهیم گوناگون و ویژگی مشخصه باندهای فوتونی)

۱-۲-۲- اولین باند در  $K \approx 0$

۲-۲-۲- باندهای فوتونی نزدیک مرز ناحیه بریلوین (BZ) برای  $k$

۳-۲-۲- روند مقید کردن فوتون: باندهای دی الکتریک و هوا

۴-۲-۲- سرعت گروه کند

۵-۲-۲- چگالی حالات

۳-۲- مفهوم مخروط نور و مثالی از باند خارج از محور (off-Axis) یک بعدی

## ادامه فصل ۲

# خلاصه ای از ویژگی های اساسی بلورهای فوتونی

- ۲-۴- ساختار باند بلورهای فوتونی دوبعدی و سه بعدی
  - ۲-۴-۱- مثال هایی از باند فوتونی دوبعدی
  - ۲-۴-۲- مثال هایی از باند فوتونی سه بعدی
- ۲-۵- چگونگی کشف ساختار باند به طور تجربی
- ۲-۶- مدهای نقص
  - ۲-۷- ویژگی های اساسی و مشترک ساختار باند فوتونی
    - ۲-۷-۱- وجود شکاف باند فوتونی
    - ۲-۷-۲- وجود مدهای نقص یا محلی
    - ۲-۷-۳- سرعت غیر عادی گروه
    - ۲-۷-۴- وابستگی های قابل توجه قطبش
    - ۲-۷-۵- ظهور باندهای ویژه
  - ۲-۸- کاربرد بلورهای فوتونی

# مقدمه

- در این فصل خلاصه ای از ویژگیهای اساسی بلورهای فوتونی را مطرح میکنیم.
- برای درک این موضوع، باید مطالبی را بیاموزیم تا فصلهای بعدی را بهتر بفهمیم.
- برای این منظور، ابتدا خلاصه ای از ساختار باند فوتونی، ویژگیهای برجسته آنها و ادوات و بلورهای فوتونی را نشان می دهیم،
- همچنین مفاهیم اساسی و قوانین بنیادی یا روابط مورد نیاز برای فهم اساسی فیزیکی را با استفاده از تشریح اساسی ساختار باند فوتونی یک بعدی شرح و نمایش میدهیم.
- درحالات دیگر، ساختار نواری را بدون شرح چگونگی بدست آمدنشان، به کار می بریم.

# 2.1 One-Dimensional Photonic Crystal: Band Calculation

## 2.1.1 Bloch Theorem

- A 1D periodic multilayer of dielectric films is illustrative;
- ❖ Example: A lossless mirror (Bragg reflector) or a quarter-wave plate.
- $a_A, a_B$  : thickness of the two layers,
- $\epsilon_A, \epsilon_B$  : dielectric constants,

periodicity of this 1D PC

$$a = a_A + a_B,$$

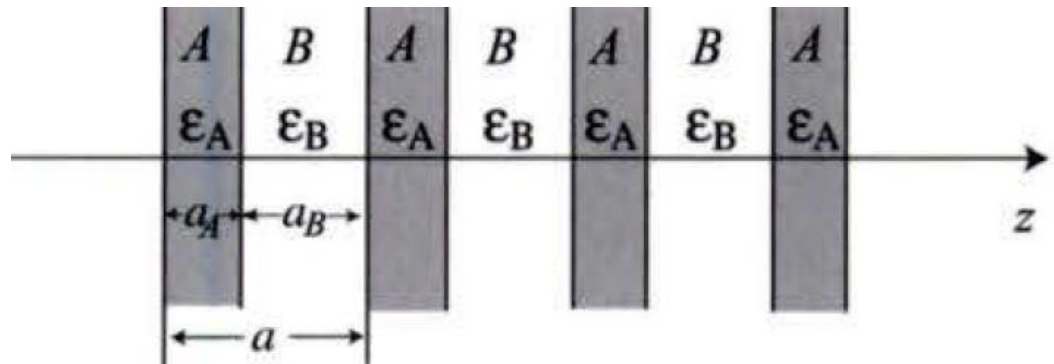


**Fig. 2 .1.** 1D stack of A and B films in the  $z$  direction. The length of the unit cell  $a = a_A + a_B$  defines the periodicity of this 1D PC.

## 2.1.1 Bloch Theorem (2)

- $\mu_0$  : the vacuum **permeability** in our nonmagnetic **PC** ;( $\mu_r=1$ )
- the **direction** of the **polarization** of  $\mathbf{E}(z)$  as the **x** direction and that of  $\mathbf{B}(z)$  in the **y** direction.  $\boxed{\mathbf{B}(z) = \mu_0 \mathbf{H}(z)}$
- Using the **scalar symbol** for the **amplitudes**, the **electric field** satisfies:

$$\frac{\partial^2}{\partial z^2} \mathbf{E}(z, t) - \frac{1}{c^2} \frac{\partial^2}{\partial t^2} \varepsilon(z) \mathbf{E}(z, t) = 0 \quad (2.1)$$

with the **periodic dielectric constant**  $\varepsilon(z)$  defined by

$$\varepsilon(z) = \begin{cases} \varepsilon_A & \text{if } z \text{ is in } A \\ \varepsilon_B & \text{if } z \text{ is in } B \end{cases} \quad (2.2)$$

## 2.1.1 Bloch Theorem (3)

➤ The **periodic function**  $\varepsilon(z)$  ( $-\infty < z < \infty$ ) is expanded into a **Fourier series**:

$$\varepsilon(z) = \sum_{p=-\infty}^{\infty} \varepsilon_p e^{i \frac{2\pi p}{a} z}. \quad (2.3)$$

Here the **basis functions**  $\left\{ e^{i \frac{2\pi p}{a} z} \right\}_{p=-\infty}^{\infty}$  have **periodicity** of the **lattice** and

$\frac{2\pi p}{a}$  ( $p = 0, \pm 1, \pm 2, \dots$ ) defines the **reciprocal lattice "vector"**.

The **Fourier coefficients** are given by

$$\varepsilon_p = \frac{1}{a} \int_0^a dz \varepsilon(z) e^{-i \frac{2\pi p}{a} z}, \quad (2.4)$$

## 2.1.1 Bloch Theorem (4)

➤ the pre-factor  $1/a$  being the **inverse** of the **unit cell "volume"**, over which the integral is made. For our **unit cell** of

$$\varepsilon(z) = \begin{cases} \varepsilon_A & 0 < z < a_A \\ \varepsilon_B & a_A < z < a \end{cases} \quad (2.5)$$

(2.4) yields

$$\varepsilon_p = \begin{cases} \varepsilon_A \frac{a_A}{a} + \varepsilon_B \frac{a_B}{a} & \text{for } p = 0 \\ \frac{i}{2\pi p} (\varepsilon_A - \varepsilon_B) \left( e^{-i\frac{2\pi p}{a} a_A} - 1 \right) & \text{for } p \neq 0. \end{cases} \quad (2.6)$$

We assume the **harmonic oscillation** in the **temporal** behavior

$$E(z, t) = e^{-i\omega t} E(z).$$

## 2.1.1 Bloch Theorem (5)

➤ To find the *solutions* of wave equation (2.1), a **Bloch form** is substituted for  $E(z)$ , which is given by

$$E(z) = \sum_{p=-\infty}^{\infty} c_p e^{i(k+p\frac{2\pi}{a})z}. \quad (2.7)$$

This is a *plane-wave expansion (PWE)* form of the *PB solution*.

➤ Inserting (2.3) and (2.7) into (2.1) and putting the *pre-factor* of the plane wave  $e^{i(k+(2\pi p/a)z)}$  to *zero*, we find

$$\left(k + \frac{2\pi p}{a}\right)^2 c_p - \sum_{p'=-\infty}^{\infty} \left(\frac{\omega}{c}\right)^2 \varepsilon_{p-p'} c_{p'} = 0 \quad (p = 0, \pm 1, \pm 2, \dots) \quad (2.8)$$

## 2.1.1 Bloch Theorem (5-2)

Inserting (2.3) and (2.7) into (2.1) and putting the *pre-factor* of the plane wave  $e^{i(k + (2\pi/a))z}$  to *zero*, we find

$$\frac{\partial^2}{\partial z^2} E(z, t) - \frac{1}{c^2} \frac{\partial^2}{\partial t^2} \varepsilon(z) E(z, t) = 0 \quad (2.1)$$

$$\varepsilon(z) = \sum_{p=-\infty}^{\infty} \varepsilon_p e^{i \frac{2\pi p}{a} z}, \quad (2.3)$$

$$E(z) = \sum_{p=-\infty}^{\infty} c_p e^{i(k + p \frac{2\pi}{a})z}. \quad (2.7)$$

secular equation: معادله مشخصه

$$\left(k + \frac{2\pi p}{a}\right)^2 c_p - \sum_{p'=-\infty}^{\infty} \left(\frac{\omega}{c}\right)^2 \varepsilon_{p-p'} c_{p'} = 0 \quad (p = 0, \pm 1, \pm 2, \dots) \quad (2.8)$$

## 2.1.1 Bloch Theorem (6)

➤ These are **linear coupled equations** for the **coefficients**  $\dots, c_{-1}, c_0, c_1, c_2, \dots$

The **solutions** exist only when  $\omega$  satisfies the **secular equation** constructed from the **coefficients** of the **coupled equations**:

$$\det \begin{vmatrix} \dots & \dots & \dots & \dots & \dots \\ \dots & (k - \frac{2\pi}{a})^2 - (\frac{\omega}{c})^2 \epsilon_0 & -(\frac{\omega}{c})^2 \epsilon_{-1} & -(\frac{\omega}{c})^2 \epsilon_{-2} & \dots \\ \dots & -(\frac{\omega}{c})^2 \epsilon_1 & (k)^2 - (\frac{\omega}{c})^2 \epsilon_0 & -(\frac{\omega}{c})^2 \epsilon_{-1} & \dots \\ \dots & -(\frac{\omega}{c})^2 \epsilon_2 & -(\frac{\omega}{c})^2 \epsilon_1 & (k + \frac{2\pi}{a})^2 - (\frac{\omega}{c})^2 \epsilon_0 & \dots \\ \dots & \dots & \dots & \dots & \dots \end{vmatrix} = 0 \quad (2.9)$$

We note the **regularity** of the **matrix elements**; the **diagonal elements** are

$$\dots, \left(k - \frac{4\pi}{a}\right)^2, \left(k - \frac{2\pi}{a}\right)^2, (k)^2, \left(k + \frac{2\pi}{a}\right)^2, \left(k + \frac{4\pi}{a}\right)^2, \dots$$

## 2.1.1 Bloch Theorem (7)

➤ The *Fourier components*  $\{\epsilon_p\}$  of the dielectric function  $\epsilon(z)$  appear in each **row** in the order

$$\dots, \epsilon_2, \epsilon_1, \epsilon_0, \epsilon_{-1}, \dots$$

with  $\epsilon_0$  present at the **diagonal position** of the matrix.

➤ That the solutions of (2.1) could be found in this way is wholly attributed to the **Bloch form** (2.7) assumed for the solution. It satisfies

$$E(z + a) = e^{ika} E(z), \quad (2.10)$$

which is the **Bloch theorem**, to be met by any solution of a **periodic system**.

➤ It is the **wave number**  $k$  that specifies the **Eigen-solutions**.

## 2.1.1 Bloch Theorem (8)

- The **periodicity** of the solutions with respect to **k**:

solution for **k** of (2.8) or (2.9) = for **k + p(2π/a)** with an integer **p**

- These two **k** lead to the same form in (2.7), as seen by renumbering the coefficient **c<sub>p</sub>**, and to the same eigenvalues for **ω** in (2.9), as seen by using the **regularity** of the **matrix elements**.

- Since the identical solutions are obtained for the set of wavenumbers **k**, **k+(2π/a)**, . . . ., all possible normal modes of (2.9) are covered by letting **k** run only over the first Brillouin zone (**BZ**), which is for the present **1D** system a region of **k** defined by

$$\boxed{-\frac{\pi}{a} \leq k < \frac{\pi}{a}.} \quad (2.11)$$

For a given value of **k** in the first BZ, the secular equation (2.9) gives the eigenvalues **ω<sub>1</sub>, ω<sub>2</sub>, . . .**.

## 2.1.1 Bloch Theorem (9)

- The **number** of the **eigenvalues** is fixed by the **size** of the **matrix** truncated in the secular equation.
- As **k** varies, each of the **eigenvalues** changes gradually. As a result, (2.9) gives a set of continuous functions of **k**,  $\omega_1(\mathbf{k})$ ,  $\omega_2(\mathbf{k})$ ,  $\dots$ .
- They are the dispersion curves of the **PBs**, of our **1D** system. The subscript **n** of  $\omega_n(\mathbf{k})$  is usually called a **band index**.
- (We sometimes use **n** as a superscript as in  $\mathbf{v}_g^{(n)}$ , the group velocity of *nth band*.)
- For the concrete case of **A=Si** ( $\epsilon_A=12$ ), **B=air** ( $\epsilon_B=1$ ), and  $\mathbf{a}_A=\mathbf{a}_B=\mathbf{a}/2$ , the band structure is given in **Fig. 2.2**.

# 2.1.1 Bloch Theorem (10)

**Fig. 2. 2.** *Band structure* of the 1D photonic crystal shown in [Fig. 2.1](#) for A= Si and B = air.

The case of  $a_A = a_B = a/2$  with  $\epsilon_A=12$  (dielectric constant of Si in the visible range) and  $\epsilon_B=1$  is shown.

Both the frequency  $\omega$  and wavenumber  $k$  are shown in **dimensionless** units.

[Fig. 2.1](#)

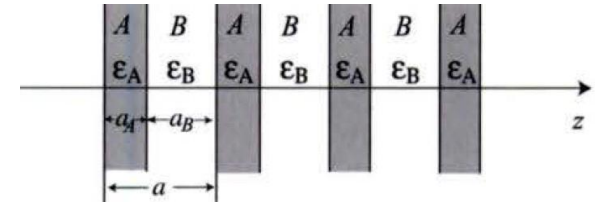
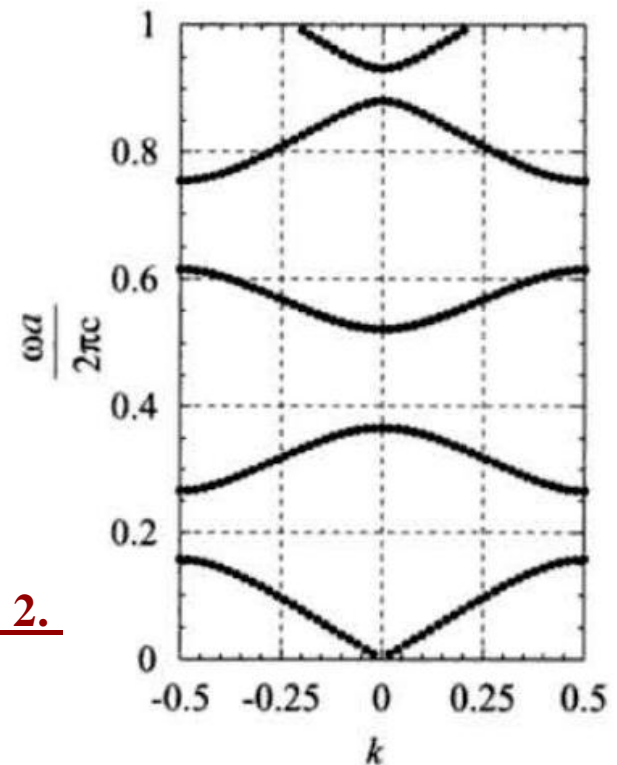


**[Fig . 2. 2.](#)**



## 2.1.1 Bloch Theorem (11)

- If we take account of a **larger range** of integer  $p$  in truncating the sum of (2.7), the **matrix of the secular equation** becomes **bigger**.
- In calculating Fig. 2.2 we have used **11 plane waves** ( $-5 \leq p \leq 5$ ) in (2.7).
  - ❖ As the size of the secular determinant increases, so does the **number of solutions** for  $\omega$  for a **fixed**  $k$ .
- With **increase** of the **number** of plane waves, the contributions of the *shorter waves* are incorporated, for the **larger** the wavenumber  $|k + (2\pi p/a)|$  is, the **shorter** becomes the wavelength of  $\exp i(k + (2\pi p/a)z)$ .
  - ❖ As a result, if we attempt to obtain the **PBS** in a higher frequency range, we necessarily **need** to treat a larger secular matrix.

## 2.1.1 Bloch Theorem (12)

---

- ❖ The actual trend that a **PB** of **higher frequency** is better represented by a larger *number of plane waves*, is seen in Fig. 2.3, which shows the calculated band frequency at  $\mathbf{k} = \pi/a$  to be improved progressively with the **increase** of the **cutoff** size of the **secular matrix**.
- ❖ It is important here to understand the **PBS** of a system in terms of the **dispersion relation** of photons in the **empty lattice**.

## 2.1.1 Bloch Theorem (13)

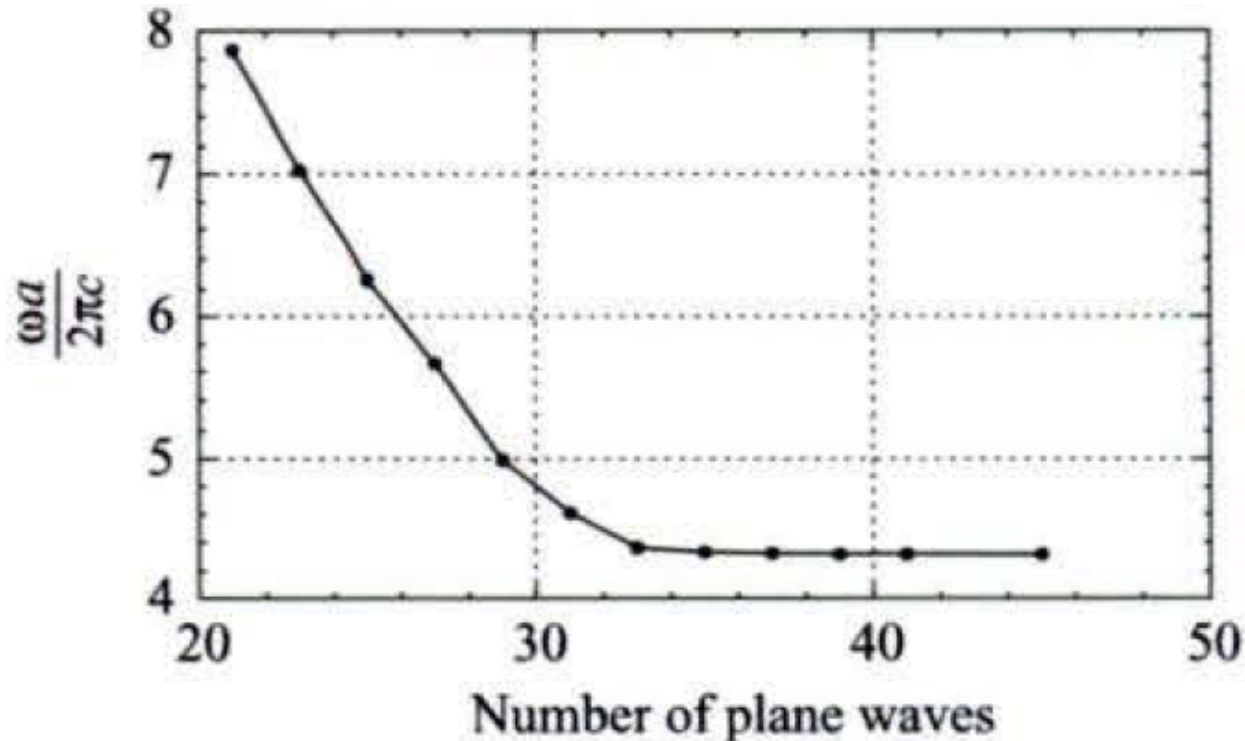


**Fig. 2.3.** Convergence of the **band energy** as a **function** of the number of **plane waves** used in the calculation. The **result** is given for the **20th band** at the **BZ edge**. The **parameters** used in the band calculation are the **same** as those used in **Fig. 2.2**

## 2.1.1 Bloch Theorem (13)

- An empty lattice of a PC is a fictitious system which has only the periodicity of that PC but is identical to free space otherwise.
- In an empty lattice, therefore,  $\epsilon_{\pm 1}, \epsilon_{\pm 2}, \dots$  all vanish identically except  $\epsilon_0 = 1$  in (2.9). The PBS of the empty lattice is obtained by folding the free space dispersion curve  $\omega = ck$  at the edge of the first BZ.
- This is because what remains in the secular matrix of (2.9) are solely the diagonal elements

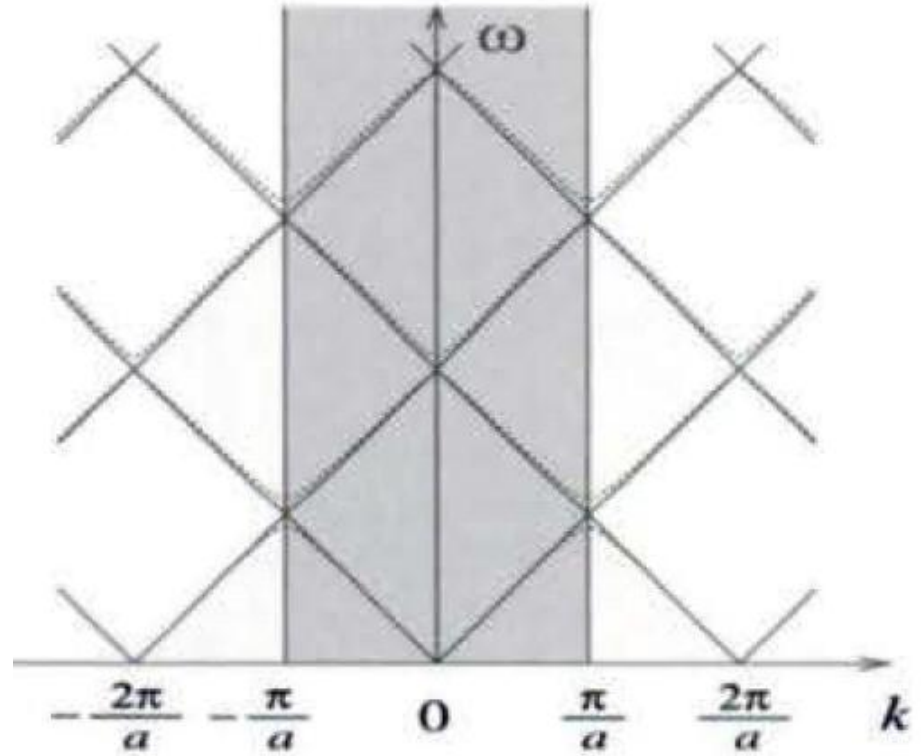
$$(k + 2\pi p/a)^2 - (\omega/c)^2.$$

- The empty-lattice test is especially useful in a PC of weak periodicity. See Fig. 2.4 for the PBS of a model system.

## 2.1.1 Bloch Theorem (14)

**Fig. 2.4.** Band structure of a 1D photonic crystal of weak periodicity. The straight lines show the dispersion curves of the empty lattice,  $\omega = c|k + (2\pi p/a)|$ , ( $p=0, \pm 1, \pm 2, \dots$ ).

The band structure with small band gaps is the one calculated for  $a_A = a_B = a/2$  with  $\varepsilon_A = 2$  and  $\varepsilon_B = 1$



## 2.1.2 **Scaling** Property of Photonic Band Structure (1)

- From (2.1) and (2.8) we can deduce an important *scaling property*.
- We introduce, in place of  $\mathbf{k}$  and  $\omega$ , the **dimensionless** wavenumber  $\mathbf{k}'$  and frequency  $\omega'$ , which are defined by

$$k = k' \left( \frac{2\pi}{a} \right), \quad \omega = \omega' \left( \frac{2\pi c}{a} \right) \quad (2.12)$$

or

$$k' = \frac{ka}{2\pi}, \quad \omega' = \frac{\omega a}{2\pi c}. \quad (2.13)$$

- ❑  $\mathbf{k}'$  : wavenumber of **photons** measured in units of  $2\pi/a$
- ❑  $\omega'$  : frequency measured in units of  $2\pi c/a$
- **reciprocal lattice points**: (In the **new scale** of the wavevector,)  $\dots, -2, -1, 0, 1, 2 \dots$
- Thus the first BZ is defined in the  $\mathbf{k}'$  axis to be  $-0.5 < \mathbf{k}' < 0.5$ .
- ❑ When the **secular equation** (2.9) is rewritten using  $\mathbf{k}'$  and  $\omega'$ , the size  $a$  can be **removed** everywhere.

## 2.1.2 **Scaling** Property of Photonic Band Structure (2)

❖ To see it, let us return to the Fourier component (2.4). We find

$$\begin{aligned}\varepsilon_p &= \frac{1}{a} \int_0^a dz \varepsilon(z) e^{-i \frac{2\pi p}{a} z} \\ &= \int_0^1 dz' \varepsilon(az') e^{-i 2\pi p z'} \\ &= \int_0^1 dz' \tilde{\varepsilon}(z') e^{-i 2\pi p z'} \\ &\equiv \tilde{\varepsilon}_p\end{aligned}\tag{2.14}$$

where

$$\tilde{\varepsilon}(z') = \varepsilon(az')\tag{2.15}$$

$\tilde{\varepsilon}(z')$  is the dielectric function expressed using the new coordinate  $z'$  measured in units of  $a$ .

## 2.1.2 **Scaling** Property of Photonic Band Structure (3)

➤ The **conclusion** is that in terms of the dimensionless quantities of  $\mathbf{k}'$ ,  $\omega'$  and  $\tilde{\epsilon}_p$ , (2.8) is transformed to

$$(\mathbf{k}' + \mathbf{p})^2 c_p - \sum_{\mathbf{p}'} \omega'^2 \tilde{\epsilon}_{\mathbf{p}-\mathbf{p}'} c_{\mathbf{p}} = 0. \quad (2.16)$$

❖ This **final result** has nothing to do with the **periodicity**  $\mathbf{a}$  of the **PC** under consideration.

➤ Therefore, if there are two PCs and their **dielectric functions** are identical when expressed using the lattice constant  $\mathbf{a}$  as the unit of length, the **PBSs** of the two systems are the **same**, when exhibited using  $\omega'$  as functions of  $\mathbf{k}'$ .

## 2.1.2 **Scaling** Property of Photonic Band Structure (4)

❖ For example, **two PCs** of repeated A and B:

the first having:

$$a = 2 \mu\text{m}, a_A = 0.8 \mu\text{m}, a_B = 1.2 \mu\text{m}$$

and the **second** one having:

$$a = 1 \text{ mm}, a_A = 0.4 \text{ mm}, a_B = 0.6 \text{ mm},$$

- **Two PCs** have the same PBS when expressed using  $\omega'$  and  $k'$ , if  $\epsilon_A$  and  $\epsilon_B$  of the two cases are identical.
- In the scaled units, the dispersion curve  $\omega = ck$  of a free photon gives  $\omega' = 0.5$  at the BZ edge  $k' = \pm 0.5$ .
- Because of these **scaling properties**, PBSs are usually discussed and displayed in these **scaled units**.

## 2.1.2 **Scaling** Property of Photonic Band Structure (5)

---

- In the above example, the BZ edge  $\pm 0.5$  corresponds to the wavelength of the PB of the order of **microns** and **millimeters**, respectively.
- In two systems having such a **huge difference** of scales, and hence involving totally **different wavelengths** of PBs, identical values of **dielectric functions** are hardly expected.

# 2.2 One-Dimensional Photonic Crystal: (1)

## Various Concepts and Characteristic Features of Photonic Bands

---

In the calculated **PBS**, several characteristic features of **BSs** are seen, which are, in fact, common not only in **1D** but also in **2D** and **3D PCs**. Let us again take a look at Fig. 2.2.

2.2.1 First Band at  $k \approx 0$

2.2.2 Photonic Bands for  $k$  near the **BZ** Boundary

2.2.3 Tendency of Photon Localization: **Dielectric** and **Air Bands**

2.2.4 Slow Group Velocity

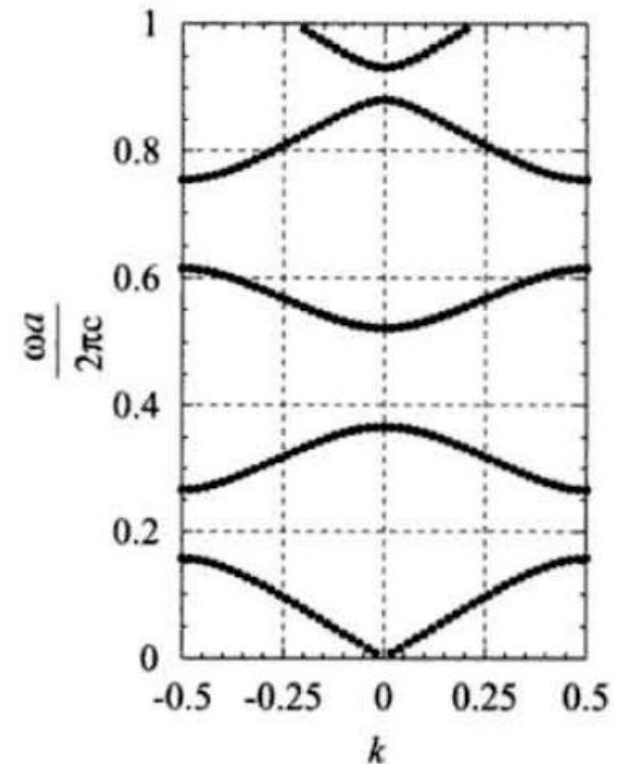
2.2.5 Density of States

## 2.2 One-Dimensional Photonic Crystal: (2)

### Various Concepts and Characteristic Features of Photonic Bands

#### 2.2.1 First Band at $k \approx 0$

- The **first band**, the **lowest** of all in frequency, has a linear dispersion relation near the center of the **BZ**.
- In view of the **empty-lattice** test, this feature is natural; since the state with  $\mathbf{k} \approx \mathbf{0}$  in the **first band** has a **wavelength** much longer than the lattice constant. ( $\lambda > a$ )



## 2.2 One-Dimensional Photonic Crystal: (3)

### Various Concepts and Characteristic Features of Photonic Bands

#### 2.2.2 Photonic Bands for $k$ near the BZ Boundary

- ❖ In the **BZ edge**, the **dispersion curves** are gradually **curved**.
- ❖ At the edge  $k' = 0.5$ , the **PB** state is an equal admixture of  $e^{ikx}$  and  $e^{-ikx}$  and **propagates** neither to right nor to left by forming a **standing wave**.
- ❖ *This is why the **group velocity**  $v_g$  of the photon **vanishes** there:*

$$v_g \equiv \frac{\partial}{\partial k} \omega_1(k) = 0 \quad \text{at } k = 0.5 \frac{\pi}{a}. \quad (2.17)$$

- Beyond the **BG**, there is a partner of the **standing-wave** with  $v_g = 0$  at the **BZ edge**.

## 2.2 One-Dimensional Photonic Crystal: (4)

### Various Concepts and Characteristic Features of Photonic Bands

#### 2.2.3 Tendency of Photon Localization: Dielectric and Air Bands

- To show the **difference** of the **two states** at the **BZ edges**, the **intensity** of the **electric field** is plotted in Fig. 2.5.
- Below the BG (band  $n = 1$ ) has a higher intensity within the region of higher  $\epsilon$ -value, while the **reverse** is true for the state above the BG.
- ❖ In this sense we often call the **lower band** of the pair a **dielectric band**
- ❖ and the **higher band** an **air band**, having in mind a periodic repetition of **dielectric** and **air**.
- This type of distribution of the **electric field** is more or less seen in the pair of states at the **BZ edge** in the higher frequency range, though the contrast gets gradually obscured due to the nodes appearing both in **dielectric** and **air regions**.

## 2.2 One-Dimensional Photonic Crystal: (5) Various Concepts and Characteristic Features of Photonic Bands

### 2.2.3 Tendency of Photon Localization: Dielectric and Air Bands

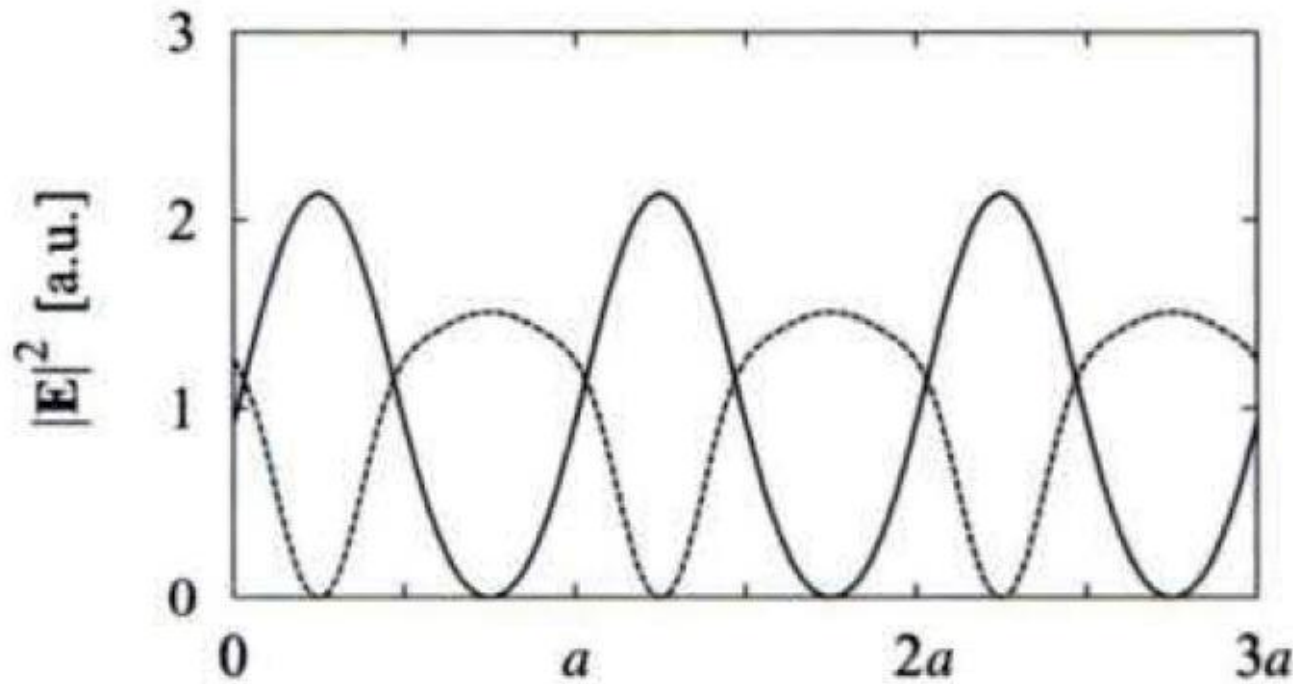


**Fig. 2.5.** Squared electric field as a function of  $z$  of the states at the **BZ** edge. The solid curve shows the first band (dielectric band) and the dashed curve shows the second band (air band) for the band structure shown in Fig. 2.2

## 2.2 One-Dimensional Photonic Crystal: (6)

### Various Concepts and Characteristic Features of Photonic Bands

#### 2.2.3 Tendency of Photon Localization: Dielectric and Air Bands

❖ The contrasting **feature** of the **two bands** stems from the general trend for **photons** that a **higher  $\epsilon$**  induces a **stronger localization** of photons. To see it, let us return to the wave equation (2.1).

$$\frac{\partial^2}{\partial z^2} E(z, t) - \frac{1}{c^2} \frac{\partial^2}{\partial t^2} \epsilon(z) E(z, t) = 0 \quad (2.1)$$

❖ For the stationary state of  $\omega$ , we have  $\partial^2/\partial t^2 \approx -\omega^2$ . Adding  $(\omega/c)^2 E(z)$  on both side of (2.1) then yields

$$-\frac{\partial^2}{\partial z^2} E(z) - \frac{\omega^2}{c^2} (\epsilon(z) - 1) E(z) = \frac{\omega^2}{c^2} E(z). \quad (2.18)$$

## 2.2 One-Dimensional Photonic Crystal: (7)

### Various Concepts and Characteristic Features of Photonic Bands

#### 2.2.3 Tendency of Photon Localization: Dielectric and Air Bands

$$-\frac{\partial^2}{\partial z^2} E(z) - \frac{\omega^2}{c^2} (\varepsilon(z) - 1) E(z) = \frac{\omega^2}{c^2} E(z). \quad (2.18)$$

➤ To compare it with the Schrodinger equation

$$-\frac{\hbar^2}{2m} \frac{\partial^2}{\partial z^2} \psi(z) + V(z) \psi(z) = E \psi(z) \quad (2.19)$$

for a particle of mass  $m$  and energy eigenvalue  $E$  in the potential energy

➤ By comparison, we see at once that  $-\frac{\omega^2}{c^2} (\varepsilon(z) - 1)$

plays the role of the potential  $V(z)$  (the dimensions are not of potential, however).

➤ Therefore we see that a substance with  $\varepsilon$  higher than unity works as an attractive potential relative to free space, by having a negative potential.

## 2.2 One-Dimensional Photonic Crystal: (7)

### Various Concepts and Characteristic Features of Photonic Bands

#### 2.2.3 Tendency of Photon Localization: Dielectric and Air Bands

$$-\frac{\partial^2}{\partial z^2} E(z) - \frac{\omega^2}{c^2} (\epsilon(z) - 1) E(z) = \frac{\omega^2}{c^2} E(z). \quad (2.18)$$

➤ To compare it with the Schrodinger equation

$$-\frac{\hbar^2}{2m} \frac{\partial^2}{\partial z^2} \psi(z) + V(z) \psi(z) = E \psi(z) \quad (2.19)$$

for a particle of mass  $m$  and energy eigenvalue  $E$  in the potential energy  $V(z)$ .

➤ By comparison

$$-\frac{\omega^2}{c^2} (\epsilon(z) - 1)$$

plays the **role** of the **potential**  $V(z)$ .  
(however the **dimensions** are not of **potential**).

➤ Therefore we see that a substance with  $\epsilon > 1$  works as an **attractive potential relative** to free space, by having a **negative potential**.

## 2.2 One-Dimensional Photonic Crystal: (8)

### Various Concepts and Characteristic Features of Photonic Bands

#### 2.2.3 Tendency of Photon Localization: Dielectric and Air Bands

- This is **why** the band having a **higher electric-field intensity** at **A** ( $\epsilon_A = 12$ ) than **B** ( $\epsilon_B = 1$ ) is found to have a **lower frequency**.
- The quantity  $\omega^2/c^2$  plays the role of an **energy eigenvalue** of the **electron**.
- Because  $\omega^2/c^2$  is always **positive** in the **photonic case**, there **cannot** be a **bound state** in an **ordinary sense**,
- i.e., the *situation* of a **photon** being *localized* completely in an **attractive potential** can **never** be achieved.
- The leakage of photons as an **outflow** of electromagnetic energy is thus inevitable in the **photonic case**.

**Table 1. Electron-photon similarity**

	<i>Electron (Schrödinger)</i>	<i>Photon (Maxwell)</i>
Field	$\psi(r, t) = \psi(r) \exp(-i\omega.t)$	$\vec{H}(\vec{r}, t) = \vec{H}(\vec{r}) \exp(-i\omega.t)$
Specific term	$V(r)$	$\vec{E}(\vec{r})$
Hermitian operator	$H = \frac{-\hbar^2 \nabla^2}{2m} + V(r)$	$\Theta = \nabla \times \left( \frac{1}{\epsilon(r)} \nabla \times \right)$
Eigenvalue equation	$H\psi = E\psi$	$\Theta\vec{H} = \left( \frac{\omega^2}{c^2} \right) \vec{H}$

$$-\frac{\hbar^2}{2m} \frac{\partial^2}{\partial z^2} \psi(z) + V(z)\psi(z) = E\psi(z)$$

$$-\frac{\partial^2}{\partial z^2} E(z) - \frac{\omega^2}{c^2} (\epsilon(z) - 1)E(z) = \frac{\omega^2}{c^2} E(z).$$

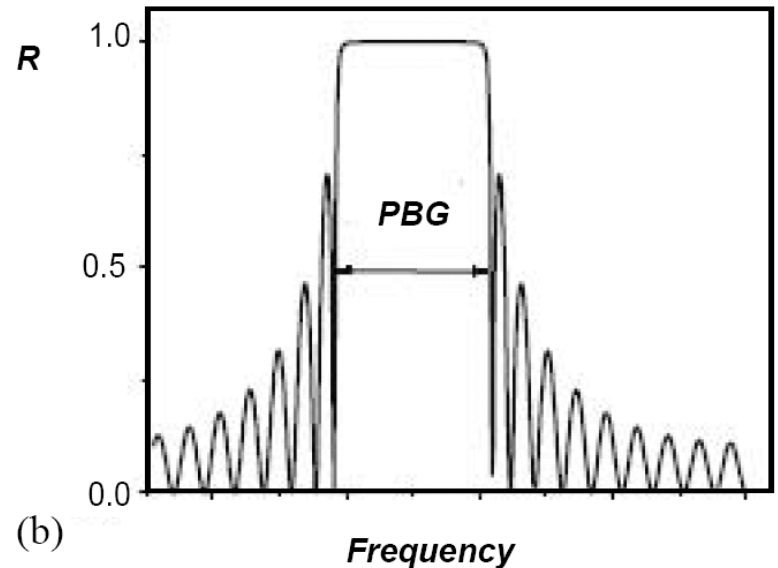
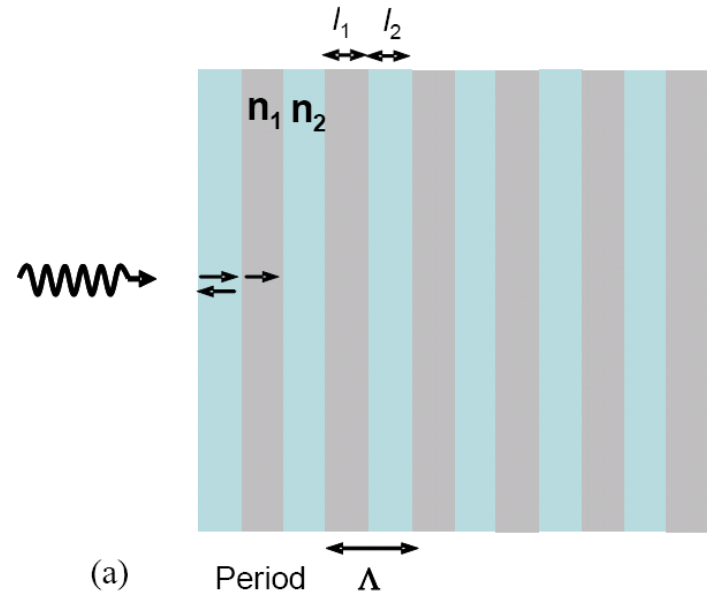
# Bragg's mirror

(a)  $\Lambda$  is the lattice period;

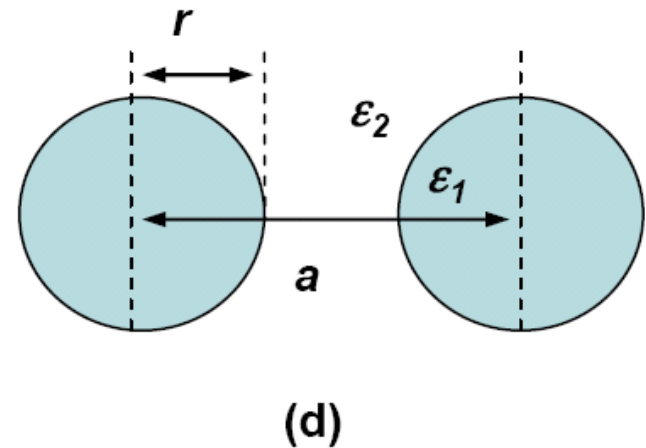
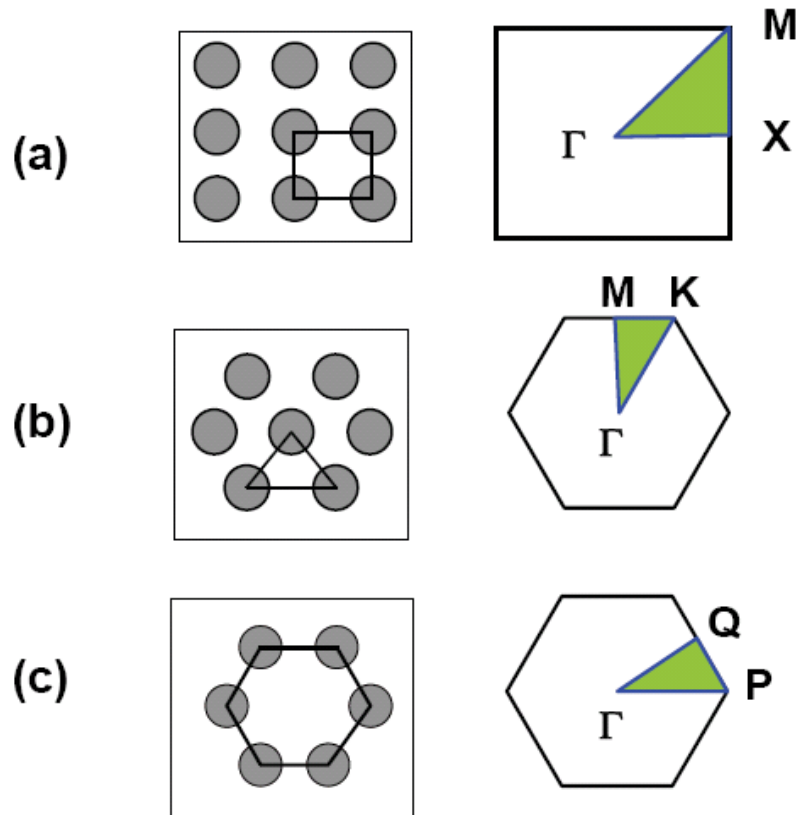
$$\lambda \approx \lambda_B = \frac{2n_0 a}{m}$$

$$\omega = v|k| \quad \Delta\lambda = \frac{\Delta n}{n_0} \lambda_B$$

(b) the reflected intensity indicating the PBG



Examples of **2D-PBG** and their **first Brillouin's zone**:  
**(a) square cell**, **(b) triangular** and **(c) hexagonal**; and  
**(d) definition of the lattice radius  $r$  and period  $a$ .**



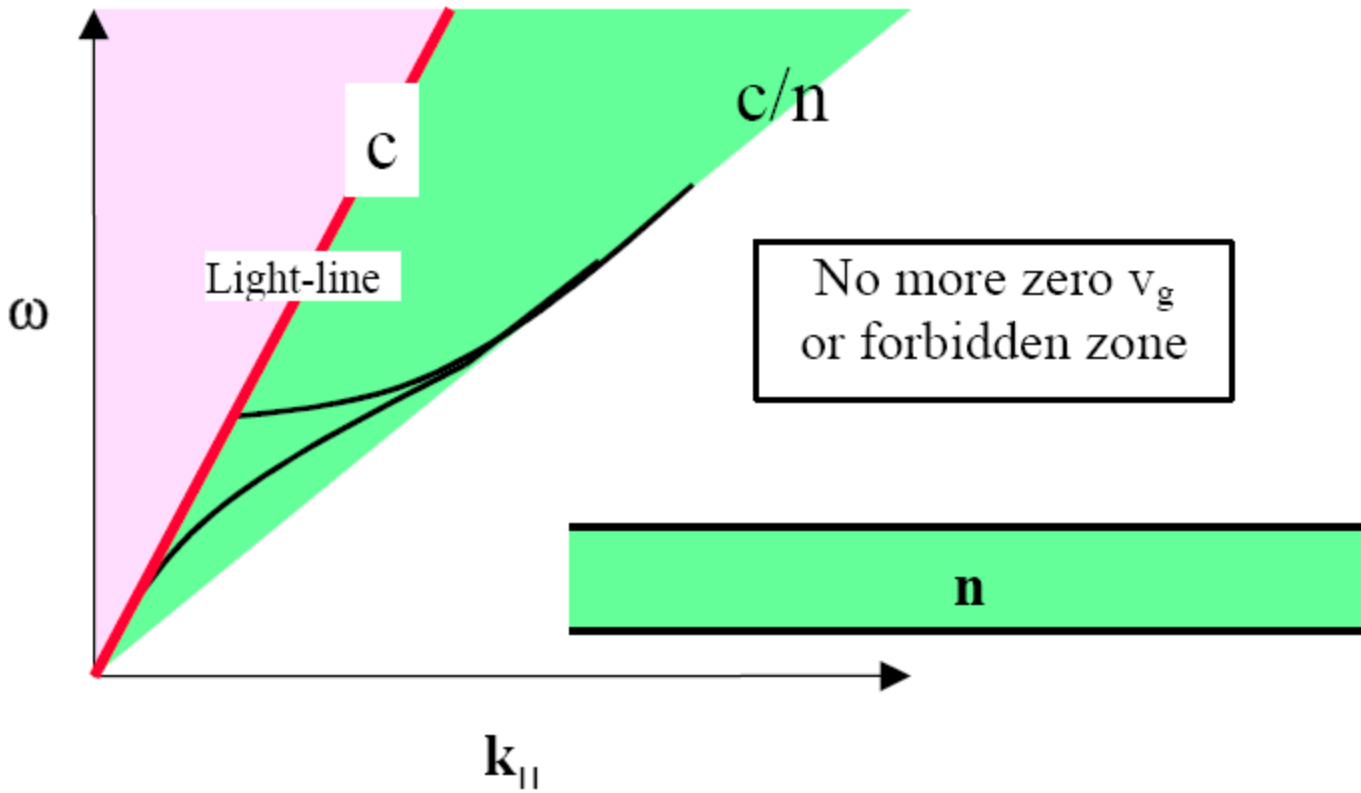


**Figure 1.6.** Case of index guiding: *light-line*

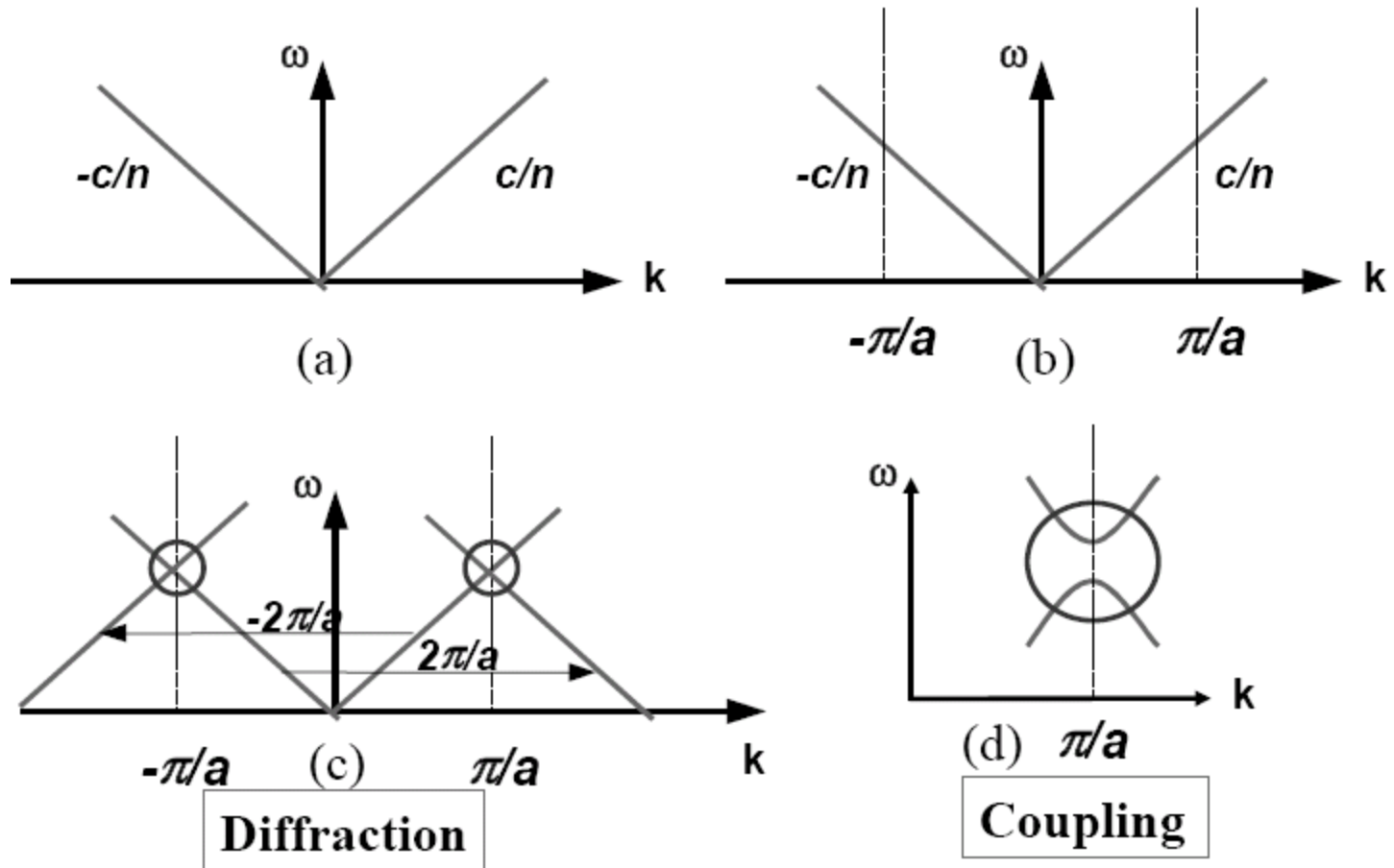


**Figure 1.9.** The **dispersion characteristics** of optical modes in a periodic medium are widely determined by **diffraction processes** and **optical mode coupling** properties

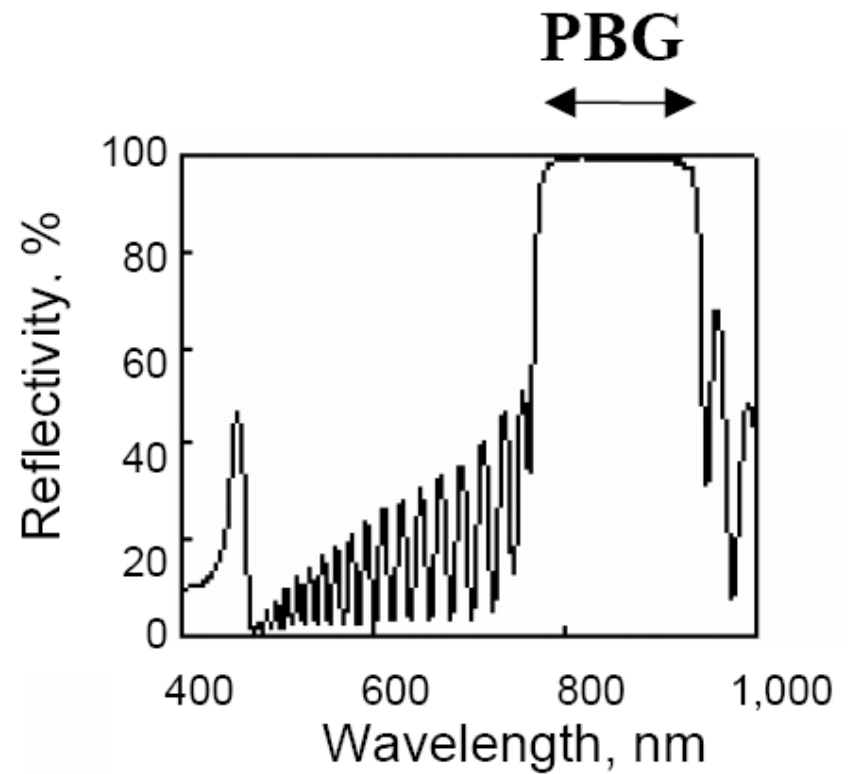
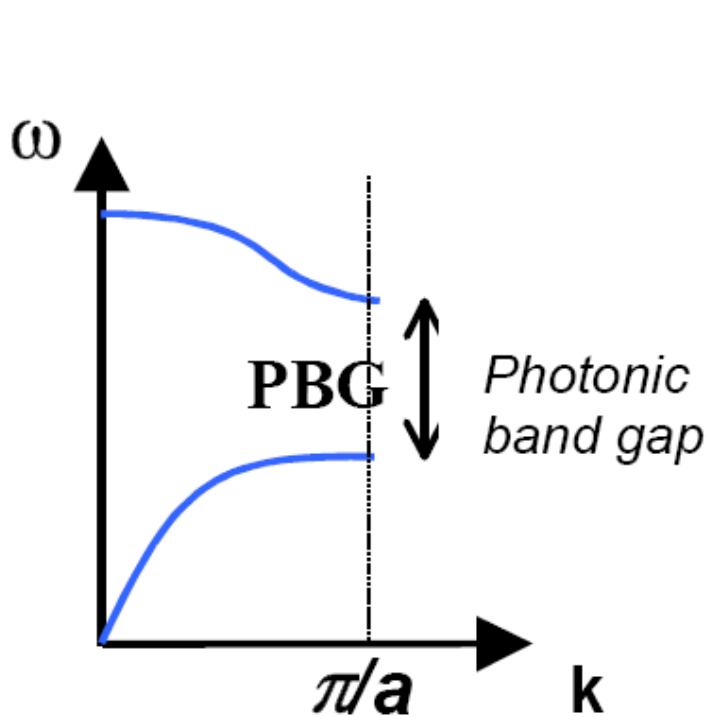


**Figure 1.10.** Photonic band gap (PBG) and bandwidth of a Bragg reflector

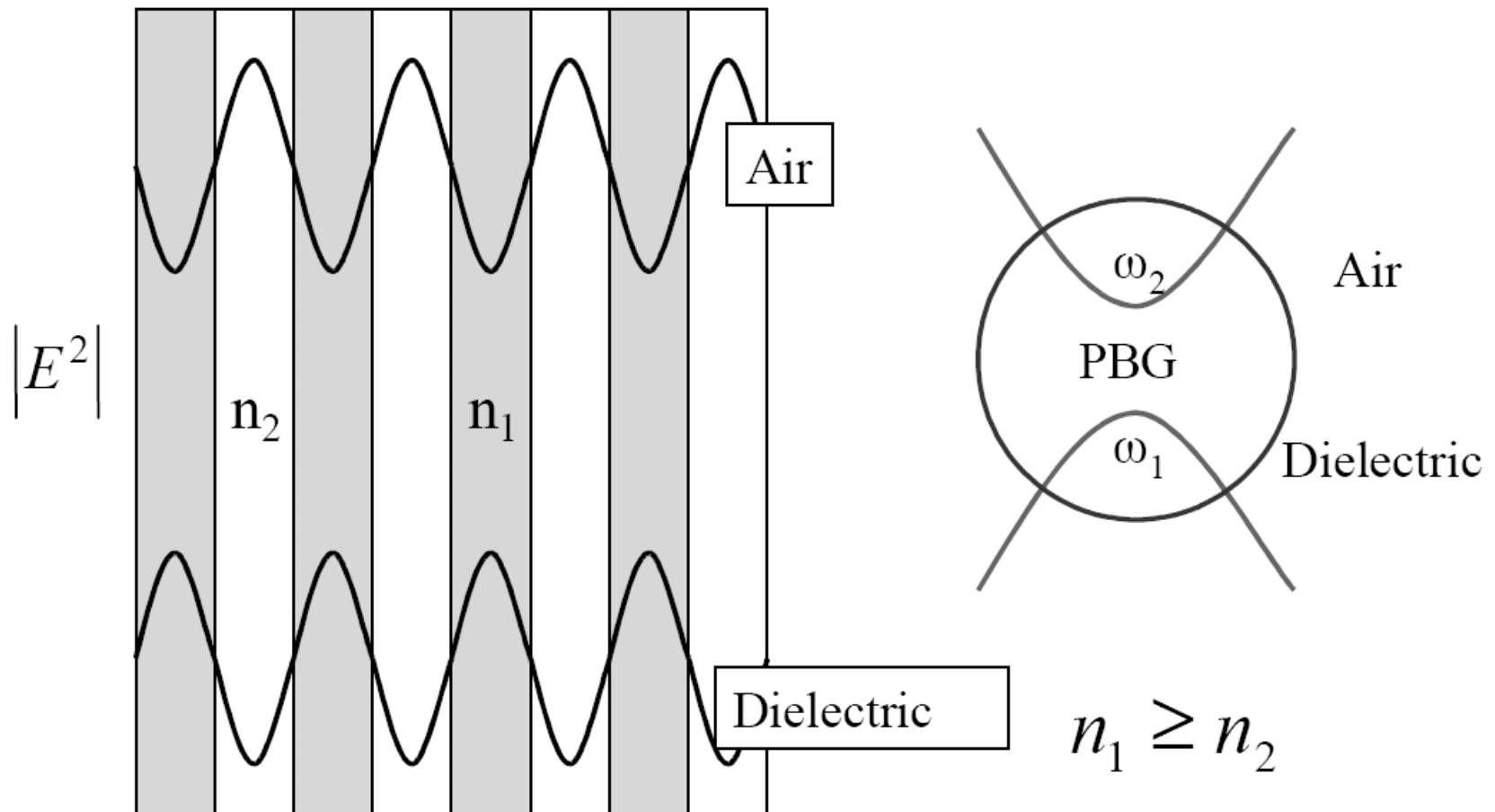


**Figure 1.11.** Air band and dielectric band at the photonic band edges

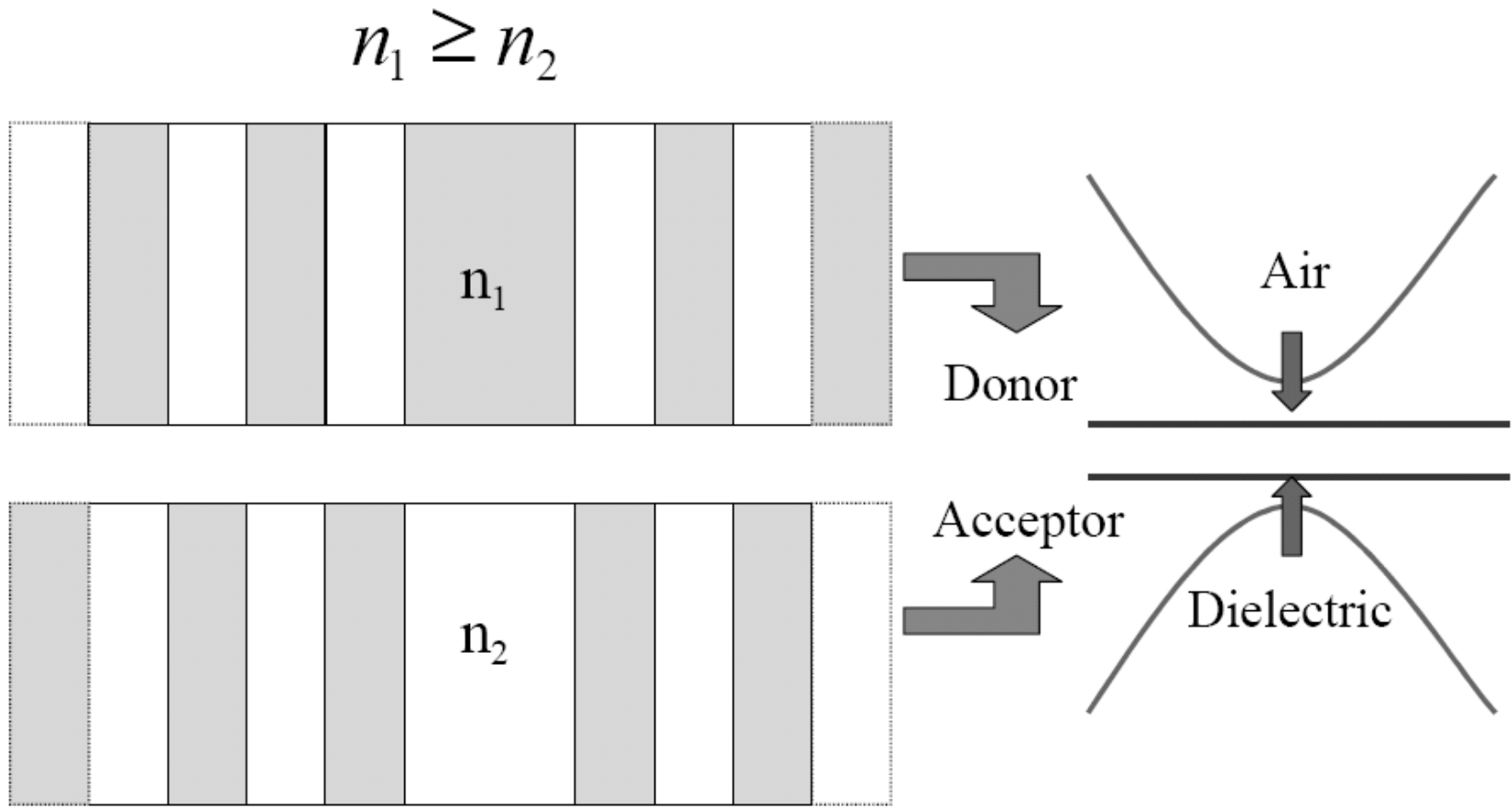


**Figure 1.13.** Donor or acceptor type localized state

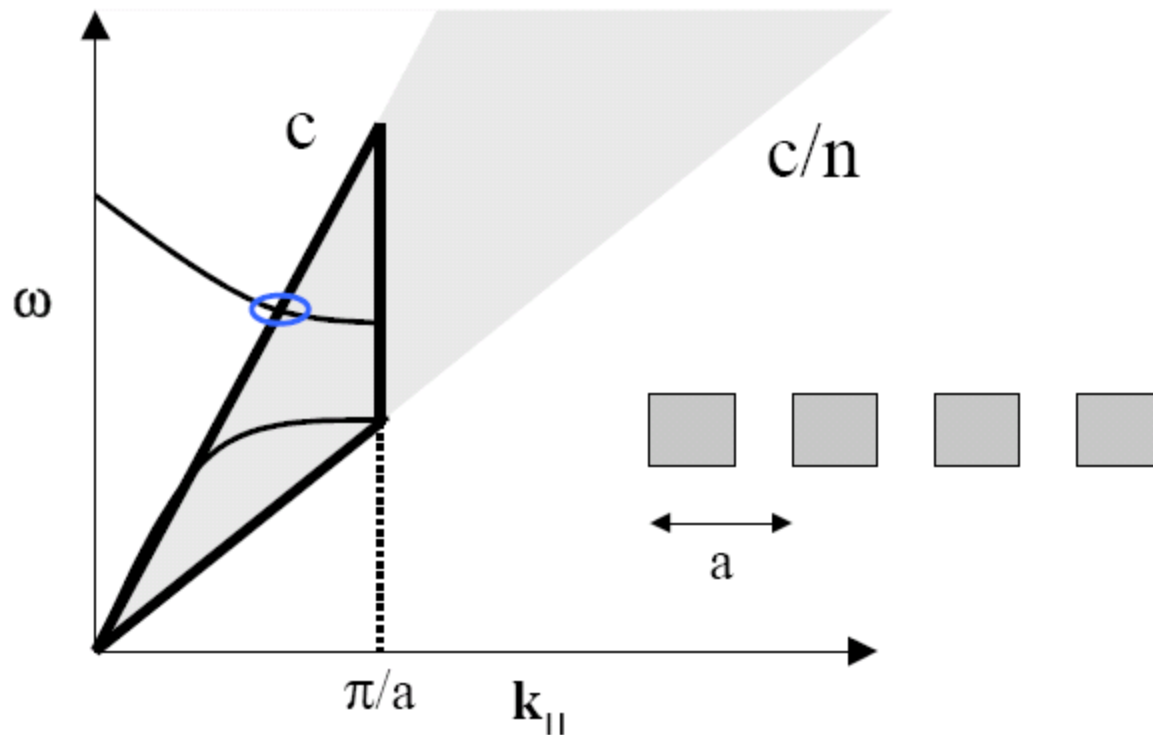


**Figure 1.16.** 1D photonic crystal in a **dielectric waveguide**: coupling processes between propagating and counter-propagating waves, and between **waveguided** and **radiated mode**

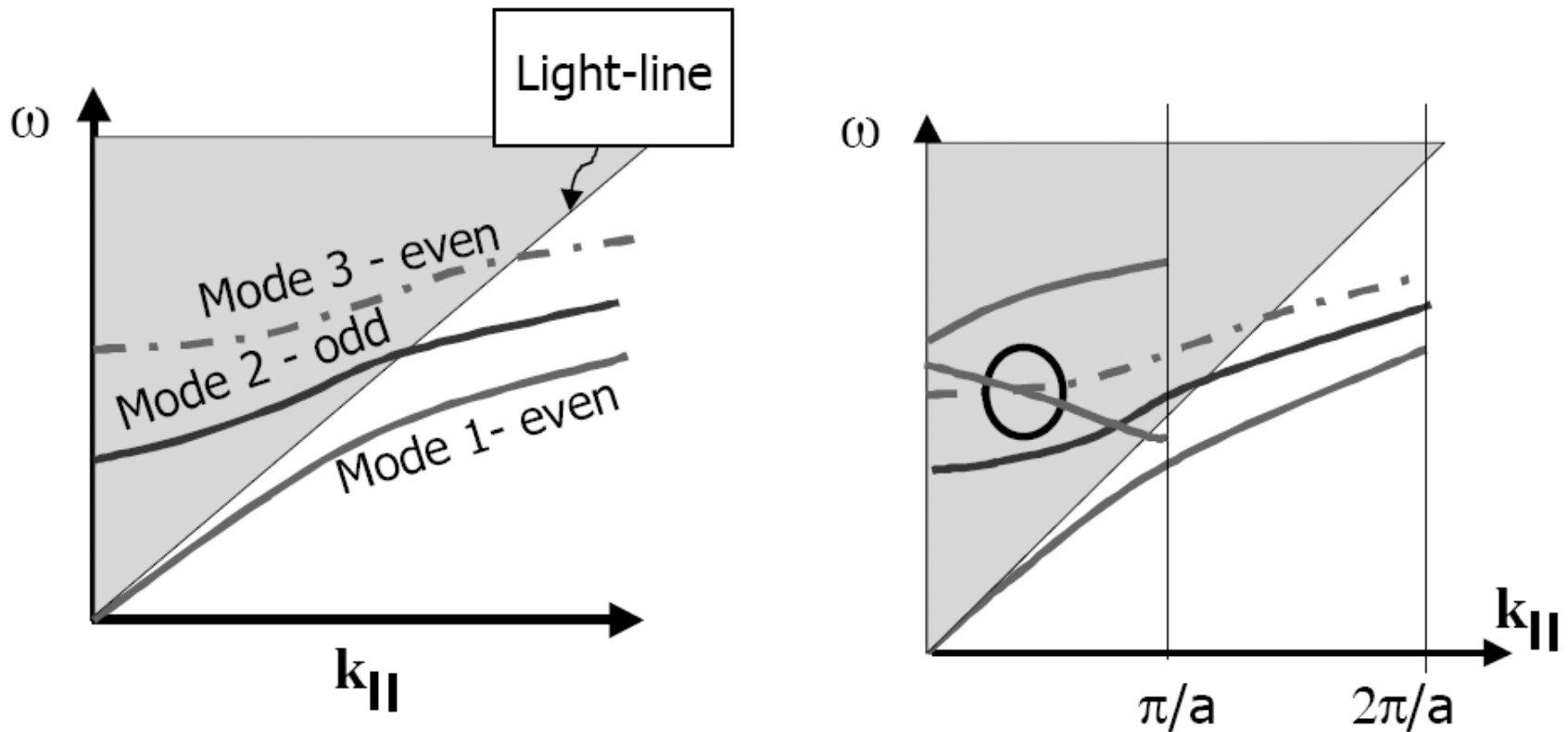


**Figure 1.17.** Coupling between waveguided modes of different orders (here with the same even symmetry: the only crossing point where coupling is possible is shown in the circle)

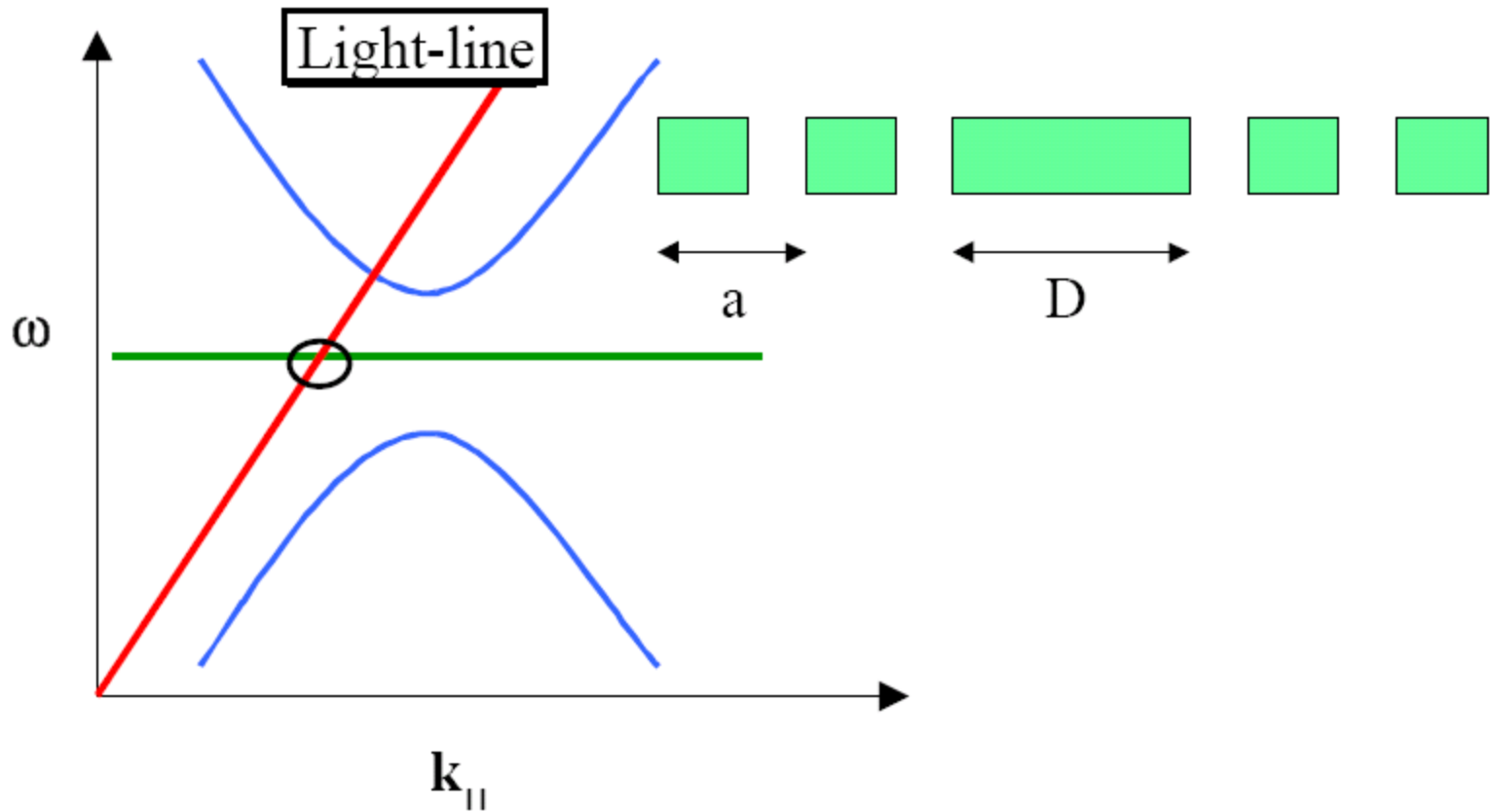
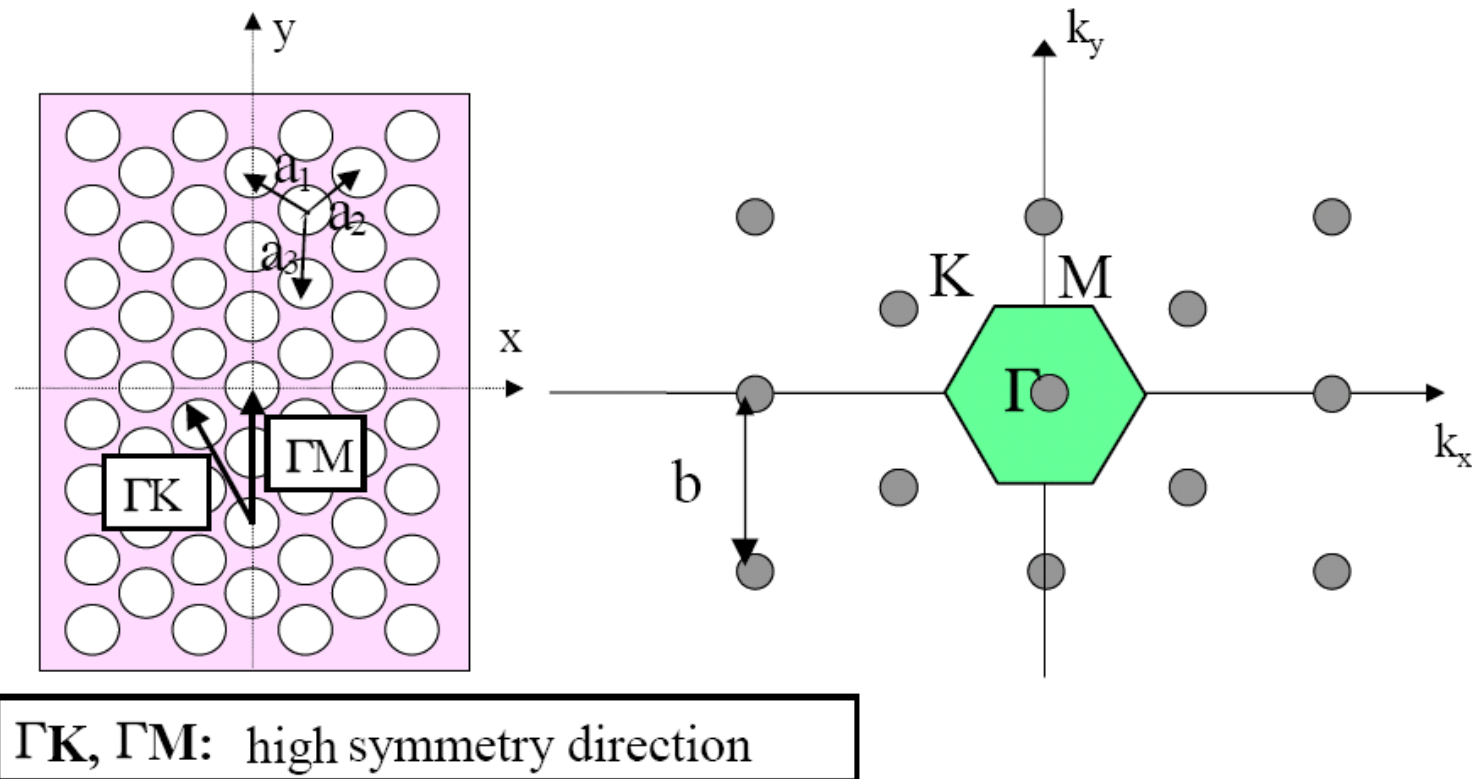


**Figure 1.18. Dispersion characteristics** of a localized **defect** or of an **optical cavity**: there always exist components of the  **$\mathbf{k}$**  vector located above the **light-line**



$\Gamma K, \Gamma M$ : high symmetry direction

**Figure 1.25. Direct and reciprocal triangular lattices.** The two so called  $\Gamma M$  and  $\Gamma K$  high symmetry directions of the crystal are shown.

The **first Brillouin zone** is included in the hexagon drawn in the reciprocal lattice.  $b$  is the module of the **base vector** of the reciprocal lattice.

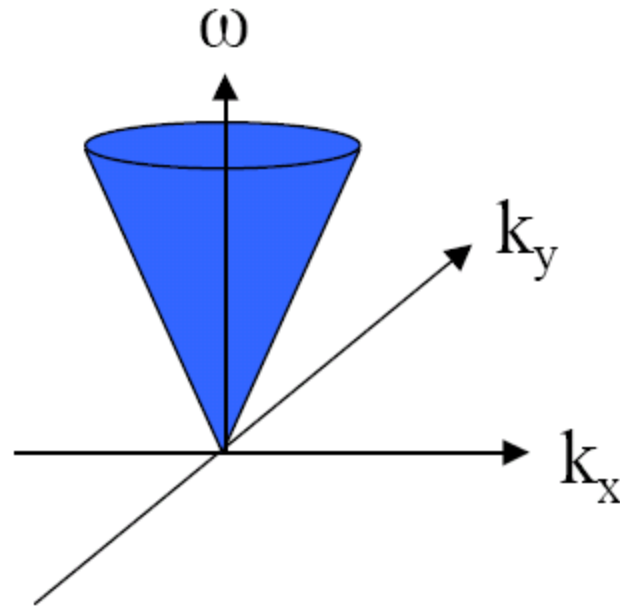
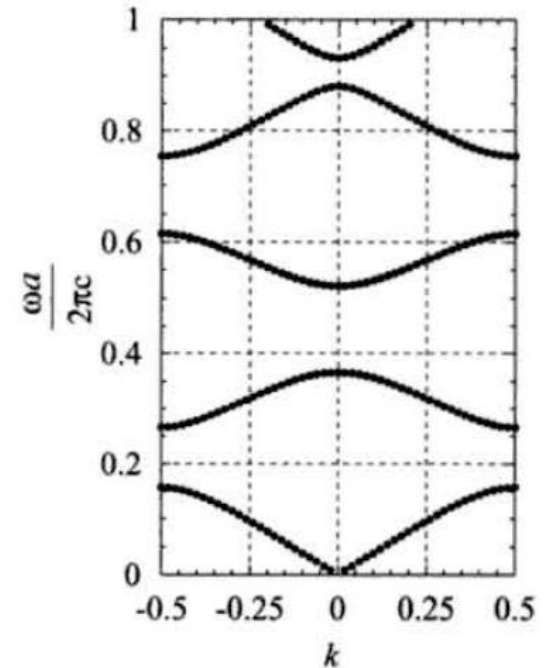


**Figure 1.26.** Conical surface **dispersion** of a two-dimensional **homogenous** medium

## 2.2.4 Slow Group Velocity

- Photons propagate very slowly near the BZ edge due to the slowing down of  $v_g$ .
- The slow  $v_g$  is a feature generally observed in the PBS not only in the BZ edge region, but also in the vicinity of the  $\Gamma$  point, as seen in Fig. 2.2.
- ❑ At  $k = 0$ ,  $v_g$  of each of the bands vanishes.



- In 2D and 3D structures, the band repulsion takes place more often than in 1D PCs and makes the band edges appear frequently inside the BZ.
- Since the states at band edges have vanishing  $v_g$ , we encounter the feature of small  $v_g$  more often in a 2D or 3D PC than in a simple 1D system.

## 2.2.5 Density of States (1)

■ The **density of states (DOS)** of photons,  $\rho(\omega)$ , is defined so that the *number of states*  $N(\omega)$  within the frequency region  $[\omega, \omega + \Delta\omega]$  of an infinitesimally small interval  $\Delta\omega$  is given by

$$N(\omega) = \rho(\omega)\Delta\omega. \quad (2.20)$$

■ Since  $k = 2\pi n/L$ ,  $L$  being the **size** of the **1D** system, number  $N(\omega) =$  **number** of the allowed  $k$  values within the interval  $\Delta k$  determined by the prescribed allowance  $\Delta\omega$ .

➤ From Fig. 2.6, (a **small part** of the **dispersion curve** of a band  $\omega = \omega_n(k)$ ), we have, for an infinitesimal  $\Delta\omega$ ,

$$\Delta\omega = \frac{\partial}{\partial k}\omega_n(k)\Delta k \quad \text{i.e.} \quad \Delta k = \left(\frac{\partial}{\partial k}\omega_n(k)\right)^{-1} \Delta\omega. \quad (2.21)$$

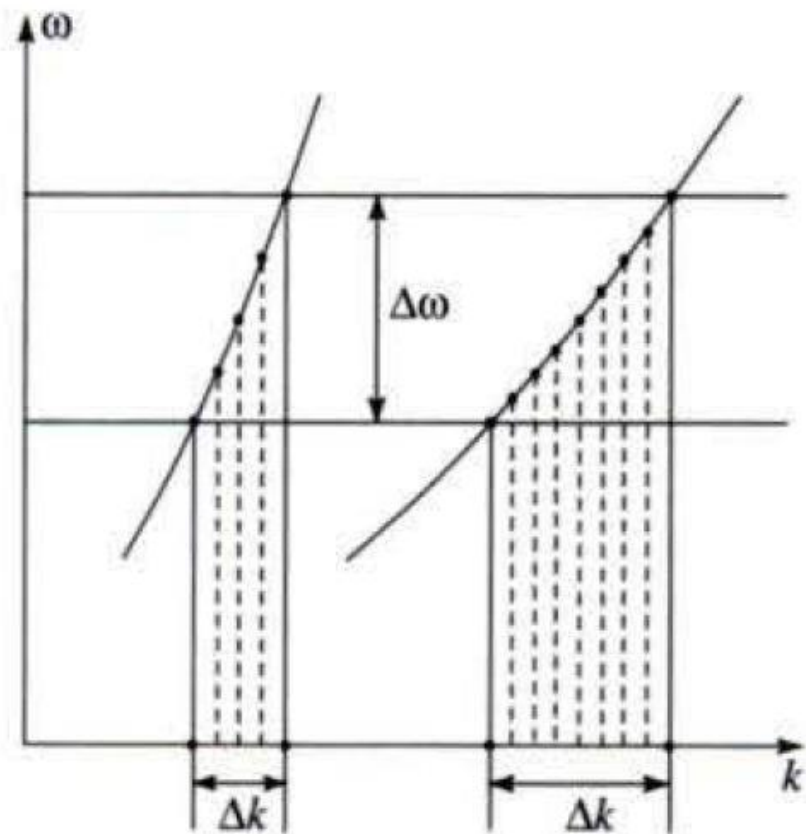
## 2.2.5 Density of States (2)

$$\Delta\omega = \frac{\partial}{\partial k}\omega_n(k)\Delta k \quad \text{i.e.} \quad \Delta k = \left(\frac{\partial}{\partial k}\omega_n(k)\right)^{-1} \Delta\omega.$$

**Fig. 2.6.** DOS versus the curvature of photonic bands.

As a band becomes flatter, the number of the states lying in a given range  $\Delta\omega$  increases.

The spacing between the quantized values of  $k$  is  $2\pi/L$ .



## 2.2.5 Density of States (3)

$$\Delta\omega = \frac{\partial}{\partial k}\omega_n(k)\Delta k \quad \text{i.e.} \quad \Delta k = \left(\frac{\partial}{\partial k}\omega_n(k)\right)^{-1}\Delta\omega. \quad (2.21)$$

Dividing  $\Delta k$  by the spacing  $2\pi/L$  of the quantization yields  $N(\omega)$ . Therefore, it follows that

$$N(\omega) = \rho(\omega)\Delta\omega. \quad \longrightarrow \quad \rho(\omega) = 2\frac{L}{2\pi} \left(\frac{\partial}{\partial k}\omega_n(k)\right)^{-1} \quad (2.22)$$

❖ The **DOS** is thus related to the **inverse of  $v_g$** ,

- The prefactor **2** of being given to take account of the **two polarizations** of photons propagating in the **z** direction of the system shown in Fig. 2.1.
- The allowance  $\Delta k$  for a given  $\Delta\omega$  increases with the **decrease of the curvature** of the **dispersion curve**.

## 2.2.5 Density of States (4)

- The **feature** of **enhanced DOS**: (**group velocity anomaly**)
- For example, the emission probability of **photons** of frequency  $\omega$  from an atom in a **PC** is proportional to  $\rho(\omega)$  and it is **natural** to expect an enhanced light emission from the atoms at the frequency of the **DOS peaks**.
- ❑ The **suppression** of the **DOS**: by the **existence** of the region of **zero DOS** at the **frequency regions** of **PBGs**.
- ❑ In the **PBG regions** we have the **zero emission rate** of photons from an **atom**.
- ❑ **Control** of the **light emission rate** by designing a **PC** to meet one demand and another is one of the **ultimate goals** of the technological application of **PCs**.
- ❑ One reason for the **increasing** demand for high-quality **2D** and **3D systems** is that these characteristics of **group velocity** or **DOS** manifest themselves much more dramatically in a **PC** of **higher dimension**.

## 2.3 Concept of the Light Cone and Example of One-Dimensional Off-Axis Band

- ❖ **Finite PCs**, especially those with **finite thickness** in **one direction** and **infinite** extension in the other **two directions**, are treated repeatedly both theoretically and experimentally.
- ❖ In such a system, called in this book a **slab type PC** or simply a **slab PC**, it is important to consider whether light coming from an outside homogeneous medium can couple to the **inside modes** through the **entrance boundary plane**.
- ❖ If there is a **coupling** the **mode** is called a **leaky mode** because it is not an eigenmode in a strict sense because of its leakage to the outer space through the coupling.
- ❖ The leakage gives a **finite lifetime** to the **mode**.

## 2.3 Concept of the Light Cone and Example of One-Dimensional Off-Axis Band (2)

- A **mode** with wavevector  $\mathbf{k}_1$  and frequency  $\omega_1 = \omega(\mathbf{k}_1)$  of an **outside region** can be **coupled** to one with  $\mathbf{k}_2$  and  $\omega_2$  in a **PC**.
- The spatial dispersion  $\omega_2(\mathbf{k}_2)$  is determined by the **PBS** calculation.
- In this coupling process, the conservation of both energy and  $\mathbf{k}_{\parallel}$ , the wavevector **component parallel** to the **surface**, is established between the two outside fields, such that

$$\omega_1 = \omega_2 \quad \text{and} \quad (\mathbf{k}_1)_{\parallel} = (\mathbf{k}_2)_{\parallel}. \quad (2.23)$$

□ In a **homogeneous** substance of uniform refractive index  $n$  the **light cone** is literally a **cone** in the  $(\omega, \mathbf{k}_{\parallel})$  space defined by the relation:

$$\omega = \frac{c}{n} |\mathbf{k}_{\parallel}|. \quad (2.24)$$

## 2.3 Concept of the Light Cone and Example of One-Dimensional Off-Axis Band (3)

➤ When the region is air with  $n = 1$  and the  $x$  axis is chosen in the direction of  $\mathbf{k}_{\parallel}$ , it holds that

$$\omega = \frac{c}{n} |\mathbf{k}_{\parallel}|. \quad (2.24)$$



$$\omega = ck_x. \quad (2.25)$$

- we often call the light cone as the light line.
- The concept of the light cone was first introduced as early as 1966 by K. L. Kliewer and R. Fuchs, as a concept used to distinguish the leaky and nonleaky modes of a dielectric slab.
- In PCs, this concept was first used in 1982 to examine the photonic modes of a periodic system of finite thickness, a slab PC in the present terminology, by Inoue and Ohtaka.
- The classification between leaky and nonleaky modes is still an important fundamental in the technological application of PCs, because a PC of practical use is always bounded by surfaces, as in slab-type PCs and PC fibers.

## 2.3 Concept of the Light Cone and Example of One-Dimensional Off-Axis Band (4)

➤ We take the boundary to be the **xy plane**, with  $n_1$  for  $z < 0$ , and  $n_2$  for  $z > 0$  with  $n_1 > n_2$ .

➤ The plane of incidence is taken as the **xz plane** with the incident angle of  $\theta_1$

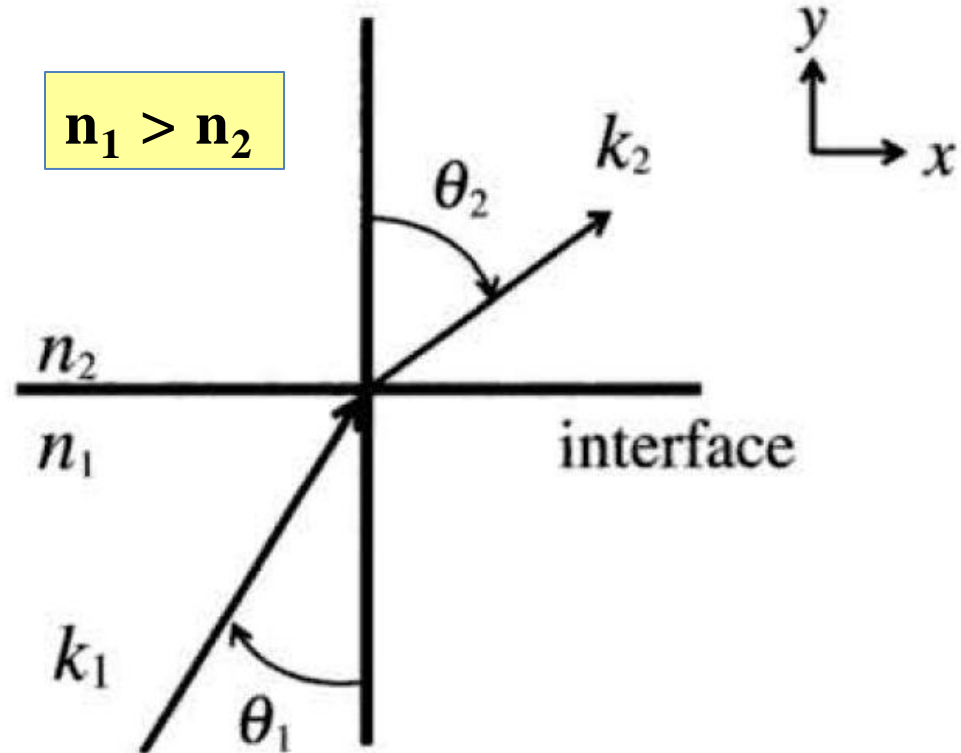


**Fig. 2. 7.** A schematic drawing of **refraction** at a **boundary**

## 2.3 Concept of the Light Cone and Example of One-Dimensional Off-Axis Band (5)

- In Fig. 2.8 we plot two straight lines, one corresponding to a light line (the dispersion relation) in medium 1, and the other in medium 2, respectively, which are expressed as  $\omega = (c / n_i)k_{\parallel}$  with  $i$  referred to 1 or 2.
- These lines just correspond to the cases where light propagates in parallel to the plane in the respective media.
- Suppose in medium 1 one mode on the point B has the same energy  $\omega$  as that on A.

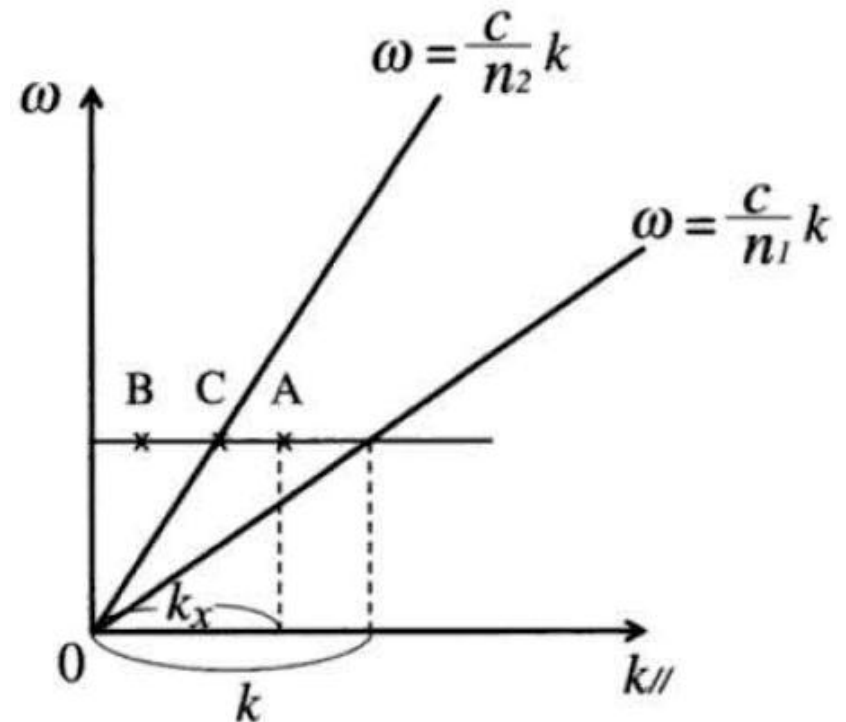


**Fig. 2.8.** A schematic drawing of an example explaining the concept of the light line

## 2.3 Concept of the Light Cone and Example of One-Dimensional Off-Axis Band (6)

- Since the magnitude of  $\mathbf{k}$  of the mode with the  $k_{\parallel}$  component is given by  $\omega = (c/n_1)k$ , the mode is nothing other than one propagating with an angle  $\theta_1$  such that

$$\sin \theta_1 = k_{\parallel}/k = k_x/(c^{-1}n_1\omega). \quad (2.26)$$

- Therefore, all modes in the medium are presented on the **left-hand side** of the line: **any light modes** do not exist on the **right-hand side**.
- The same is also true with medium 2. As a consequence, light that is incident on the boundary plane with wave  $k_{\parallel}$  on the **left-hand side** of medium 2 can go inside medium 2 with the refraction angle  $\theta_2$  given by

$$\sin \theta_2 = k_{\parallel}/k = k_x/(c^{-1}n_2\omega). \quad (2.27)$$

## 2.3 Concept of the Light Cone and Example of One-Dimensional Off-Axis Band (7)

- ❑ On the other hand, light with  $\omega$  and  $k_{\parallel}$  on the **right-hand side** cannot go inside medium 2, but is totally reflected back into medium 1.
- ❑ Therefore, from the above two equations the critical condition is given by the **light line** of medium 2, such that

$$\sin \theta_c = n_2/n_1, \quad (2.28)$$

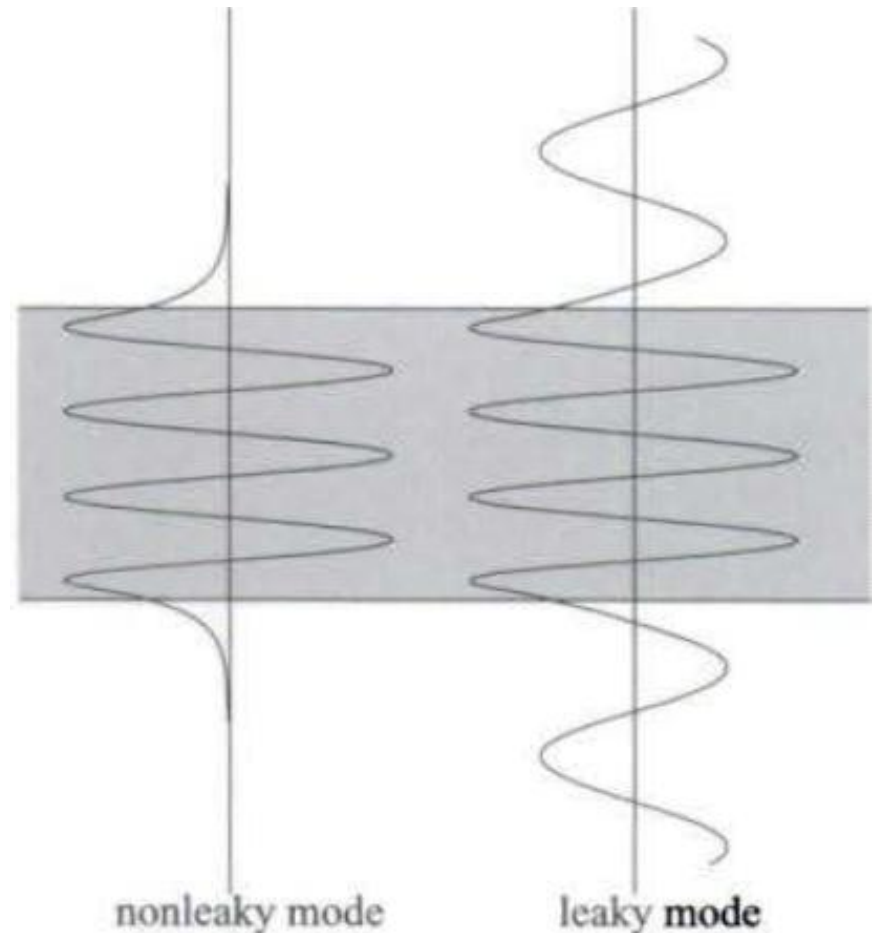
- ❑ In the case of total reflection  $\theta > \theta_c$ , there is no wave propagating at large distances from the boundary in medium 2.
- ❑ However, this does not indicate that the light field vanishes completely in medium 2 for  $z > 0$ .
- ❑ Namely, the evanescent wave can propagate along the boundary plane, the wavevector  $k_x$  of which is expressed as

$$k_x = (n_1/c)\omega \sin \theta_1 = n_1(2\pi/\lambda) \sin \theta_1. \quad (2.29)$$

## 2.3 Concept of the Light Cone and Example of One-Dimensional Off-Axis Band (8)

- ❖ Those features which discriminate the leaky modes and guided modes are shown in Fig. 2.9. See Sects. 3.4 and 4.3 for leaky modes.

**Fig. 2.9.** *Leaky modes* and *guided modes*. The outside fields are those of plane-wave light in the *leaky modes*, while they are *evanescent light* in the *guided modes*.

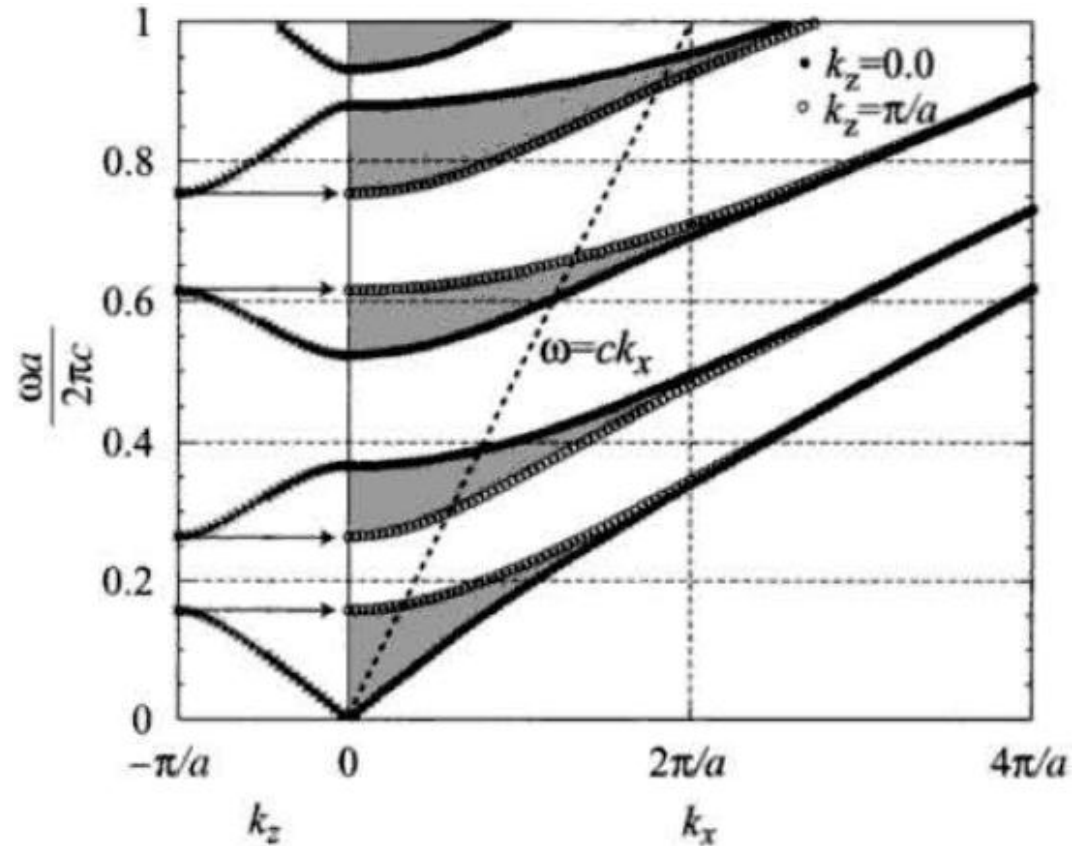


## 2.3 Concept of the Light Cone and Example of One-Dimensional Off-Axis Band (9)

**Fig. 2.10.** The *off-axis modes* in a 1D multiple-Layer film. Two layers **A** and **B** are stacked in the **z** direction.

The *dispersion curves* of the modes of  $k_y = 0$  and polarized in the **y** direction are plotted as functions of  $k_z$ , the boundary of the grey regions being given by the dispersion curve with  $k_z = 0$  or  $k_z = \pi/a$ .

From the points at  $k_x = 0$ , the dispersion curves of the modes of  $k_x = 0$  are drawn on the **left band side** in the **first BZ**;  $0 < k_z < \pi/a$



## 2.3 Concept of the Light Cone and Example of One-Dimensional Off-Axis Band (10)

- As the simplest case, let us consider the *off-axis modes*, i.e., the *mode* with  $k$  not *perpendicular* to the layers or film, in the *multiple-layers* film described.
- The structure considered here is the same as that shown in Fig. 2.1, except that it is not infinitely long but semi-infinite by the presence of the surface.
- Let  $k_x$  be the wavevector component parallel to the surface between the semi-infinite **1D PC** and *air*.
- Now the **guided mode** is specified by  $k_z$  and  $k_x$ .

## 2.3 Concept of the Light Cone and Example of One-Dimensional Off-Axis Band (11)

- ❑ In Fig. 2.10 is shown the *dispersion* of the **TM** (*s-polarized*) *guided modes* of the **1D PC** used in Fig. 2.2.
- ❑ The band structure with  $k_x = 0$  is given on the left as a function of  $k_z$ , which is reproduced from Fig. 2.2.
- ❑ The shaded regions of the *band structure* on the right show the continuum of bands coming from the freedom of the  $k_z$  values.
- ❑ For a *multilayer stack* of *finite* thickness, bounded by a surface parallel to the *xy plane*, only the modes below the *light line*, shown by the dashed line in the figure, are true *guided modes* confined completely inside the PC, while those above the *light line* are actually the *leaky modes* which can *escape* from the **PC** into *air*.

# 2.4 Band Structures of Two- and Three-Dimensional Photonic Crystals

## 2.4.1 Examples of Two-Dimensional Photonic Band

- As for **PBS** in **2D** and **3D PCs**, many examples will be presented in the subsequent chapters in relation to the concrete samples fabricated.
- So, here we show only a few typical examples.
- First, in Fig. 2.11 we show an example of a **2D PC** with the **square lattice** of **dielectric rods** of circular cross-section.
- The first **BZ** corresponding to this structure is also a square lattice, where there exist two high symmetry points, i.e. , **X**  $(a/\pi, 0)$  and **M**  $(a/\pi, a/\pi)$  other than the  **$\Gamma$  point**  $(0, 0)$  (for the naming of these special points, see Appendix A) .

## 2.4.1 Examples of Two-Dimensional Photonic Band (2)

- ❑ The **eigenmodes** for this structure can be specified by the **polarization**. That is, those are classified into the **E(H)-polarized** modes with **E(H) parallel** to the dielectric cylinders, which are called **TM-(TE-) modes**, respectively.
- ❑ It is seen that an ample variety of **PBSs** manifest themselves in the **2D PC** as compared to **1D PCs**.
- ❑ First, each band belongs to the specific irreducible representation of the relevant point group that depends not only on polarization, but also on the **k** direction.
- ❑ For example, if the **mirror plane** is present for the lattice, the respective bands are classified to **even** or **odd** symmetry ones according as **E** becomes symmetric or **anti-symmetric** with respect to the mirror plane.
- ❑ In this case the **odd modes**, or **odd-parity modes** *cannot be coupled to the external plane wave* at normal incidence for **symmetric reasons**.
- ❑ This situation is met frequently in 2D and 3D PCs, although it does not occur in 1D PCs. Those modes are called the "**uncoupled modes**".

## 2.4.1 Examples of Two-Dimensional Photonic Band (3)

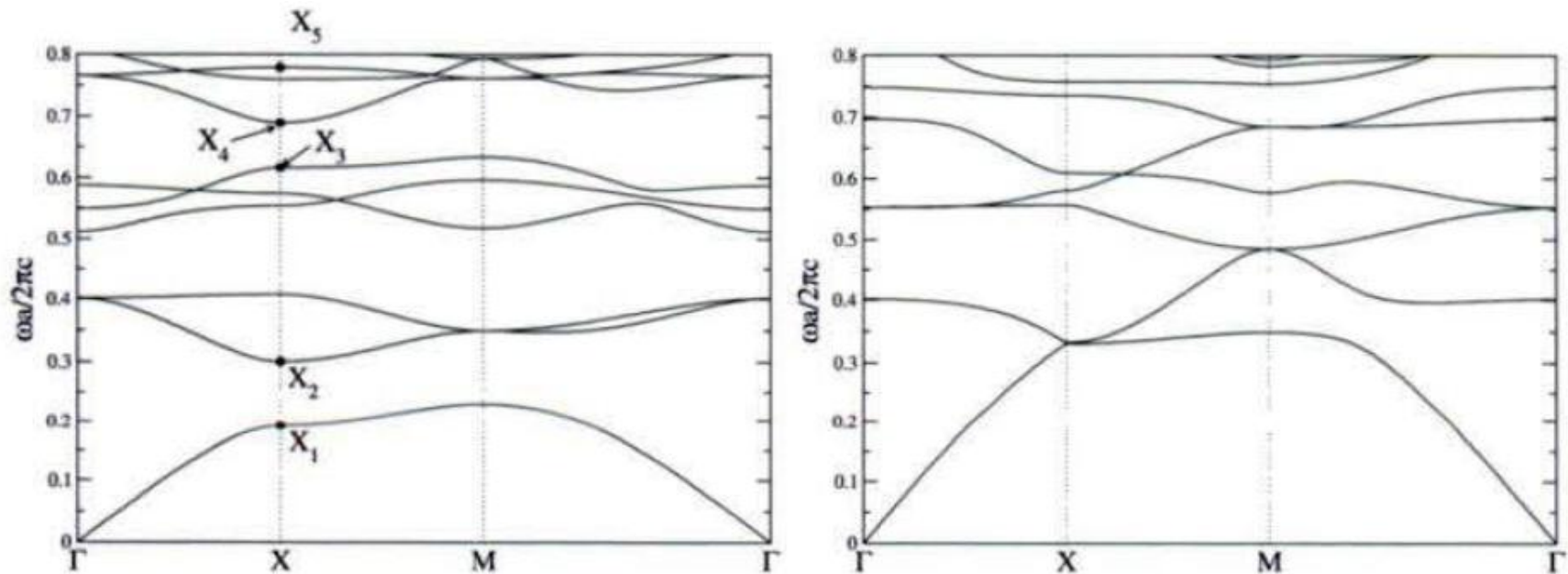


**Fig. 2.11.** Photonic band structure of a 2D PC of cylinders arrayed in a square lattice: TM bands (left) and TE bands (right). The cylinders of  $\epsilon = 12$  (Si) are arrayed in a lattice in the air. The ratio of the radius  $r$  of cylinders to  $a$  is  $r/a = 0.3$ . The states  $X_1$  through  $X_5$  at the X point are examined below

## 2.4.1 Examples of Two-Dimensional Photonic Band (4)

- ❑ Second, there exist three **PBGs** for **TM-modes**, although the PBG common to both polarized modes does not open in this case.
- ❑ Third, there are a **number** of very narrow bands and the  $v_g$ -anomalies occur not only at the zone edge but also in the interior of the first BZ.
- ❑ The appearance of so many narrow bands can be understood by the **empty lattice** test.
- ❑ Figure 2.12 shows the **BS** of the empty-lattice for  $\mathbf{k}_{\parallel}$  along the  $\Gamma$ -X axis, i.e.,  $\mathbf{k}_{\parallel} = (k_x, 0)$  as a function of  $k_x$ .
- ❑ In obtaining it, we drew the dispersion curves for **plane-wave light** of wavevector  $\mathbf{k}_{\parallel} + \mathbf{h}_{\parallel}$

$$\omega = c|\mathbf{k}_{\parallel} + \mathbf{h}_{\parallel}|, \quad (2.30)$$

with  $\mathbf{h}_{\parallel}$  given by

$$\mathbf{h}_{\parallel} = \frac{2\pi}{d}(\pm 1, 0), \frac{2\pi}{d}(0, \pm 0), \frac{2\pi}{d}(\pm 1, \pm 1), \quad (2.31)$$

- ❑ etc. and plotted the curves by putting  $\mathbf{k}_{\parallel} = (k_x, 0)$ .
- ❑ In short, some of them originate from the flat bands in the empty 2D lattice; notice that this is not the case for 1D.

## 2.4.1 Examples of Two-Dimensional Photonic Band (5)

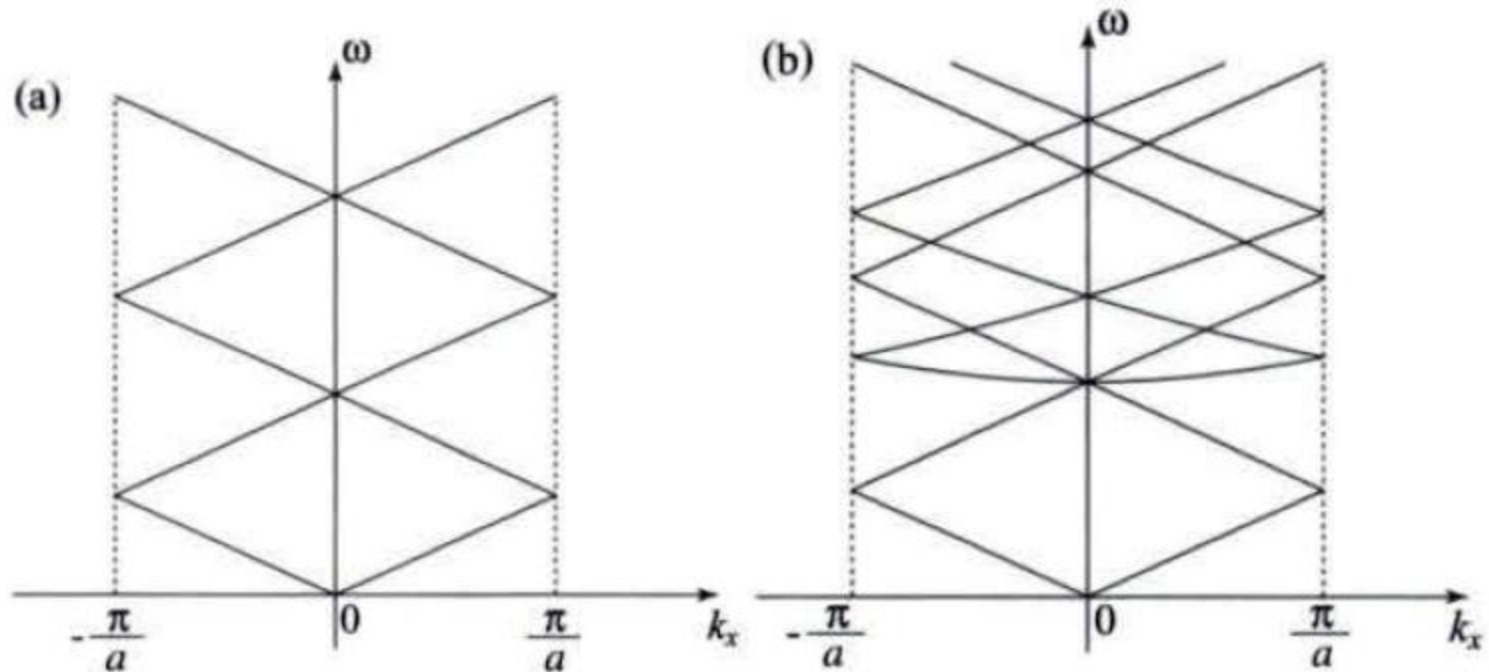


**Fig. 2.12.** Photonic band structure of **empty lattice**: (a) 1D photonic crystal and (b) 2D photonic crystal of square lattice ( $\Gamma$ - X) direction

## 2.4.1 Examples of Two-Dimensional Photonic Band (6)

- Next, the eigenvector of the PB of  $(nk_{\parallel})$  gives the intensity of the electric field,  $|\mathbf{E}_{nk_{\parallel}}(\mathbf{r})|^2$ , associated with that Bloch state.
- Without specifying the normalization of the eigenvectors, Fig. 2.13 shows the intensity of the electric field  $|\mathbf{E}_{nk_{\parallel}}(\mathbf{r})|^2$  in arbitrary units, for the bands  $n = 1$  and  $2$  of Fig. 2.11 at the X point of the first BZ.
- We see the typical feature of a dielectric band in the lower band-state  $X_1$ . The air-band characteristic of the  $X_2$  state is less obvious than the dielectric-band feature of  $X_1$ , however.
- As for the band states with higher energy marked by  $X_3$  to  $X_5$ , a similar plot of intensity reveals that the distinction between the dielectric and air bands becomes progressively vague, since the mixing among the increasing number of plane waves of shorter wavelengths comes in.

## 2.4.1 Examples of Two-Dimensional Photonic Band (7)

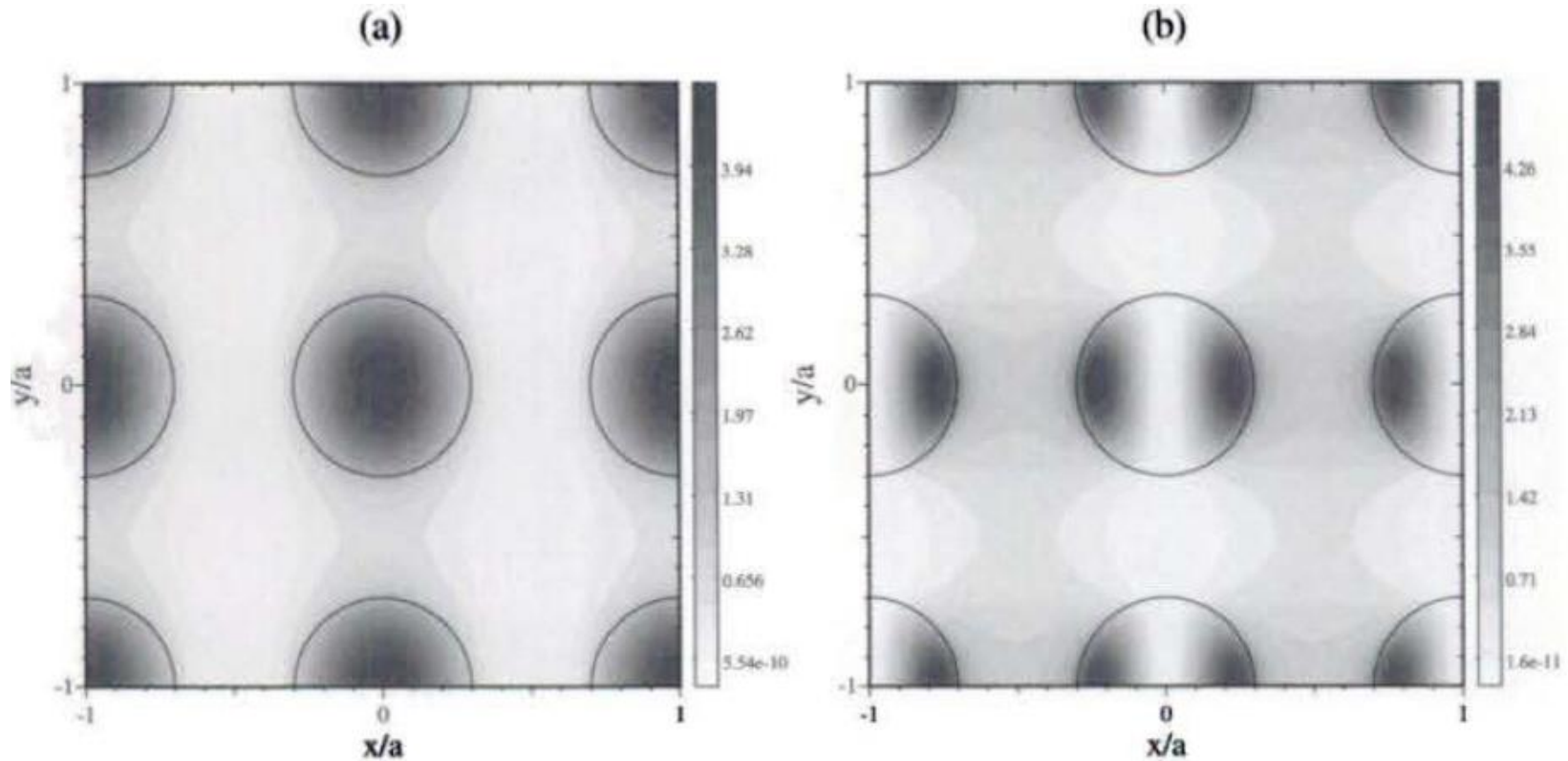


**Fig. 2.13.** Plot of intensity  $|\mathbf{E}(\mathbf{r})|^2$  of the states  $\mathbf{X}_1$  and  $\mathbf{X}_2$  of Fig. 2.11 (arbitrary units). The state  $\mathbf{X}_1$  (left) has a typical dielectric-band character in (a) and band  $\mathbf{X}_2$  (right) shows an air-band character in (b).

## 2.4.1 Examples of Two-Dimensional Photonic Band (8)

- ❖ In Fig. 2.14 is shown another example of a 2D PBS for a triangular lattice of air holes; the 2D BZ corresponding to this structure is shown in Appendix A.
- ❖ It is well-known that the PBS for this structure exhibits a 2D PBG, irrespective of polarization, as is seen in Fig. 2.14, if the difference of  $c$ : between the background material and air (holes) is large enough; in this example the difference is 12 used for Si against 1.
- ❖ Rather unusually, for this structure the gap does not open for E-polarized modes between the lowest (first) and the second-lowest (second) bands, but instead, it does between the higher-energy bands.
- ❖ This is because the first and second bands for E-polarized modes are degenerate at the K point [9].
- ❖ Note that the notation X and J are sometimes used in the literature (also in this book) in place of M and K, respectively.

## 2.4.1 Examples of Two-Dimensional Photonic Band (9)

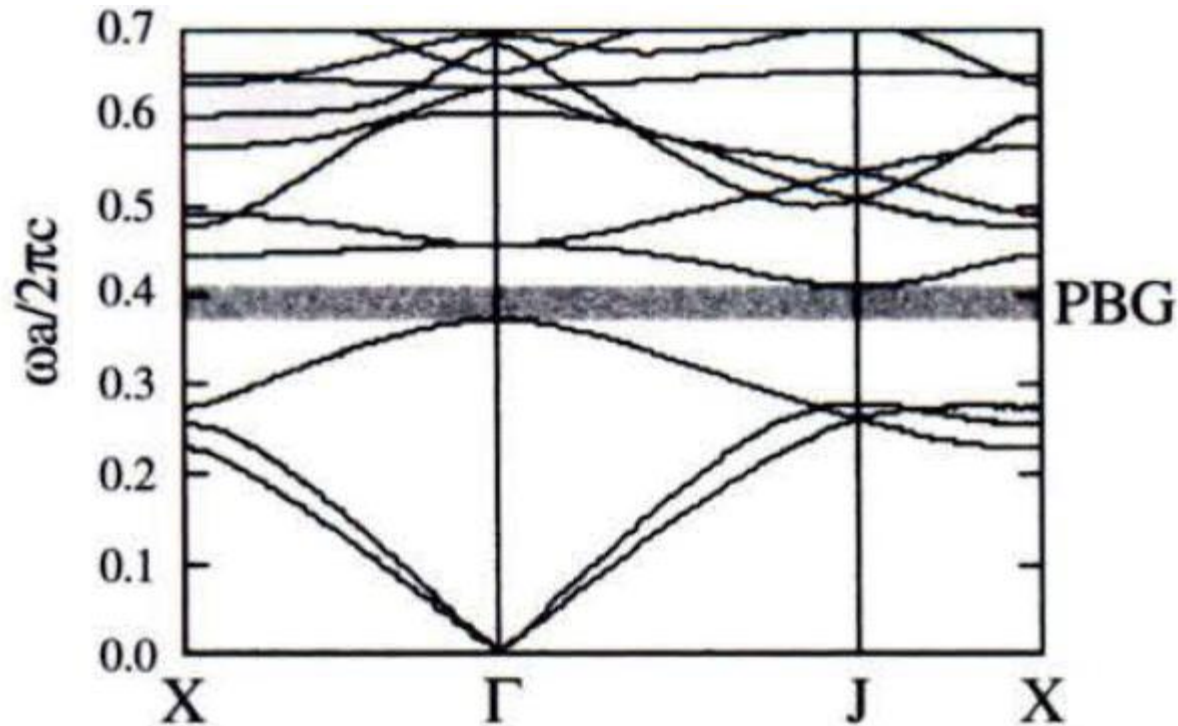


**Fig. 2.14.** An example of 2D photonic band structure with a 2D photonic band gap (a **triangular air-hole structure**)

## 2.4.2 Example of Three-Dimensional Photonic Band

- In Fig. 2.15 is shown an example of a calculated PBS with a full 3D BG in an inverse diamond lattice structure, which is composed of the respective tetra-bonds consisting of air-rods (diameter  $R$ ) in the dielectric of  $\epsilon = 7$  ;  $R/a = 0.1$  is adopted in calculation.
- The shape of the first BZ corresponding to this structure is the face-centered cubic (fcc) lattice, as shown in Appendix A.
- There, it is seen that a full BG opens in all directions.

## 2.4.2 Example of Three-Dimensional Photonic Band (2)

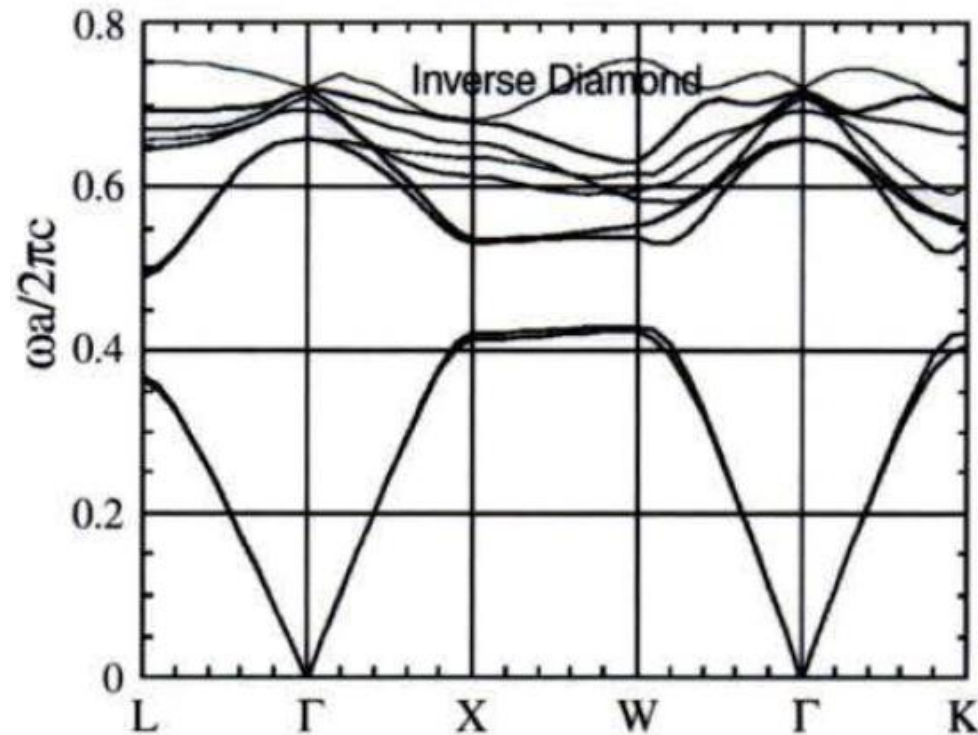


**Fig. 2.15.** An example of 3D photonic band structure with the diamond lattice structure (a sample of inverse diamond structure)

## 2.4.2 Example of Three-Dimensional Photonic Band (3)

- ❖ This PBG corresponds to the well-known **BG of electron** in semiconductors such as **GaAs**, which also has the same **BZ structure** of the **fcc lattice**.
- ❖ As is well known, a **BG** for **GaAs** exists between the valence and conduction bands.
- ❖ Notice that the two band structures (photonic and electronic) resemble each other in many respects, which arises from the resemblance of the two different wave equations.
- ❖ In particular, the existence of the **BG** is common between the two. However, the two differ from each other in some respects.
- ❖ For example, in the photon case one can **excite** any state, while in the electron case one can do so only when the state is **not occupied**.
- ❖ This is because the **photon** is a **boson** governed by **Bose-Einstein** statistics, whereas the **electron** is a **fermion** governed by **Fermi-Dirac** statistics.

## 2.5 How to Experimentally Explore the Band Structure (1)

- ❑ How can we experimentally get information about individual PBSs corresponding to a sample? We explain very briefly the methods below.
- ❑ A simple and reliable method is to observe either the **transmittance (T)** or **reflectance (R)** spectrum, or both in general, as a function of wavelength over a broad range.
- ❑ We need to do so with the propagation direction of incident light varied. This can be done by preparing samples with the surface **normal directed** in several high-symmetry directions such as  **$\Gamma - K$** ,  **$\Gamma - M$** , etc.
- ❑ Therefore it needs rather a troublesome task.
- ❑ However, in some simple cases, information about such spectra only for the particular directions may suffice for the purpose.

## 2.5 How to Experimentally Explore the Band Structure (2)

- ❖ For wavelengths corresponding to a stop band,  $T$  drops very much, whereas  $R$  should be unity, since there exist no photon modes inside in that direction for the external light to couple to, causing it to be reflected completely.
- ❖ However, it is important to note that the reverse is not necessarily true.
- ❖ In other words, observation that the external light is completely or totally reflected over a wavelength range does not necessarily indicate that the range corresponds to a stop band.
- ❖ This is because complete reflection or drastic attenuation of  $T$  occurs for a range of the *uncoupled band*, which has already been explained in the preceding section.
- ❖ Next, to what extent the incident light can couple to an individual band (*coupled band*) of a PC depends on the band itself, or the character of the band.

## 2.5 How to Experimentally Explore the Band Structure (3)

- Finally, in the case of a practical sample  $T$  drops considerably *even* for a coupled band, whenever the quality of the sample under study is not good.
- Also, another problem exists from a practical point of view in that we have to make a measurement by using a sample with **finite periods**, although the PBS is calculated, with a few exceptions, for an **infinitely** long sample.
- If the number of periods of the sample is too small, say, 5 or 10, the correspondence of the **T-spectrum** between the observed and the calculated PBS is not good.
- Except these points, the correspondence is very good between theories and experiments carried out for PCs.
- This is because the calculated PBS is reliable enough due primarily to the lack of photon-photon scattering; in contrast the one-electron approximation is often not good in the electronic case because of the existence of **electron-electron** and **electron-phonon** (vibration) interactions.

## 2.6 Defect Modes (1)

- ❑ Thus far we have described and discussed a regular or completely periodic PC lattice, i.e., one that can be called a **bulk PC**.
- ❑ It is rather easy to technically introduce a **defect** or **disorder** to a particular lattice **point** or **place**, or thereby.
- ❑ As a consequence, this kind of defect causes, generally speaking, breakdown of the symmetry that a PC has originally possessed.
- ❑ An **eigen-mode** due to the **defect** is possible to newly manifest itself in a PBG.
- ❑ As an example of the zero- dimensional (**0D**) or point defect in a **1D** and **2D PC** of air cylinder or dielectric pillar type, we have only to enlarge or lessen the size (diameter), for example, of only one air cylinder at the particular lattice point, as compared to others, or the surrounding ones; the special case of this is to leave it without any air cylinder.
- ❑ Such examples of an enlarged air cylinder and without (missing) air cylinder in a **2D PC** are schematically shown in Fig. 2.16(a).

## 2.6 Defect Modes (2)

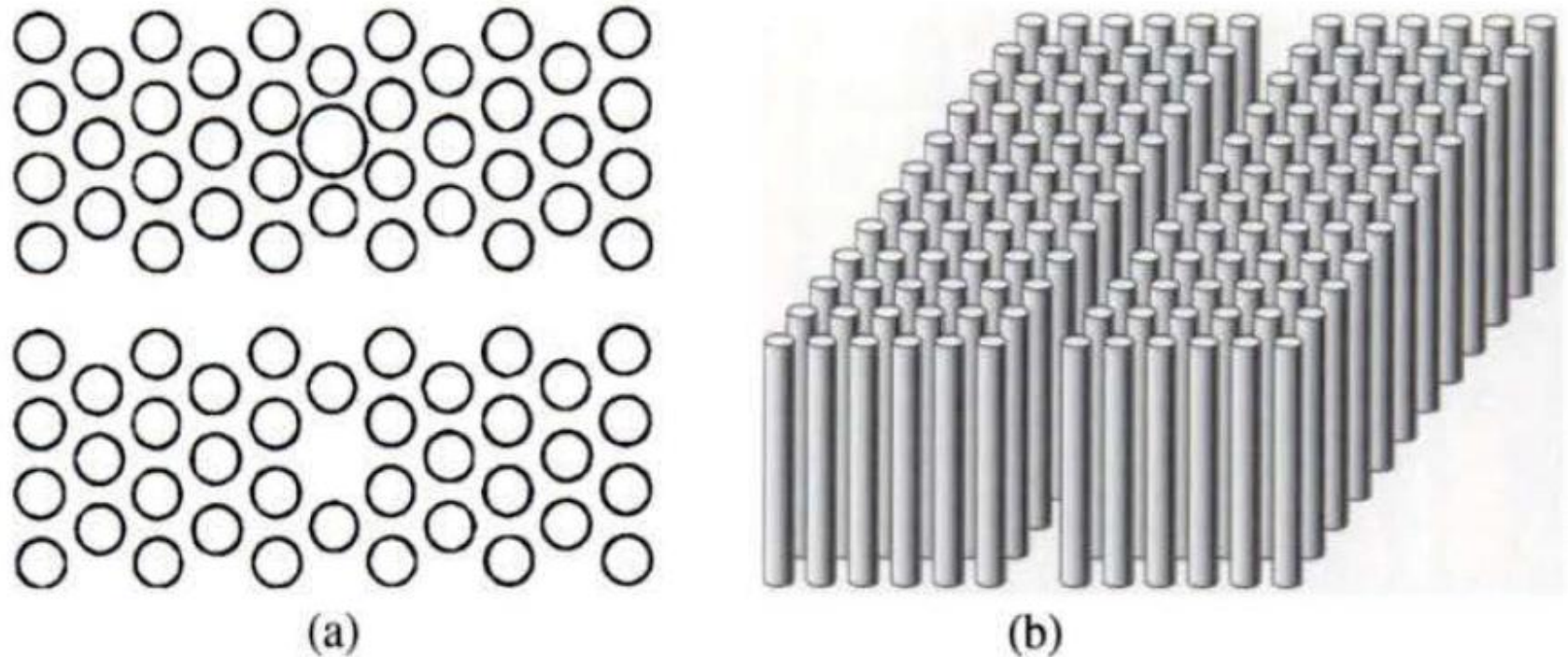


**Fig. 2 .16.** A schematic drawing of examples of the defect modes in a 2D PC. (a) **0D (point)** defect modes (top view) in an array of air holes; the **acceptor (upper)** and **donor (lower)** types, and (b) 1D (line) defect mode in an array of dielectric pillars

## 2.6 Defect Modes (3)

- Another typical example of a **0D defect** in a **1D PC** is to make the period at one lattice position different, as compared to the others.
- This kind of **0D** defect mode corresponds to an impurity state, either the donor or the acceptor state of electrons in a semiconductor; in the case of a different size of air hole introduced, **increasing** (decreasing) the hole size that causes **decrease** (increase) of the dielectric constant there corresponds to an **acceptor** (donor) state for electrons.
- In the case of PCs, in addition to the above-mentioned **0D** defects, **1D** and **2D** types of defects, i.e., line and plane defects, can also be created, which are also important in controlling light or developing unique devices in optoelectronics.
- As an example of a **1D** defect, we create it in a **2D** PC of air cylinders or dielectric pillars by leaving a single line of air cylinder imperforated, or introducing a single line of air, as is schematically shown in Fig. 2.16(b).
- One can also create it in a **3D** PC, e.g., of **air-hole** type in such a way that we leave a single line of holes unopened.
- A typical example of a **2D** defect is such that one lattice plane is left homogeneous in a **3D PC**.

## 2.6 Defect Modes (4)

---

- Now, introducing this kind of defect into the bulk PC creates newly an **eigenmode** or an **eigen band** called a **defect-mode** or a **defect-band**, generally speaking, in a BG: the point-defect modes in a **BG** correspond to the impurity modes in the electronic case, or in semiconductor.
- It is noted that the line defect band exhibits a  *$\omega - k$  dispersion* along the direction, which will be repeatedly discussed in later chapters, e.g., in Chaps. 7, 11 and 12.

# 2.7 Common and Fundamental Features of Photonic Band Structure

---

In Sec. 2.2, based on an example we have already explained several basic features of the 1D PBS. This section is devoted to newly summarize the unique and outstanding features that 2D and 3D PCs generally exhibit. As will be shown in the next section, PCs are very well suited for controlling light, i.e., both the radiation field and light propagation characteristics. This important potential is primarily based on one or two of the following features:

1. Existence of photonic band gap
2. Existence of defect or local mode
3. Anomalous group velocity
4. Remarkable polarization dependence
5. Manifestation of peculiar band
6. Others

Let us make a survey of each item one by one, taking into account how to utilize those for observing new phenomena and developing PC-based devices.

# 2.7.1 Existence of Photonic Band Gap (1)

- A question arises as to in what cases a full PBG opens.
- There exist rather severe requisites to satisfy for a 3D PC to possess such a PBG. Those are related to the crystalline structure, the difference of the relevant E-values, and the occupation ratio  $f$  between two constituted materials. It is generally recognized that the diamond lattice structure is the best in order to obtain a full PBG as well as a wide gap. This is primarily because the shape of the first BZ is close to the sphere (most sphere like) as compared to other structures such as the simple or body-centered cubic one.
- This feature is advantageous to opening a gap between the second- and third-lowest bands. However, this is not the case for the higher bands. In fact, it is known that a full PBG opens for such higher bands in a face-centered cubic lattice [12] and even in the simple cubic lattice [13].
- In Fig. 2.17 is shown the BS. It is remarked that in this case the conditions regarding the contrast of  $\epsilon$  as well as  $f$  are relatively severe, and more importantly, the relative gap width  $L/w$  is not large enough, where  $L$ ,  $w$  and  $\omega_0$  refer to the width and the center frequency of the gap, respectively.

## 2.7.1 Existence of Photonic Band Gap (2)

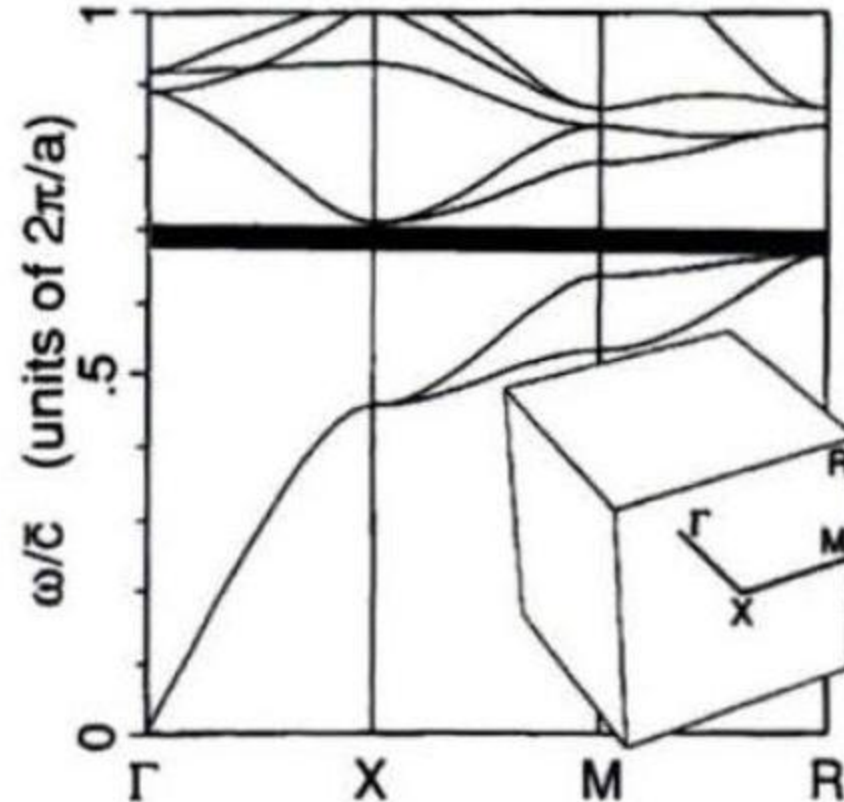


**Fig. 2.17.** Another example of 30 photonic band structure for square-shaped air rods in a simple cubic lattice:  $\epsilon_b = 13$ ,  $\epsilon_a = 1$  and  $f = 0.83$ , quoted from [13] by courtesy of Professor J. W. Haus

## 2.7.1 Existence of Photonic Band Gap (3)

---

In contrast, it is rather easier to design a sample with a 2D PBG. In both 2D and 3D cases, in a given crystal structure there is, as far as the structure is adequate, a trend that as the ratio of  $\epsilon_A / \epsilon_B$  is larger, a gap is easier to open, where A and B refer to the two constituted materials.

Here we mention how the term PBG is used. It is better to use the terminology "PBG" only for the complete BG already defined. However, it is true that in some cases people in this field use this term even for the case where there is no such BG, or for an incomplete BG: in physics we have used the term of "stop band" for the latter case. Therefore, in order to avoid confusion, we will use hereafter in this book the term "a full PBG" only in a strict sense.

## 2.7.1 Existence of Photonic Band Gap (4)

In this connection, it is important to note that the situation for a 2D PC slab (a sort of quasi-3D PC) is substantially different from the 2D case; it differs also from the 3D case. Namely, because of the existence of the so-called light cone, already explained in Sect. 2.3, any complete BG should not exist within the 2D slab plane: inside the light cone there are, in principle, continuous extended states (not eigenmodes for the PC slab) for arbitrary wavelength. However, we define a 2D PBG even for this case in such a manner that any guided modes (eigenmodes) of the PC slab are missing over a specific energy range in all 2D directions. This will be presented in more detail in Chap. 6.

Now we mention briefly a few examples of direct application of a full BG. First, unique mirrors for complete reflection without loss can evidently be developed, and in fact, some of those have already been commercially available. Next, it can be utilized for controlling the radiation from matter. For example, an emission from atoms placed inside a PC with a full 3D PBG is inhibited when the photon energy is in an energy range of the PBG. This is because the emission probability is zero, since the DOS for photons within the PBG vanishes; the probability in the radiative process is proportional to the DOS. In order to completely suppress the spontaneous emission from atoms one needs to use a 3D PC with a full 3D PBG.

## 2.7.1 Existence of Photonic Band Gap (5)

---

On the other hand, whether the probability of the spontaneous emission becomes enhanced or not at the edge of a full 3D PBG as compared to that in the homogeneous case with the same effective refractive index is not clear. First of all, the radiative lifetime of an oscillating electric dipole placed inside a PC depends not only on the DOS per unit volume, but also on a few other factors. Namely, it depends on whether the dipole is placed in the constituent material with the higher or lower dielectric constant, and on the oscillation direction, i.e., the orientation of polarization.

## 2.7.1 Existence of Photonic Band Gap (6)

---

Furthermore, the probability of the spontaneous emission depends also on in what direction the emission is observed. So, generally speaking, the probability is possible to be enhanced or reduced in the case of a 3D PC. In particular, the probability is expected to be enhanced to some extent around the band edge depending on the case. The same is also true in the case for a 2D BG. In contrast, there exists the case where the probability should increase in a divergent way at the edge of a BG for a 1D PC. This problem in quantum electrodynamics will be discussed in a bit more detail in Chap. 10.

It is important to note that in many cases we can control the radiation field and light propagation properties with use of a 3D PC without such a full PBG, except for some cases including complete suppression of the spontaneous emission described above. For the same reason, 2D PCs also serve for controlling light. Thus, we should be able to develop a variety of devices by using such a PC, irrespective of the 2D or 3D nature.

## 2.7.2 Existence of Defect or Local Modes (1)

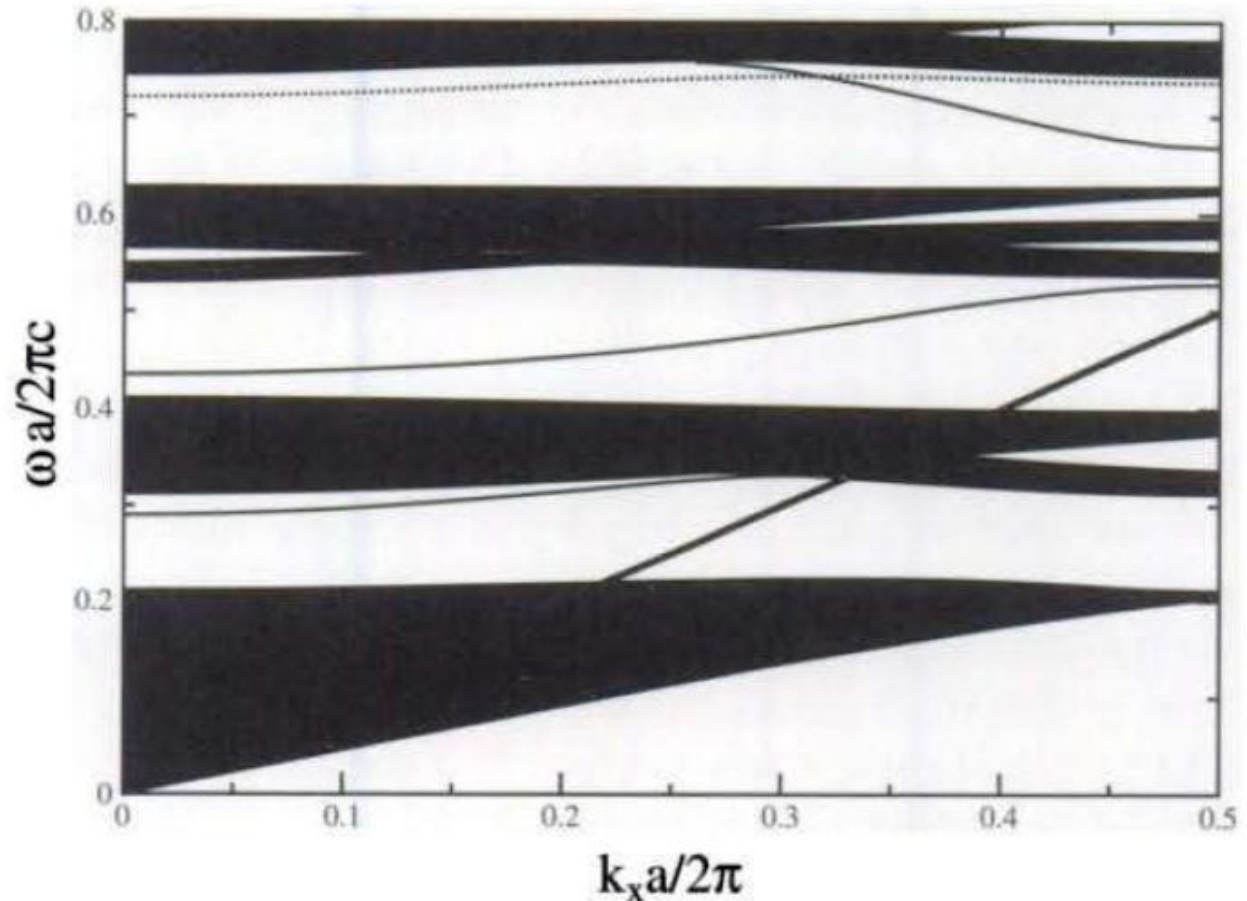
The existence of the defect modes has already been stated in the preceding section, with special emphasis placed on how to create those. Here we discuss the physical property to some extent. By exciting this mode, light can be localized around the defect or the region with disorder. Therefore, the defect mode is localized both energetically and spatially, as stated in Sect. 2.6. In the OD case, where the mode is localized in a small spatial region, the mode does not have a definite wavevector  $k$  *because of the uncertainty principle concerning  $k$  versus  $r$  in quantum mechanics. This feature is very similar to that for the impurity state, i.e., the donor or acceptor state, for electrons in a BG, as already described in Sect. 2.6. In contrast to the point-defect (OD) case, the line-defect mode shows a particular dispersion in a BG. Namely, with  $k_1$  defined to be the wavevector in the direction along the line defect, the mode frequency  $w$  varies with  $kt$  in the gap.*

## 2.7.2 Existence of Defect or Local Modes (2)

An example of such a line defect mode in a 2D PC of a triangular array of dielectric pillars in air is shown in Fig. 2.18. The present line-defect is composed of one row of missing pillars along the  $\Gamma$  - K direction (adopted as the X axis) so the band structure for the TM-modes with  $k_t$  parallel to the x axis is shown in Fig. 2.18 with  $k_x$  used for  $k_d$ ; the x and y axes are taken within the 2D plane, whereas the z axis is in the direction of the pillar axis. In Fig. 2.18 the hatched areas are obtained by projecting all the bands  $\omega_n(k_x, k_y)$  in the first BZ onto the  $\omega$  -  $k_x$  plane, these bands being often called the slab bands in the literature. The dispersion relation of the line-defect bands are shown by the thin curves between the hatched regions.

## 2.7.2 Existence of Defect or Local Modes (3)

**Fig. 2.18.** Dispersion feature of the line-defect modes in a 2D PC of dielectric pillars of  $c = 12$  arrayed in the triangular lattice in free space. The electric fields of the defect modes and the projected bands are both polarized in directions of the pillar axis. The thick line is the air light-line  $\omega = ck$ :



## 2.7.2 Existence of Defect or Local Modes (4)

---

The solid and dotted curves show the even and odd defect modes, with the parity of the defect modes defined according as  $E_z$  is symmetric and antisymmetric with respect to the mirror plane ( $xz$  plane). The parameters are  $r/a = 0.3$  and  $c = 12$ ,  $r$  being the radius of pillars and  $a$  the lattice constant. Needless to say, the defect modes shown here provide the light propagation along the  $x$  direction.

## 2.7.2 Existence of Defect or Local Modes (5)

Let us consider in a bit more detail the significance of localization of the electric (magnetic) field due to the defect or disorder mode. That light without real mass can be localized, e.g., around a particular point in space, just like the case for an electron, is very important from the physical point of view; this phenomenon of light localization should be discriminated from the case where light is confined with use of the specific boundaries such as metal walls. Anyway, the OD defect mode can be utilized, for example, either as an extremely small optical cavity, or as a very narrow band-pass filter. On the other hand, the line-defect mode already described is considered to serve as a novel type of waveguide without any propagation loss even at an abruptly bent corner [16, 17]. This type of waveguide, called a PC waveguide, becomes at present very important [18] (see also the literature in Chaps. 11 and 12, where this PC waveguide is discussed in more detail).

## 2.7.3 Anomalous Group Velocity (1)

Both  $v_g$  and group velocity dispersion (GVD) play an important role in light propagation. Theoretically,  $v_g$  is given by the slope ( $dw/dk$ ) of a band, where  $k$  refers to the magnitude of  $k$  in the relevant direction of light propagation; usually, the magnitude of  $v_g$  is estimated for the band calculated for an infinitely long or large sample. In general, there appear in a PC a lot of band portions or positions where the band slope is flat, which makes  $v_g$  anomalous. At the band edge  $v_g$  should become extremely small without fail [19-21]. Such a flat energy position is also encountered at both the maximum and minimum points of the lower and upper bands resulting from an anti-crossing between two bands with the same symmetry, as already described in Sect. 2.2. A photon with such a small  $v_g$  at those positions is sometimes called a heavy photon in analogy with the heavy electron (see Sect. 3.6)

## 2.7.3 Anomalous Group Velocity (2)

It is also important to note that very frequently a relatively flat band, i.e., a very small  $v_g$ , is encountered in a 2D and 3D PC [21, 22], as the origin of the flat band was already explained in Sect. 2.2. Moreover, there are many bands where  $v_g$  becomes negative. We call all these anomalous group velocity. That  $v_g$  is very small indicates that the electric field strength becomes very large there; the fact that the Poynting vector must be constant everywhere requires that  $E^2$  becomes large for a small  $v_g$ . This fact is very important, since the effective interaction length between light and matter becomes short enough by using such a small  $v_g$ . That is, the radiation signal in many physical phenomena such as second-harmonic generation (SHG) can be very effectively generated from a PC, or equivalently, can be greatly enhanced in a PC sample as compared to a conventional sample with the same length [23- 25]. This also makes sense in the case of a laser, because the threshold value of electrical current or fluence for pumping can be greatly reduced by utilizing a small  $v_g$  [26- 29].

## 2.7.3 Anomalous Group Velocity (3)

---

As for the GVD in PCs, it is very large in general; the line-defect mode already described can be designed to also have a large GVD [30]. This is because the GVD in a PC originating from the periodicity can be artificially altered unlike the GVD in a transparent wavelength region of a material which *is governed by the dispersion of the refractive index, i.e., essentially by the intrinsic absorption.*

## 2.7.4 Remarkable Polarization Dependence (1)

---

Characteristically, in many PCs propagation of light incident from the outside through a sample is markedly influenced or governed by the polarization; of course this property arises from the fact that the PBS under study is polarization-dependent. This property applies generally to all PCs irrespective of the dimension, with the exception of on-axis light propagation in a 1D multilayer film; notice that even in this case the BS for the off axis propagation already described in Sect. 2.3 becomes polarization-dependent. If we focus on only the guided modes, the polarization dependence is particularly remarkable even around the first BG in 2D PCs and 2D PC slabs. In contrast, it is, generally speaking, less remarkable for 3D PCs. This is particularly true with the diamond-lattice structure, as compared to the cases for a simple cubic lattice (113) and a face-centered cubic lattice [31].

## 2.7.4 Remarkable Polarization Dependence (2)

---

As a consequence, a unique polarizer can be developed by utilizing a pair of specific bands for two different polarized light beams with the same frequency. A simple example is the case that there exists a stop band for one polarized light beam, while there is a band for the other. Even for the case where there are respective bands for two different polarizations, the magnitude of  $v_9$  should be generally significantly different from each other, except for an accidental case. Based on this feature, a different kind of polarizer can also be developed for an ultra-fast light pulse. Namely, such a pulse is easily split into two, depending on the polarization, after passing through a thin PC [132]. Thus, utilizing time delay together with a gate, one can pick up only a pulse with the desired polarization.

## 2.7.5 Manifestation of Peculiar Bands (1)

There are a variety of peculiar PBs showing anomalous or singular points [33]. Roughly speaking, such an anomaly is likely to manifest itself in the higher energy region where many bands run. It has already been revealed that well established crystalline optics no longer apply to the case of a PC; it is again remarked that a PC is not a natural crystal, but an artificially fabricated one. Consequently, we need to introduce new crystalline optics or concepts, called "photonic crystal optics" to cover the case of PCs. Let us show the simplest example below to understand this fact. It is well known that all crystals except for quasi-crystals in an optical region are classified into three cases, i.e. , uniform crystalline, uni-axial crystalline, and biaxial crystalline, corresponding, respectively, to

$$\epsilon_1 = \epsilon_2 = \epsilon_3, \quad \epsilon_1 = \epsilon_2 \neq \epsilon_3, \quad \epsilon_1 \neq \epsilon_2 \neq \epsilon_3, \quad (2.32)$$

where  $\epsilon_1$ ,  $\epsilon_2$ , and  $\epsilon_3$  refer to the dielectric constants along the optic axes. This classification no longer applies to a PC; for detail, see Sect. 4.7.

## 2.7.5 Manifestation of Peculiar Bands (2)

First of all, Snell's law of refraction does not generally apply to the boundary plane between a PC and a normal material. Anyway, propagation characteristics of light at such a singular point are very complicated on one hand, and unique on the other hand. As a result, several peculiar phenomena have already been found, such that the phenomenon of tri-refringence occurs (34), and  $v_g$  cannot be determined uniquely [33]. From the view point of application, the superprism phenomenon (35) is very important, which manifests itself at a specific equi-energy surface portion of a particular band. There, the propagation direction of light going inside a PC through the interface varies remarkably with small change of wavelength of the incident light. This phenomenon showing anomalously large dispersion of wavelength versus incident angle enables one to develop, in principle, a new type of device of wavelength dispersion with the size much reduced as compared to the conventional ones.

## 2.7.5 Manifestation of Peculiar Bands (3)

---

Similarly, a phenomenon called super collimation has also been found in a PC (36): a light wave with a finite cross-section can propagate in a PC with the size unchanged, which occurs also at a specific band.

When we formally apply Snell's law for an anomalous band or at wavelengths exhibiting negative  $v_g$ ,  $n$  becomes negative. Utilizing this sort of band, one can create a superlens (an ideal lens in a sense) [37]. However, in order to implement this kind of lens,  $v_g$  must be negative over a wide range of wavelengths for all incident angles. This requisite is very severe, but it is reported that this is still possible (38).

## 2.8 Application of Photonic Crystals (1)

---

Because of their unique properties, PCs are very attractive for exploring new physical phenomena and developing novel and important devices in the field of optoelectronics as well. In this survey, we focus rather on the latter. Concerning the latter, some simple passive optical components such as narrow-band filters, unique polarizers and wonderful super-prisms described in the preceding section have already been developed, and some others are expected to be developed one after another from now on and to be commercially available in the near future.

Let us mention some applications below, other than the above-mentioned simple components. First, we describe applications to nonlinear optical phenomena, or the related active components. By utilizing the unique PBS in either 2D or 3D PCs, the phase-matching (PM) can be easily fulfilled at several wavelengths; it is well known that the PM is very important in nonlinear optical phenomena, particularly in coherent phenomena such as second harmonic generation (SHG).

## 2.8 Application of Photonic Crystals (2)

Furthermore, a novel type of PM can be expected to be utilized in PCs including 1D in this case [39). That is, an umklapp process can be utilized, since the reciprocal vector  $q$  is on the same order in magnitude with the relevant wave-vectors involved in the phenomenon under study; it has already been proved that this process is useful in SHG for a 1D periodic system (1D PC). We describe below the SHG case as an example,

$$\mathbf{k}_s = 2\mathbf{k}_i \pm \mathbf{q}, \quad \omega_s = 2\omega_i, \quad (2.33)$$

where  $k_i$  and  $k_s$ , and  $\omega_i$  and  $\omega_s$  are the wave-vectors, and angular frequencies of incident (fundamental) and second-harmonic light waves, respectively.

## 2.8 Application of Photonic Crystals (3)

As for other active components, several kinds of unique 2D PC lasers have been successfully developed. Those are categorized into two types, i.e. , one [40] utilizing an ultra-small PC cavity, or a point defect already mentioned in Sect. 2.7.2, and the other [26-28] utilizing a small  $v_g$ . *So, some of them may be in practical use soon.* The first type of laser has prominent characteristic of being extremely small. The latter type of lasers include a sort of vertically emitted laser excited by an electrical current [27], a 2D laser with a low threshold, and an small size of laser. The same is also true with a light emitter embedded in a PC slab, where the extraction efficiency of light has already been demonstrated to be greatly improved compared to the record obtained thus far [41].

## 2.8 Application of Photonic Crystals (4)

---

PC fibers, both of PBG type and refractive-index confined, are also very attractive. The latter type of optical fiber is considered to be an ideal transmission line for light, so it will be in practical use, depending on the case. Independently of the above application, it has been demonstrated that light can be generated over an extremely broad range of wavelengths by illuminating the latter type, Le., with the silica core in the central portion, using an ultra-short, i.e., sub-picosecond light pulse. This phenomenon should be utilized as a white light source for spectroscopic use (42].

## 2.8 Application of Photonic Crystals (5)

---

Next, the Smith- Purcell radiation with use of a PC is also attractive and important, because it has the possibility of developing a compact wavelength tunable coherent light source in a range from far- to near-infrared; the Smith Purcell effect is such that coherent light is radiated due to interaction between high-speed traveling charged particles and a periodic system such as a grating. It has been predicted theoretically [43] and has already been verified very recently that use of a PC instead of a grating enables one to observe the radiation much more efficiently than the previous cases (44). This topic is treated in Sect. 10.7.

## 2.8 Application of Photonic Crystals (6)

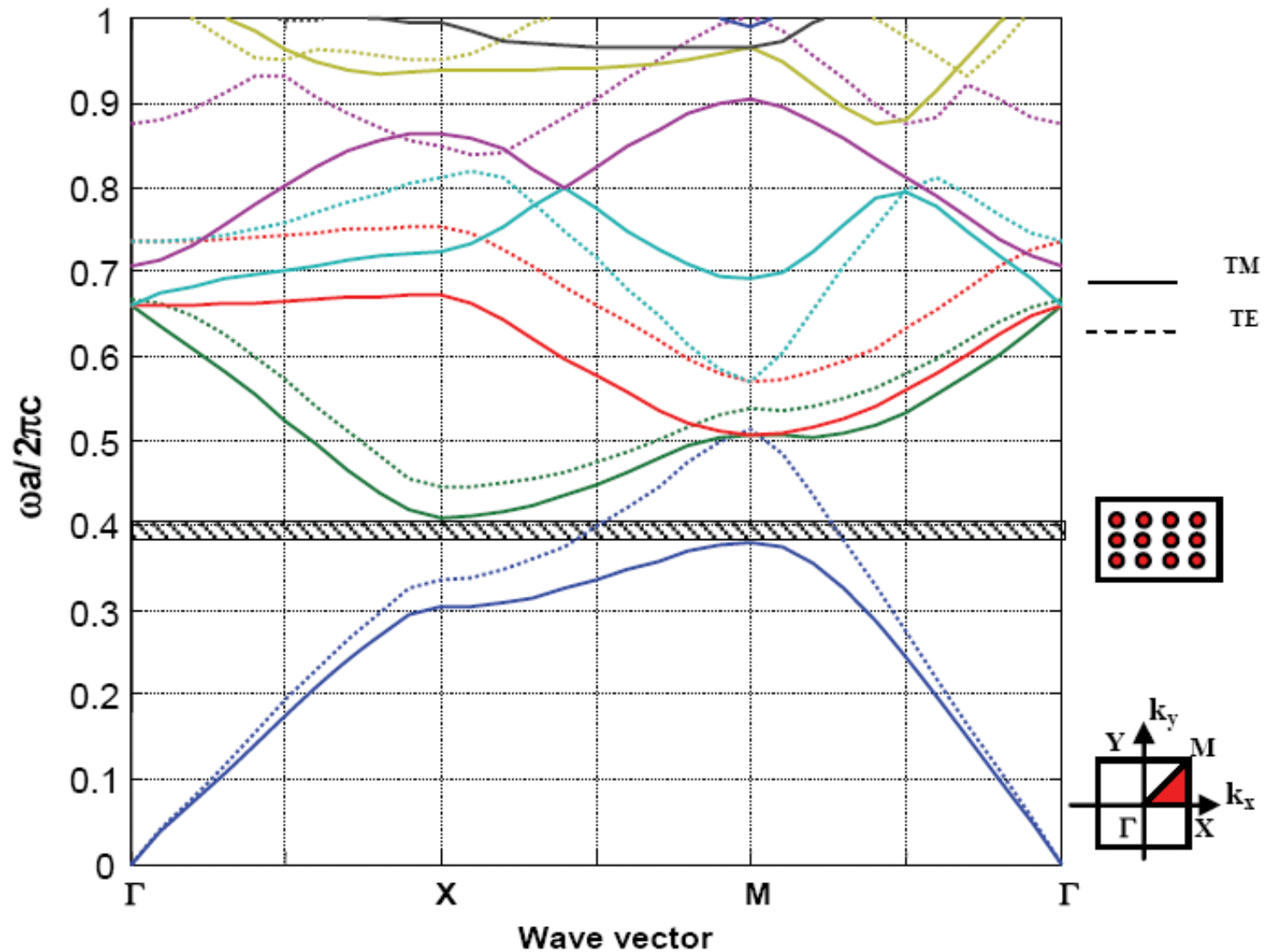
Finally, we would like to mention one of the most important applications of a PC, i.e., development of ultra-fast and ultra-compact integrated light circuits; such a development is crucially important for future telecommunications. It is considered that such a circuit based on PCs may be developed in the future. For this purpose, there are a few key components to be developed. One is a novel type of light waveguide that is capable of being bent sharply. This can be achieved by utilizing a PC-based waveguide. The PC-based waveguide is constituted of line defect modes in a 2D or 3D PC; in the case of a 2D PC of triangular lattice of air hole type, for example, a line-defect is produced by leaving a single line of air holes imperforated along one of six equivalent  $\Gamma - K$  directions. Importantly, in the PC-based waveguide the light wave is confined due to the PBG, so that it can be bent sharply without any propagation loss, while light is confined by total reflection in the lateral plane in the conventional dielectric waveguide; in the case of PC-slab waveguides, the vertical confinement of light is achieved by the total reflection. Another is the compact de-multiplexer, but we do not go into details here (see Chaps. 11 and 12).

## 2.8 Application of Photonic Crystals (7)

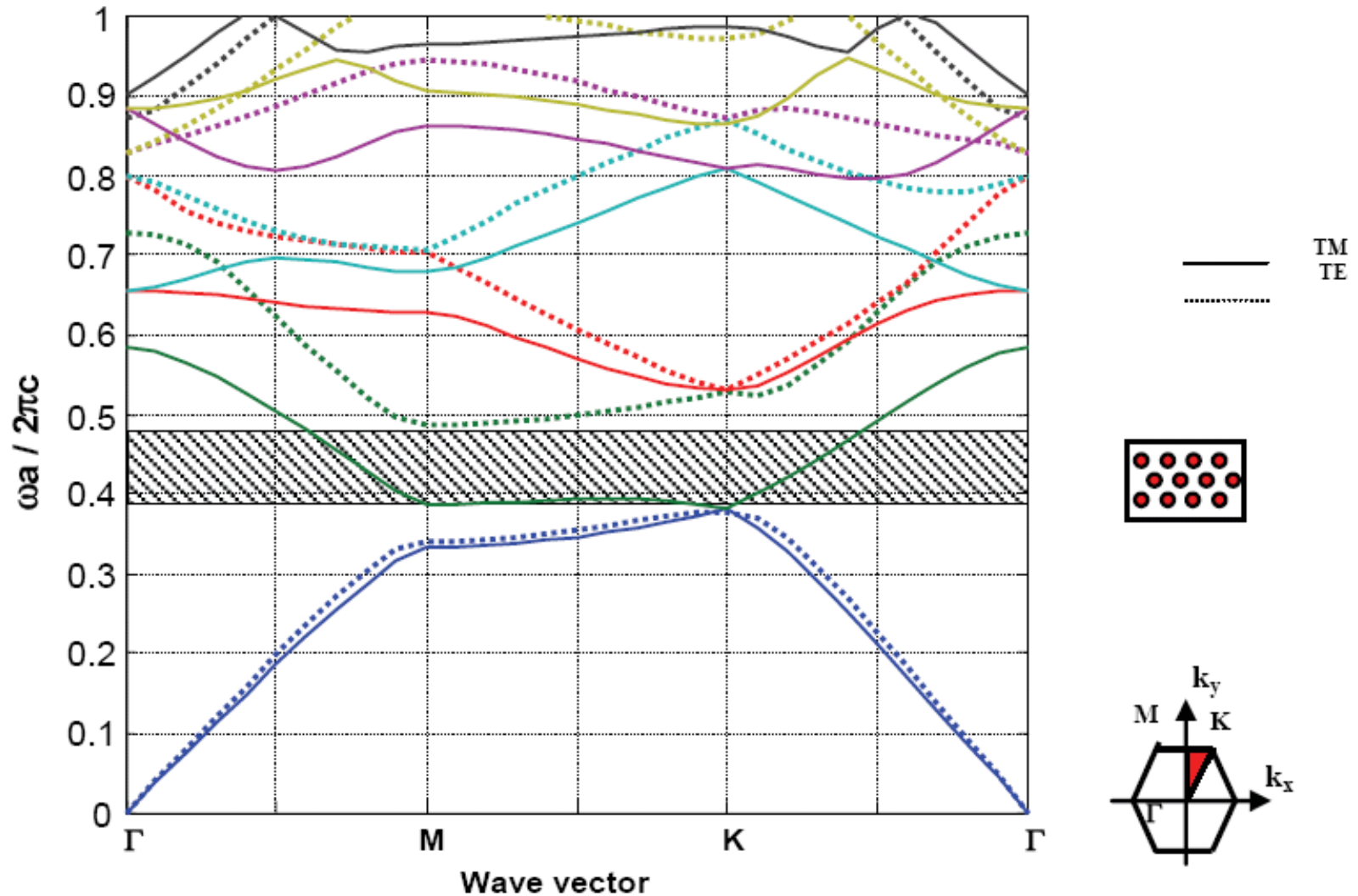
---

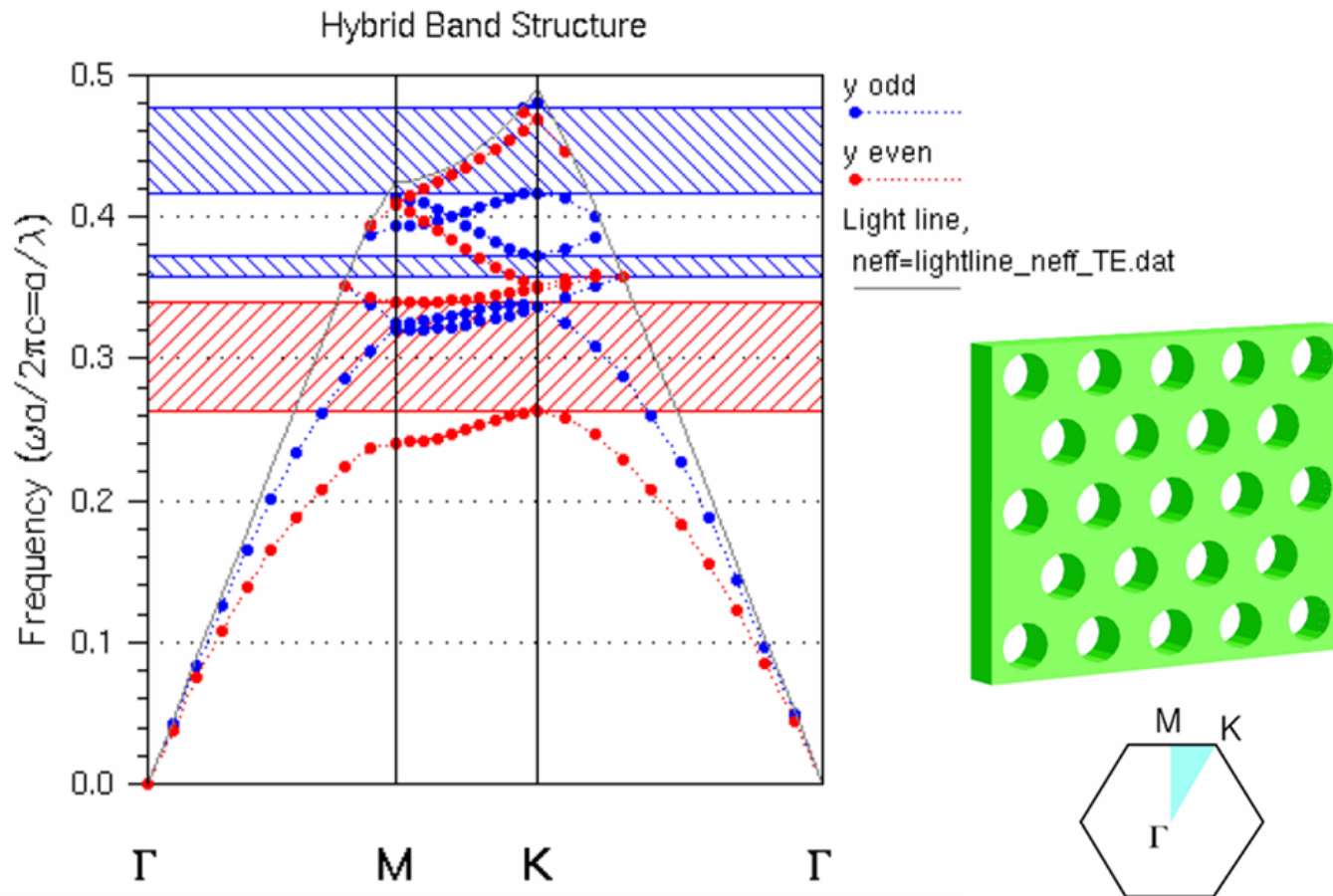
From the practical point of view, the planar type of integrated circuit, in particular, made of PC slabs, has the advantage over the 3D type. This is because it is much easier to fabricate the planar type than a 3D one. So, up until now many investigations have been devoted to this type, both theoretically and experimentally. As a result, it may be possible to finally develop such an ultra-small integrated circuit. The details will be presented also in Chap. 12.

# Structure PBG of 2D grating in LiNbO<sub>3</sub>: A square lattice



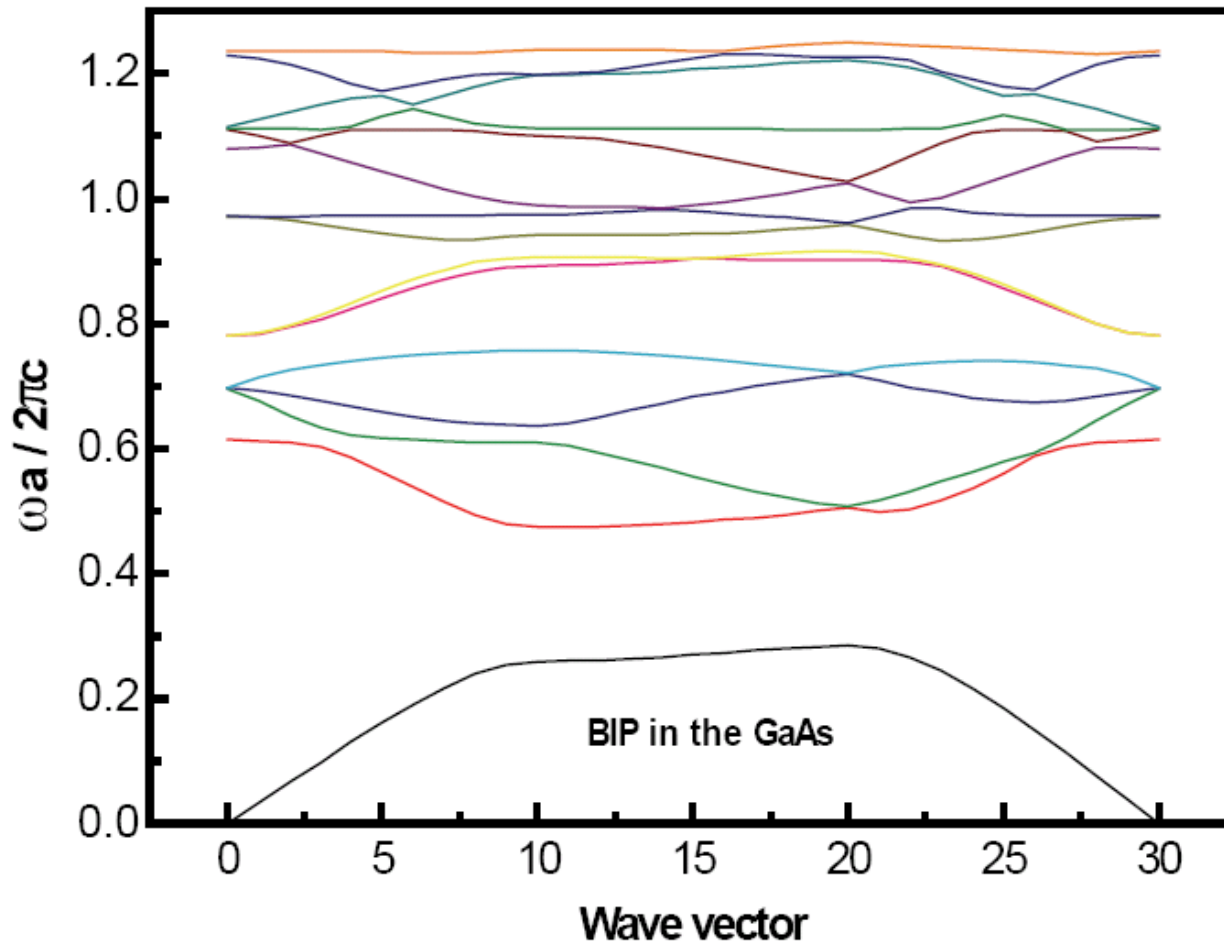
# Structure PBG of 2D grating in LiNbO<sub>3</sub>: A triangular lattice

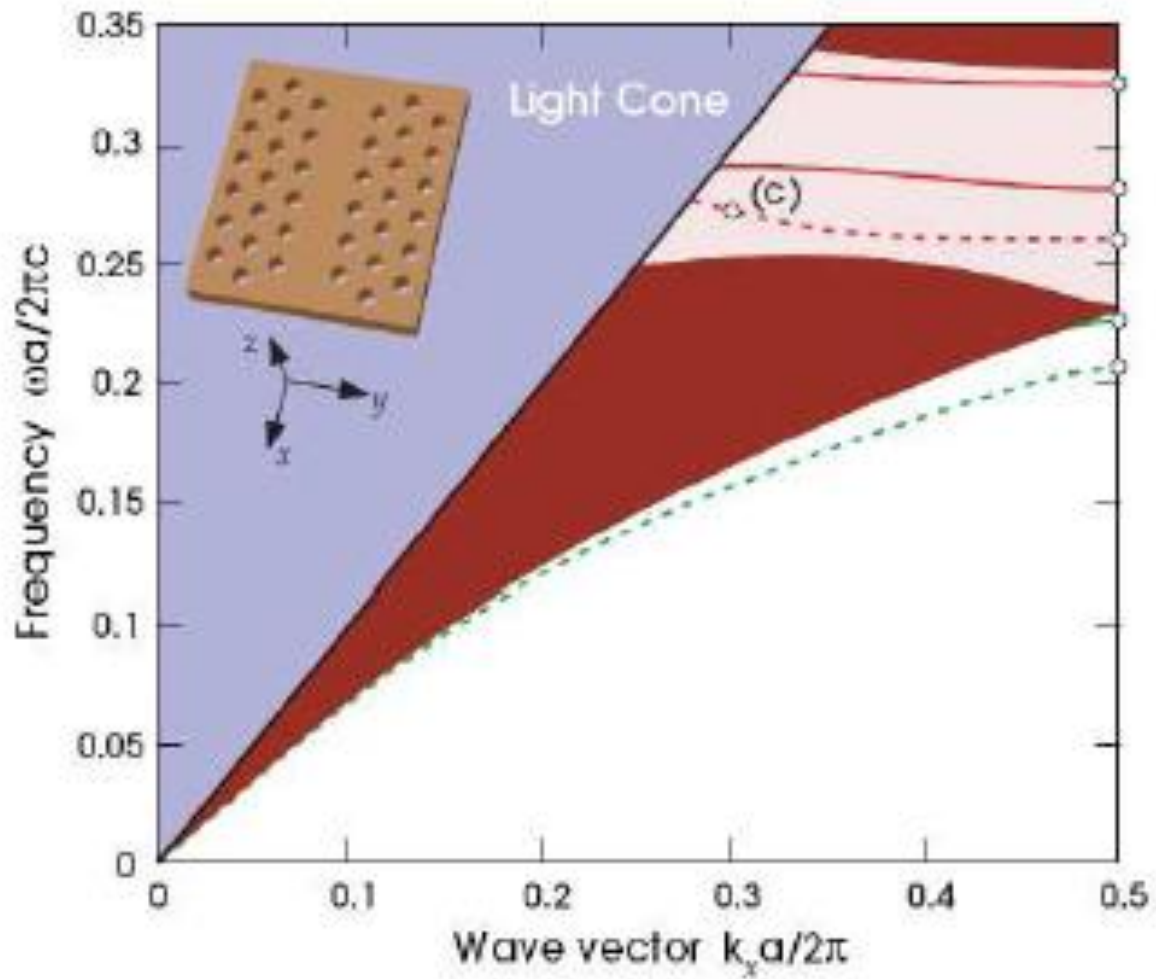




(الف) شمای ساده ای از ساختار بلور فوتونی تیغه ای حفره‌ای با شبکه مثلثی (شکل بالا) به همراه یاخته واحد آن فضای وارون (شکل پایین).  
 (ب) ساختار نوار مربوط به بلور تیغه ای شکل (الف) برای قطبش TE (نقاط قرمز) و قطبش TM (نقاط آبی).

PBG structures of **pillar triangular** lattice of  
**GaAs**,  $\epsilon_0 = 12.6$  in **air** (**TE mode**)





ساختار باند موجبر بلور فوتونی تیغه‌ای سیلیکونی با نقص خطی در جهت  $\Gamma$  K

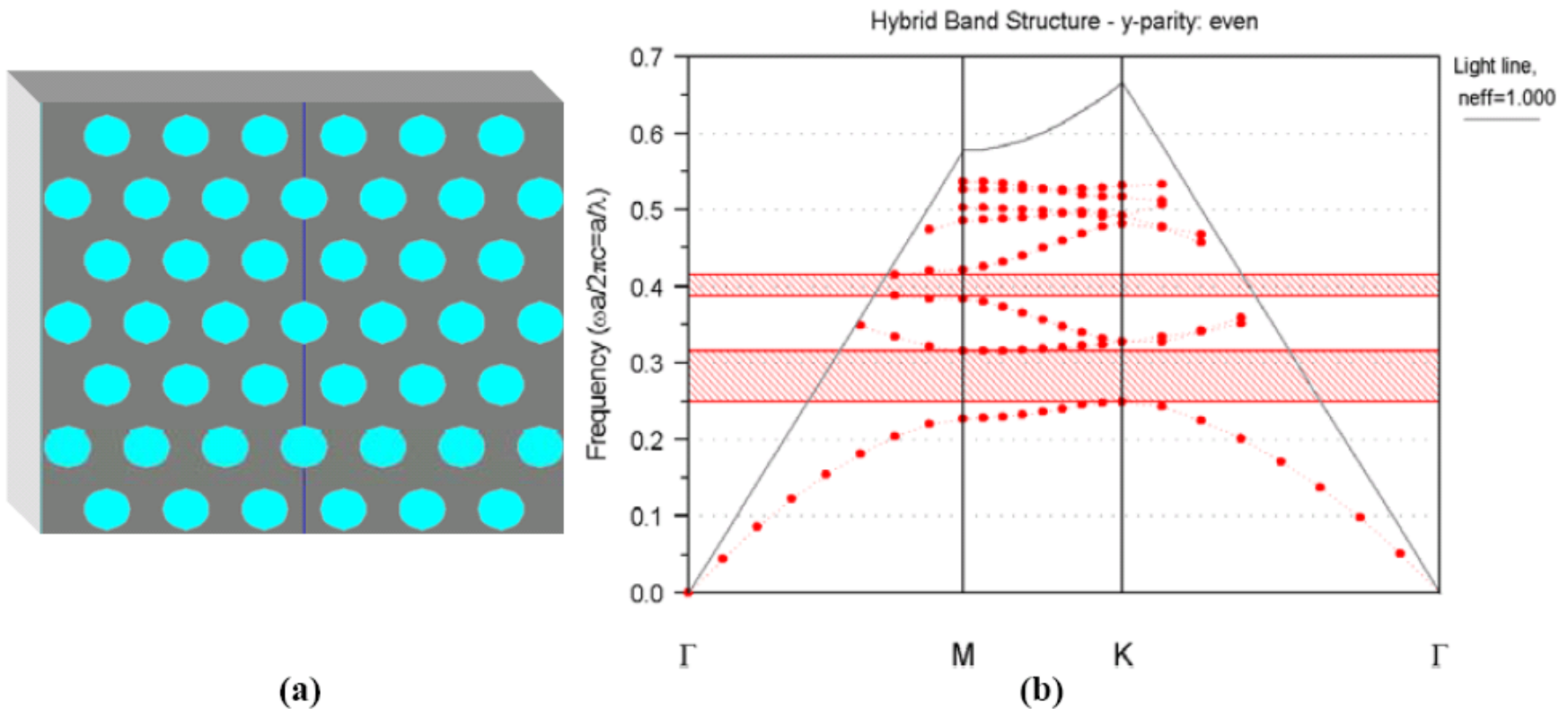
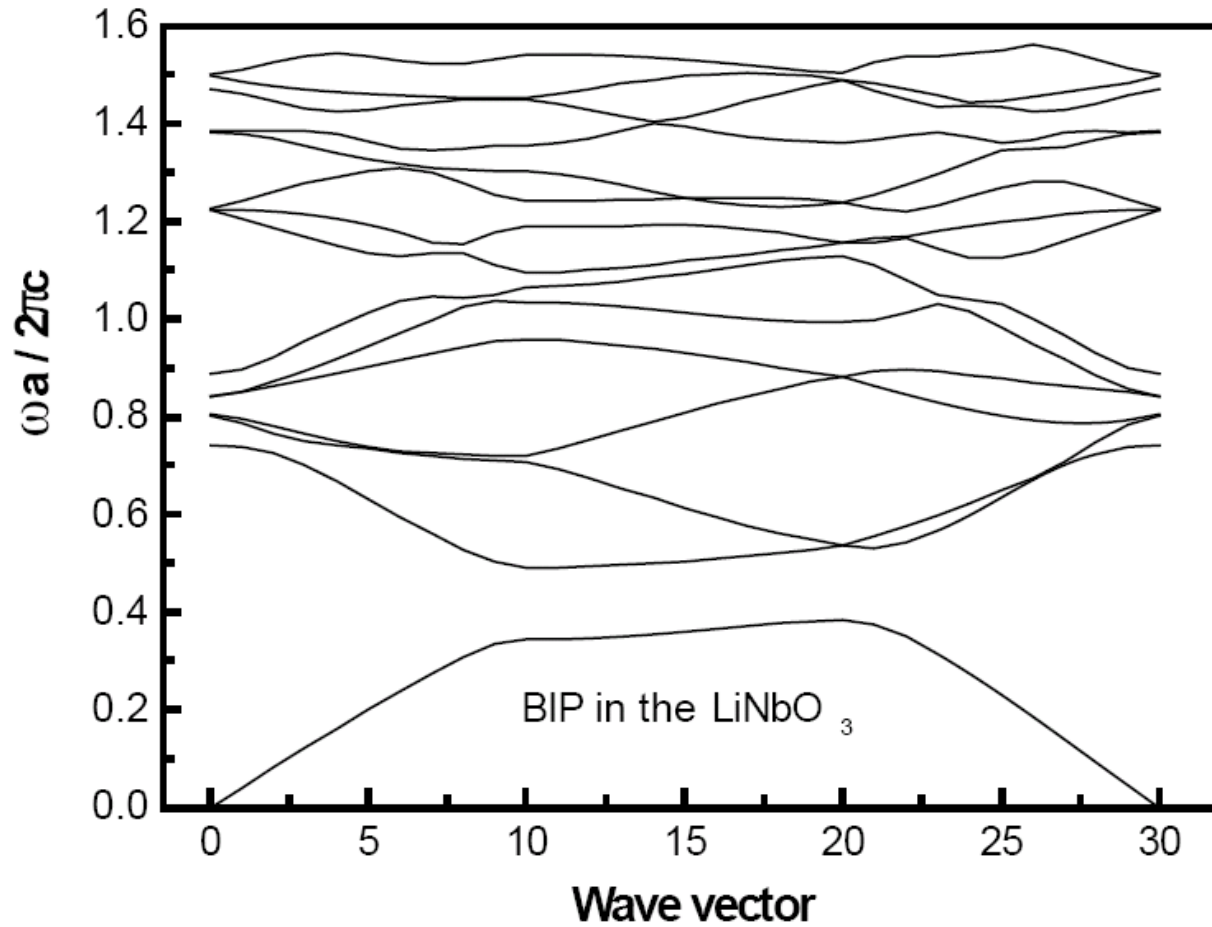
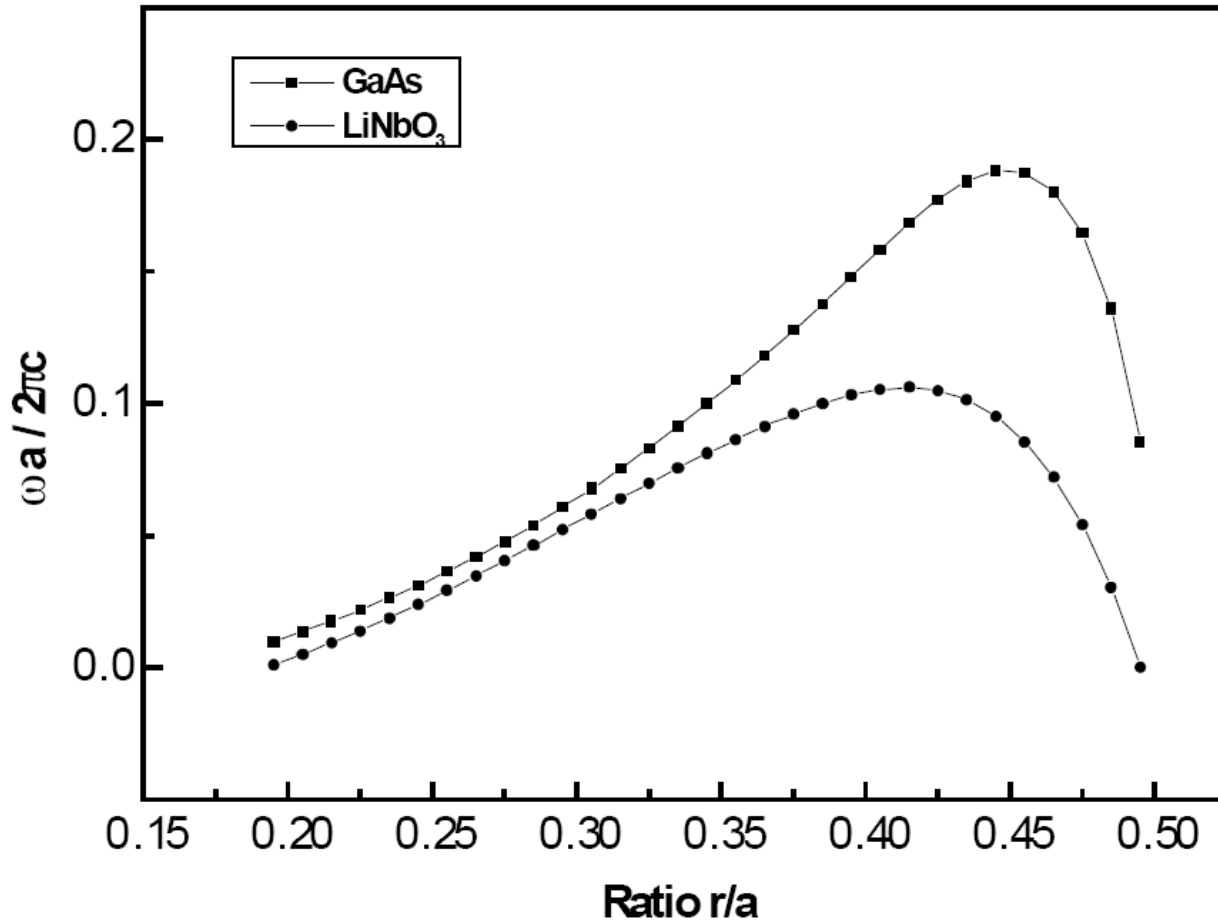


**Figure 2.2** Simulated photonic band structures for **bulk PC** with **finite height**  
 (a) Schematic of 2-D PCS **triangular lattice** structure;  
 (b) Simulated photonic band structure of 2-D triangular lattice PCS, the shadow region marked the **PBG**

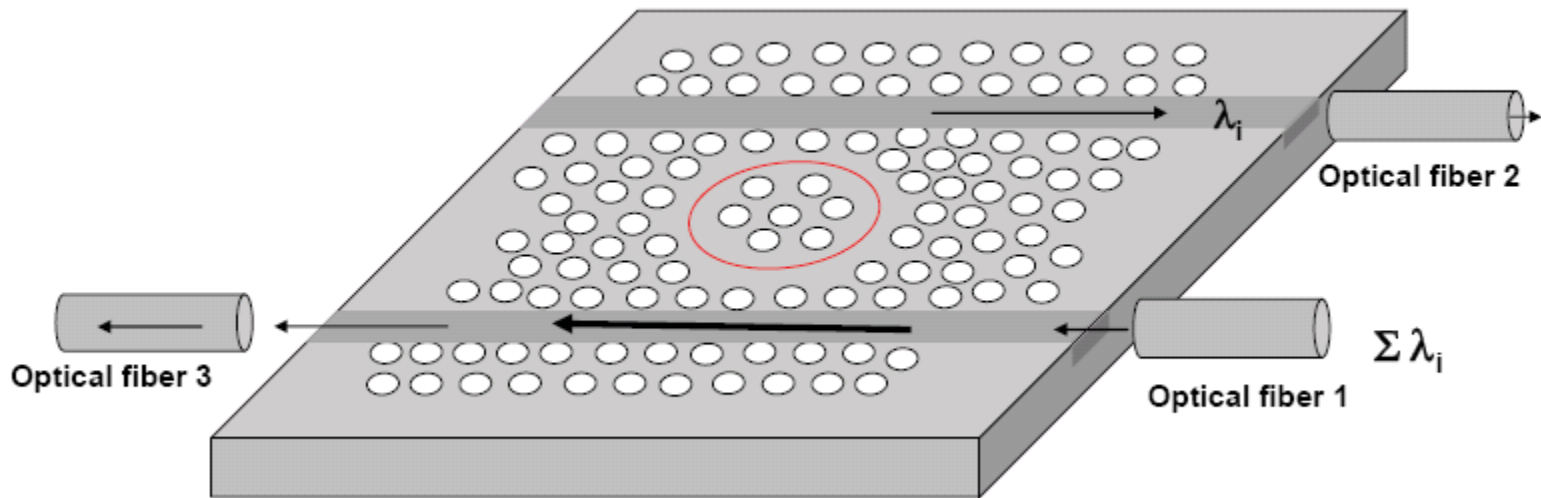
PBG structures of **pillar triangular** lattice of **LiNbO<sub>3</sub>**,  $\epsilon_0 = 4.884$  in **air** (**TE mode**)



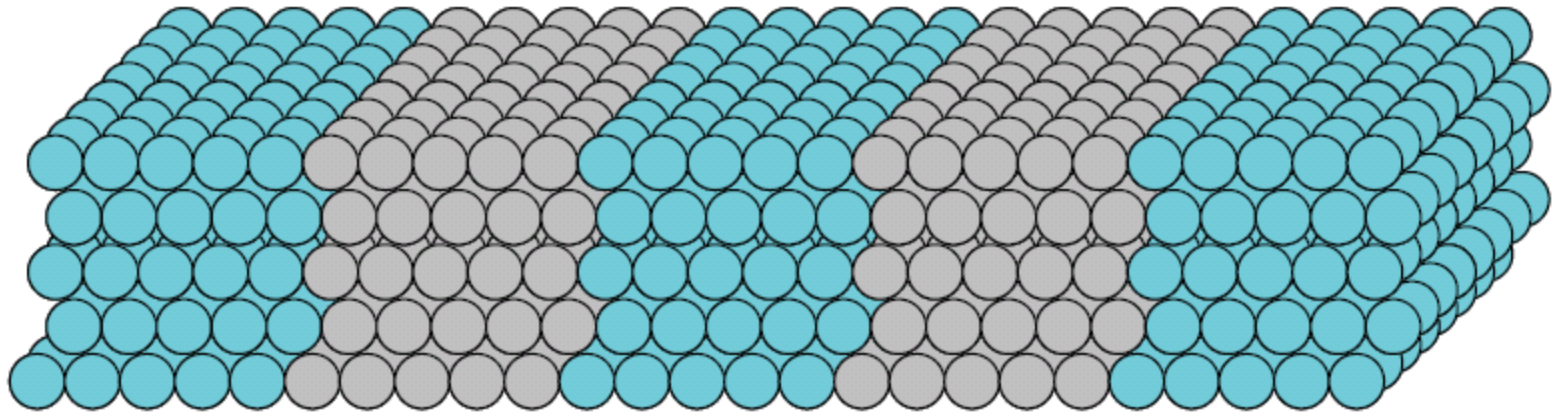
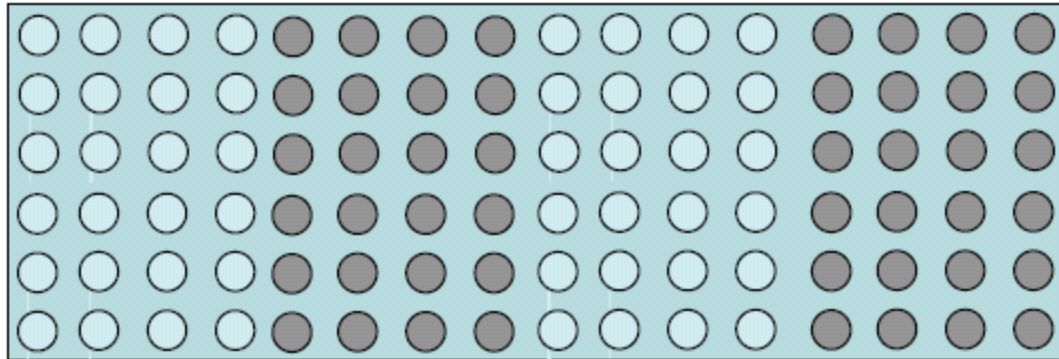
Evolution **PBG** width as a **function** of the ration **r/a** for:  
**LiNbO<sub>3</sub>**,  $\epsilon_0 = 4.884$  and **GaAs**,  $\epsilon_0 = 0.46$  (**TE mode**)



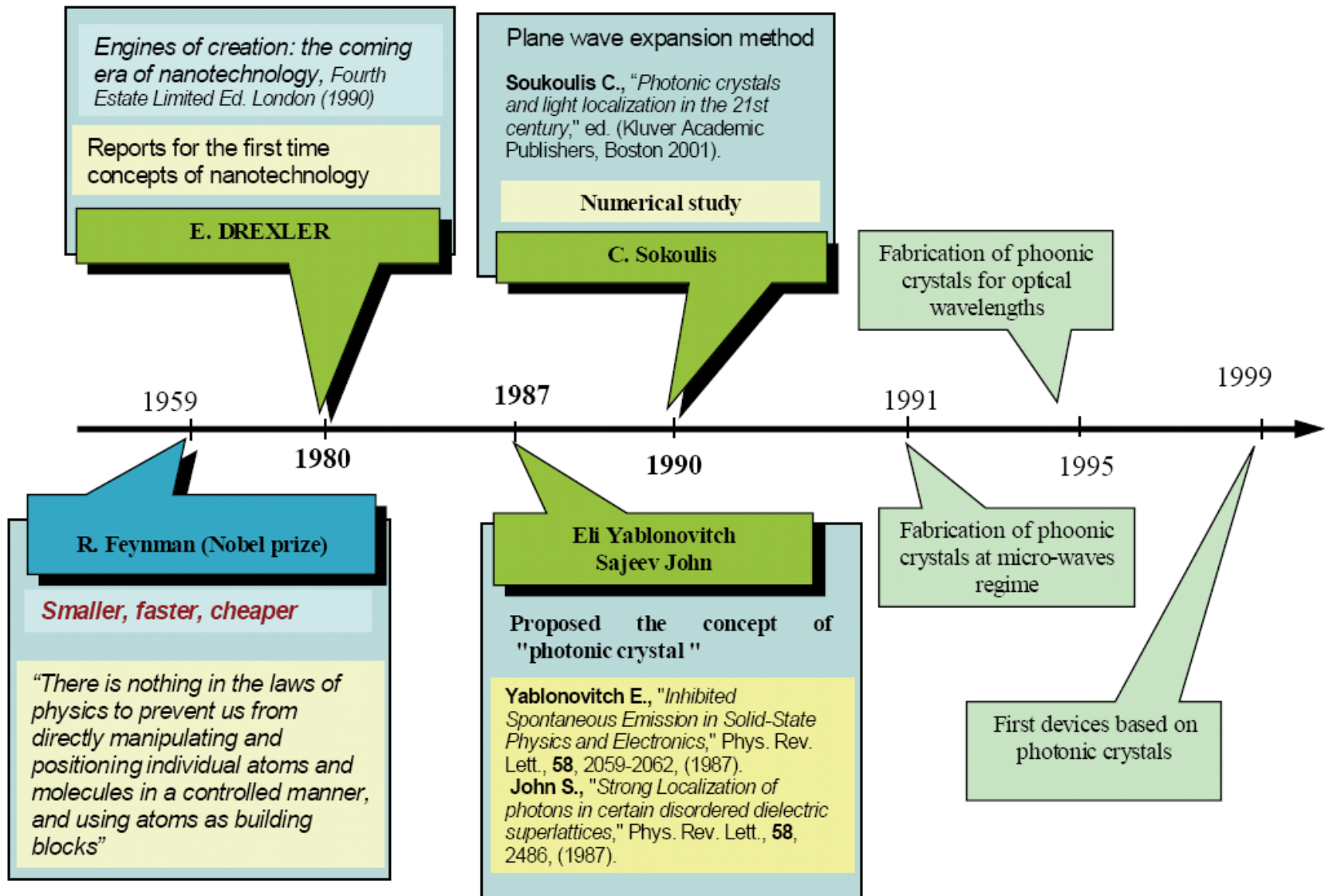
# Add and drop filter principle based on photonic crystals

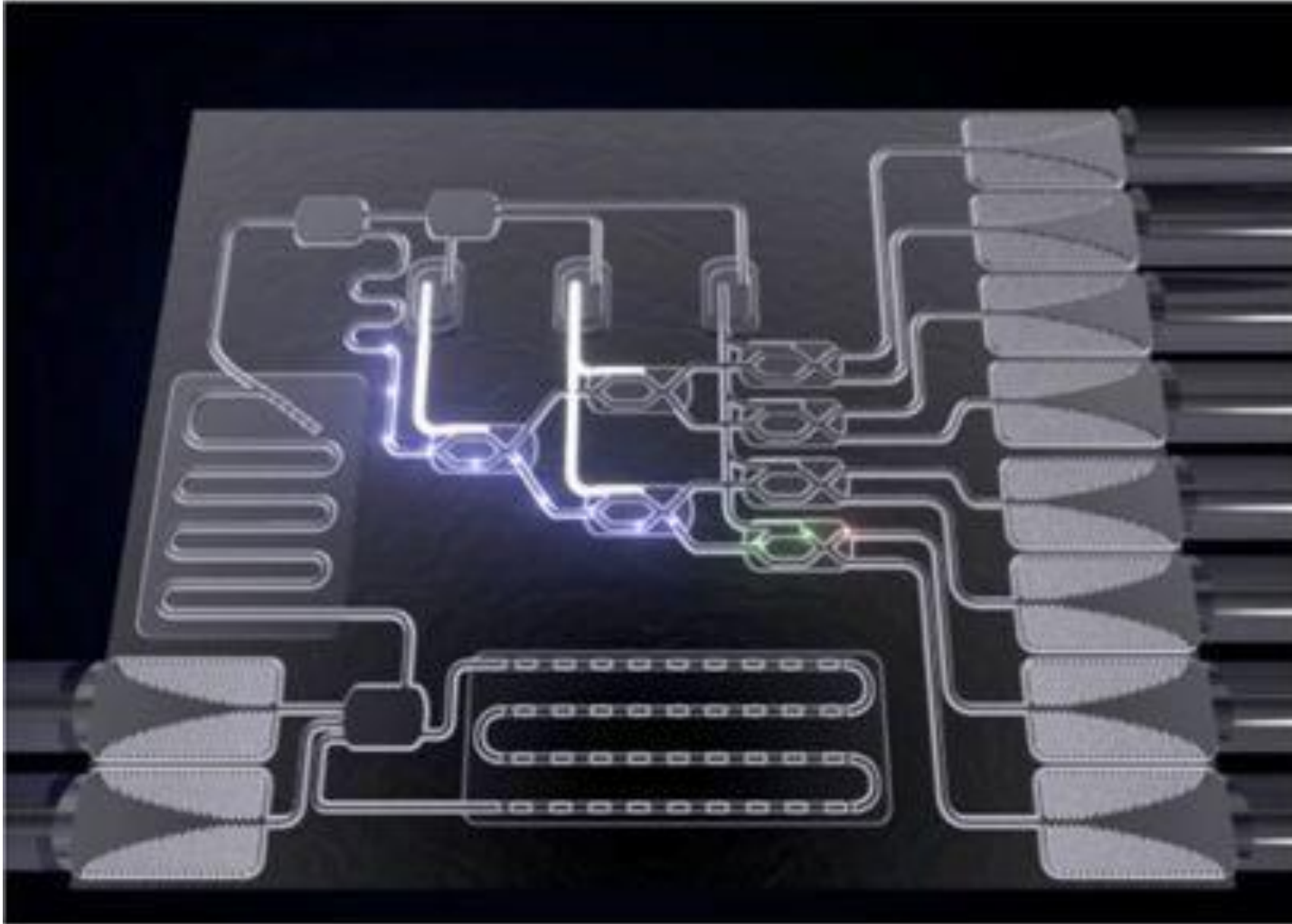


# Hetero-structure of 2D and 3D photonic crystals

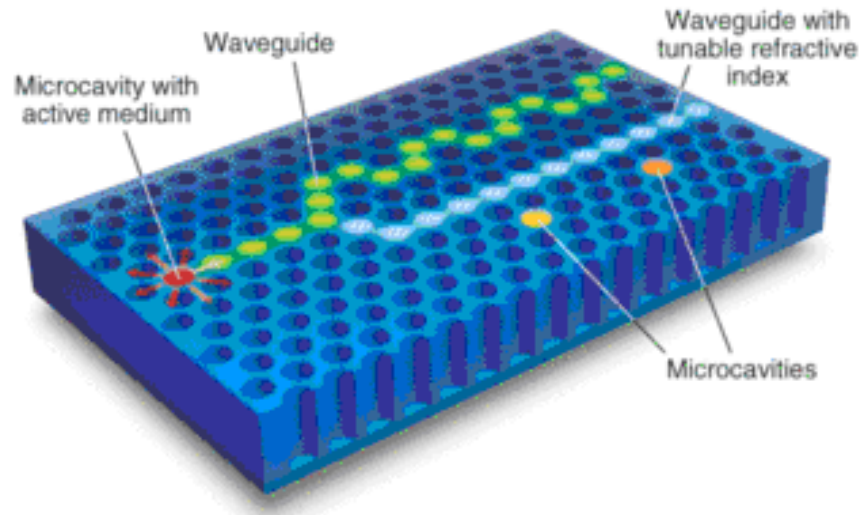


# Historical review of photonic crystal development

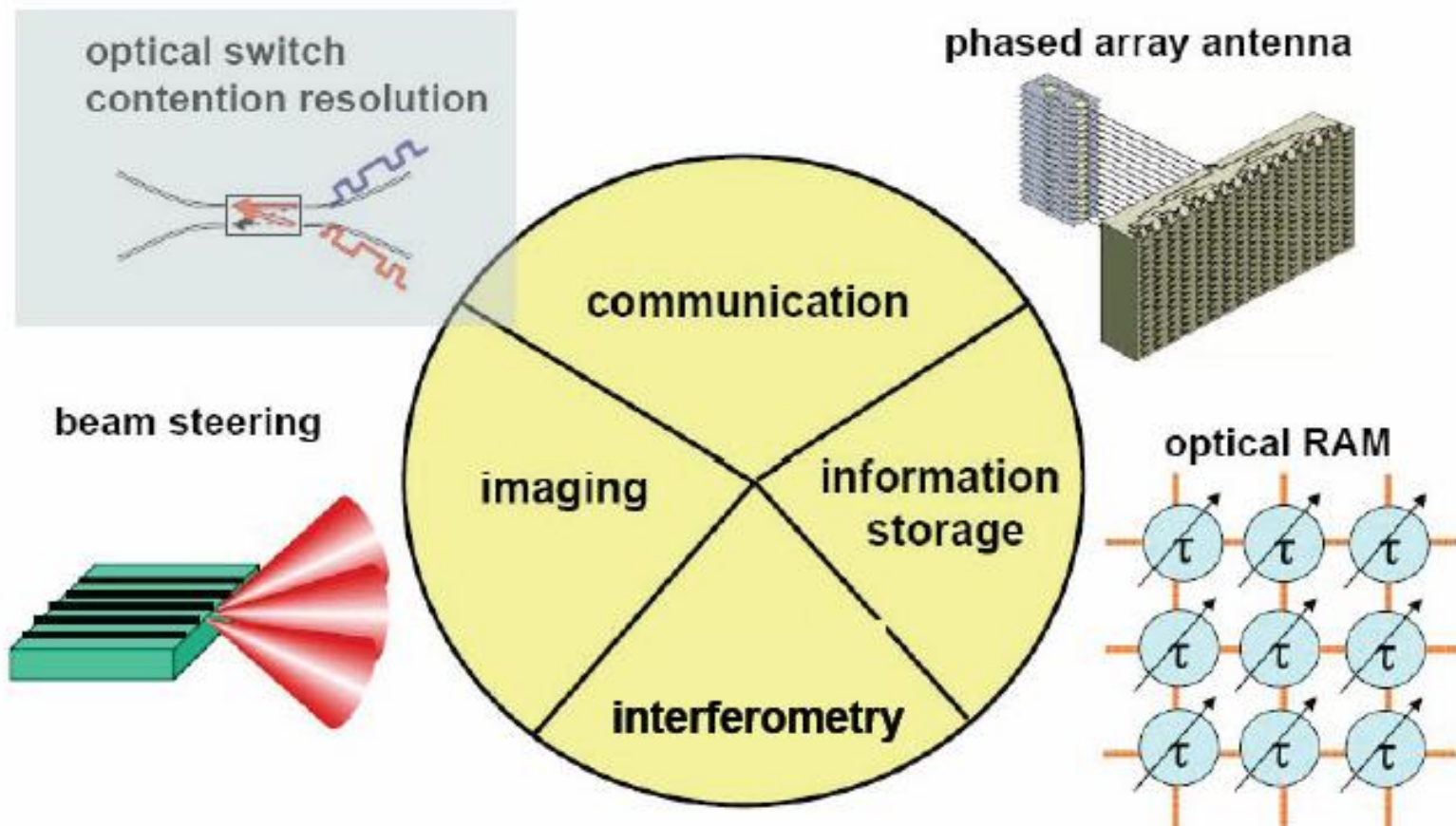




## تراشه فوتونی تمام نوری



نمونه Lab on chip



**کاربرد نور کند در زمینه‌های گوناگون**

# References (1)

---

1. E. Yablonovitch, Phys. Rev. Lett. 58, 2059 (1987)
2. E. Yablonovitch, T. J. Gmitter, and K. M. Leung, Phys. Rev. Lett. 67, 2295 (1991)
3. K. L. Kliewer and R. Fuchs, Phys. Rev. 144, 495 (1966)
4. K. L. Kliewer and R. Fuchs, Phys. Rev. 150, 573 (1966)
5. M. Inoue and K. Ohtaka, Phys. Rev. B26, 3487 (1982)
6. W. M. Robertson, G. Arjavalingham, R. D. Meade, K. D. Brommer, A. M. Rappe, and J. D. Joannopoulos, Phys. Rev. Lett. 68, 2023 (1992)
7. M. Wada, K. Sakoda and K. Inoue, Phys. Rev. B52, 16297 (1995)
8. K. Sakoda, Phys. Rev B51, 4672 (1995)
9. K. Inoue, M. Wada, K. Sakoda, A. Yamanaka, M. Hayashi, and J. W. Haus, Jpn. J. Appl. Phys. 33, L1463 (1994)
10. M. L. Cohen and T. K. Bergstresser, Phys. Rev. 141, 789 (1966)

# References (2)

---

11. E. Yablonovitch, T. J. Gmjtter, and K. M. Leung, *Phys. Rev. Lett.* 67, 3380 (1991)
12. H. S. Sozuer, J. W. Haus, and R. Inguva, *Phys. Rev.* B45, 13,962 (1992)
13. H. S. Sozuer and J. W. Haus, *J. Opt. Soc. Am. B* 10, 296 (1993).
14. S. Johnson, S. Fan, P. R. Villeneuve, and J.D. Joannopoulos, *Phys. Rev.* B60, 5751 (1999)
15. S. Noda, M. Imada, M. Okano, S. Ogawa, M. Mochizukj, and A. Cbutinan, *IEEE J. Quantum Electronics*, 38, 726 (2002)
16. A. Mahls, S. Fan and J.D. Joannopoulos, *Pbys. Rev.* B58, 4809 (1998)
17. S. Johnson, P.R. Villeneuve, S. Fan, and J. D. Joannopoulos, *Phys. Rev.* B62, 8212 (2000)
18. T. Baba, N. Fukaya, and J . Yonekura, *Electron. Lett.* 27, 654 (1999)
19. M. Scalora, R. J. Flynn, S. B. Reinhardt, R. L. Fork, M. D. Tocci, M. J. Bloemer, C. M. Bowden, H. S. Ledbetter, J. M. Bendickson, J. P. Dowling, and R. P. Leavitt, *Pbys. Rev.* E54, R1078 {1996)

# References (3)

20. A. Imhof, W. L. Vos, R. Sprik, and Ad. Lagendijk, Phys. Rev. Lett. 83, 2942 (1999)
21. K. Inoue, N. Kawai, Y. Sugimoto, N. Ikeda, N. Carlsson, and K. Asakawa, Phys. Rev. B65, 121308R (2002)
22. K. Sakoda, Opt. Express, 4, 167 (1999) [<http://fepubs.osa.org/journal/opticsexpress>]
23. M. Scalora, M. J. Bloemer, A. S. Manka, J. P. Pawling, C. M. Bourden, R. Viswanathan, and J. W. Haus, Phys. Rev. A56, 3166 (1999)
24. M. Centini, C. Sibilia, M. Scalora, G. D'Aguanno, M. Bertolotti, M. J. Bloemer, C. M. Bowden, and I. Nefedov, Phys. Rev. E60, 4891 (1999)
25. Y. Dumeige, I. Sagnes, P. Monnier, P. Vidakovic, I. Abram, C. Meriadec, and A. Levenson, Phys. Rev. Lett., 89, 043901 (2002)
26. K. Inoue, M. Sasada, J. Kawamata, K. Sakoda, and J. W. Haus, Jpn. J. Appl. Phys., 38, L157 (1999)
27. M. Imada, S. Noda, A. Chutinan, T. Tokuda, M. Murata, and G. Sasaki, Appl. Phys. Lett., 75, 316 (1999)

# References (4)

28. M. Notomi, H. Suzuki, and T. Tamura, *Appl. Phys. Lett.* 78, 1325 (2001)
29. K. Sakoda, K. Ohtaka, and T. Ueta, *Opt. Express*, 4, 481 (1999)
30. M. Notomi, K. Yamada, A. Sbinya, J. Takahashi, C. Takahashi, and I. Yokohama, *Phys. Rev. Lett.* 87, 253902 (2001)
31. K. M. Ho, C. T. Chan, and C. M. Soukoulis, *Phys. Rev. Lett.* 65, 3152 (1990)
32. M. C. Netti, C. E. Finlayson, J. J. Baumberg, M.D. B. Charlton, M. E. Zoorob, J. S. Wilkinson, G. J. Parker, *Appl. Phys. Lett.* 81, 3927 (2002)
33. K. Ohtaka, T. Ueta, and Y. Tauabe, *J. Phys. Soc. Jpn.* 65, 3068 (1996)
34. M. Netti, A. Harris, J. J. Baumberg, D. M. Whittakar, M. B. D. Charlton, M. E. Zoorob, and G. J. Parker, *Phys. Rev. Lett.* 86, 1526 (2001)
35. H. Kosaka, T. Kawashima, A. Tomita, M. Notomi, T. Tamamura, T. Sato, and S. Kawakami, *Phys. Rev. B* 58, R10096 (1998)
36. H. Kosaka, T. Kawashima, A. Tomita, M. Notomi, T. Tamamura, T. Sato, and S. Kawakami, *Appl. Phys. Lett.* 74, 1212 (1999)

# References (5)

---

37. M. Notomi, Phys. Rev. B62, 10696 (2000)
38. C. Luo, S. G. Johnson, and J. D. Joannopoulos, Appl. Phys. Lett. 81, 2352 (2002)
39. N. Bloembergen and A. J. Sievers, Appl. Phys. Lett. 17, 483 (1970)
40. O. Painter, R. K. Lee, A. Yariv, A. Scherer, J. D. O'Brien, P. D. Dapkus, and I. Kim, Science, 284, 1819 (1999)
41. T. Baba, K. Inoshita, H. Tanaka, J. Yonekura, M. Ariga, A. Matsutani, T. Miyamoto, F. Koyama, and K. Iga, J. Lightwave Technol., 17, 2113 (1999)
42. J. K. Ranka, R. S. Windeler, and A. J. Stentz, Optics Lett. 25, 25 (2000)
43. K. Ohtaka and S. Yamaguti, Optical and Quantum Electronics, 34, 135 (2002);  
S. Yamaguti, J. Inoue, O. Haeberle and K. Ohtaka, Phys. Rev. B 66, 195202 (2002)
44. K. Yamamoto et al., Abstract of International Workshop on Photonic and Electromagnetic Crystal Structures, ed. S. Yu Lin (UCLA, 2002), p. 36

